

**A Genetic Approach toward Defining the Role of Factor X
in Development and Coagulation**

A Thesis

Submitted to the Faculty

of

Drexel University

by

Shing Jen Tai

in partial fulfillment of the
requirements for the degree

of

Doctor of Philosophy

July 2005

© Copyright 2005
Shing Jen Tai. All Rights Reserved.

Dedications

The work presented here is dedicated to the author's parents, Mr. and Mrs. Tai.

Acknowledgments

The author wishes to acknowledge her mentor, Dr. Katherine High for her advice, encouragement, support, and guidance. She also wishes to acknowledge the members of her committee, Dr. Fred Allen, Dr. Patricia Labosky, Dr. Peter Lelkes, and Dr. Margaret Wheatley for their time and support. Furthermore, she likes to thank Dr. Roland Herzog, Dr. Valder Arruda, Dr. Jeff Golden, F. Parker Hudson, and Kirk Chu for their advice and assistance in the study. Finally, the author thanks her parents for their support and understanding.

Table of Contents

LIST OF TABLES	ix
LIST OF ILLUSTRATIONS.....	x
ABSTRACT	xii
1. INTRODUCTION	1
1. GENERATION AND CHARACTERIZATION OF FX KNOCK-OUT MICE.....	9
2.1 Introduction.....	9
2.2 Materials and Methods	12
2.2.1 Isolation of Murine FX Genomic DNA.....	12
2.2.2 Construction of the FX Socket-Targeting Vector	12
2.2.3 Electroporation and Selection of <i>Neo</i> -Resistant ES Cell Clones ..	15
2.2.4 Homologous Recombination between the FX Socket Construct and FX Locus.....	16
2.2.5 Isolation of ES Cell DNA and Mouse Genomic DNA	17
2.2.6 PCR Analysis on ES Cell DNA and Mouse Genomic DNA.....	18
2.2.7 Southern Blot Analysis on ES Cell DNA and Mouse Genomic DNA	19
2.2.8 Generation of FX-Deficient Mice.....	19
2.2.9 Reverse Transcriptase-Polymerase Chain Reaction (RT-PCR) on Total RNA Isolated from Liver Tissues.....	20
2.2.10 Northern Blot Analysis on Total RNA.....	20
2.2.11 Western Blot Analysis on Plasma and Extracts Isolated from Liver Tissues	21
2.2.12 Activated Partial Thromboplastin Time (aPTT) and Prothrombin Time (PT) FX Assays	22
2.2.13 Timed Mating Experiment.....	23

2.2.14 Immunohistochemical Staining for PECAM-1 and ICAM-2.....	23
2.3 Results	24
2.3.1 Construction of the FX Socket-Targeting Vector	24
2.3.2 Targeted Disruption of FX Exon 8	25
2.3.3 PCR Results	25
2.3.4 Southern Blot Results.....	27
2.3.5 Targeting Frequency	29
2.3.6 Production of FX Knock-Out Mice	29
2.3.7 Phenotypic Characterization of FX Knock-Out Neonates	30
2.3.8 Genotype Analysis of the Offspring from Heterozygous FX(+/-) Intercross.....	32
2.3.9 Evaluation of Embryonic Lethality and Phenotype of FX Knock-Out Mice	33
2.3.10 Detection of a Partial Transcript in FX Knock-Out Mice.....	34
2.3.11 Absence of FX Antigen in FX(-/-) Neonates	36
2.3.12 Coagulation Activities of Plasma from FX(-/-) Newborn Mice	38
2.3.13 Immuno-Staining of E13.5 Embryo Sections for PECAM-1 and ICAM-2	39
2.4 Discussion	40

1. GENERATION AND CHARACTERIZATION OF FX KNOCK-IN MICE	45
3.1 Introduction.....	45
3.2 Materials and Methods	49
3.2.1 Construction of the FX Plug-Targeting Vector	49
3.2.2 Electroporation and Selection of HAT-Resistant ES Cell Clones .	52
3.2.3 Isolation of ES Cell DNA and Mouse Genomic DNA	52
3.2.4 PCR Analyses on ES Cell DNA and Mouse Genomic DNA	53
3.2.5 Southern Blot Analysis on ES Cell DNA and Mouse Genomic DNA	53
3.2.6 DNA Sequencing to Confirm Substitution of TCC for CCC in FX Exon 8	54
3.2.7 Generation of Homozygous FX-Friuli [FX(F/F)] Mice.....	54
3.2.8 Western Blot Analysis of Plasma.....	54
3.2.9 Generation of FX(-/F) Mice.....	55
3.2.10 Activated Partial Thromboplastin Time (aPTT) and Prothrombin Time (PT) FX Assays	56
3.2.11 Genotypic Analysis of Offspring from Mating of FX(-/F) Mice.....	56
3.2.12 Phenotypic Analysis of Embryos Resulting from FX(-/F) Mothers	57
3.2.13 Histological Analysis of FX-deficient Mice	57
3.3 Results	58
3.3.1 Homologous Recombination between the FX Plug-Targeting Vector and FX Knock-Out Locus	58

3.3.2 PCR Results	59
3.3.3 Southern Blot Results	62
3.3.4 Targeting Frequency in the Knock-In Experiment.....	62
3.3.5 DNA Sequencing Results	63
3.3.6 Production of Homozygous FX(F/F) Mice.....	64
3.3.7 Levels of FX Antigen in FX(F/F) Mice.....	66
3.3.8 Levels of FX Activity in FX(F/F) Mice.....	66
3.3.9 Generation of FX(-/F) Mice	67
3.3.10 Levels of FX Activity in FX(-/F) Mice.....	68
3.3.11 Genotypic Analysis of the Offspring from FX(-/F) Intercross	69
3.3.12 Phenotypic Analysis of Embryos from FX(-/F) Mothers	70
3.3.13 Histological Analysis of FX-Deficient Mice.....	73
3.4 Discussion	77
1. FX EXPRESSION DURING DEVELOPMENT	89
4.1 Introduction.....	89
4.2 Materials and Methods	91
4.2.1 Timed Mating of Heterozygous FX(+/-) Mice	91
4.2.2 Synthesis of FX Riboprobes	91
4.2.3 Whole-Mount <i>In Situ</i> Hybridization (E9 to E12.5)	92
4.2.4 <i>In Situ</i> Hybridization of Paraffin-Embedded Embryo Tissue Sections (E13.5 to E15.5).....	93
4.2.5 Immunohistochemical Staining for FX Antigen	95
4.3 Results	96
4.3.1 Whole-Mount <i>In Situ</i> Hybridization (E9 to E12.5)	96

4.3.2 <i>In Situ</i> Hybridization of Paraffin-Embedded Embryo Tissue Sections (E13.5 to E15.5).....	99
4.3.3 Immunohistochemical Staining for FX Antigen	102
4.4 Discussion	105
1. SUMMARY AND FUTURE DIRECTIONS.....	110
LIST OF REFERENCES	114
VITA	121

List of Tables

1. Mouse Models of Thrombosis and Hemostasis	2
1. Genotype Distribution among Offspring from Heterozygous FX(+/-) Intercross	33
1. Genotype Distribution among Offspring of Heterozygous FX(+/-) Parents .	34
1. Coagulation Times in Seconds of FX(+/+), FX(+/-), and FX(-/-) Newborn Plasma.....	39
1. A List of Some Naturally Occurring Human FX Variants with Mutations in Exon 8	47
1. Genotype Distribution among Offspring from Heterozygous FX(+/ F) Intercross.....	65
1. FX Coagulation Activity in FX(+/+), FX(+/ F) and FX(F/F) Adult Mice.....	67
1. Genotype Distribution in Offspring Resulting from Cross of FX(F/F) Females and FX(+/-) Males	68
1. FX Coagulation Activity in FX(-/ F) Mice and Age-Matched Wild-Type Adult Mice.....	69
1. Genotype Distribution among Offspring from FX(-/ F) Intercross.....	70
1. Comparison of FX(+/-) Intercross and FX(+/ F) Intercross.....	79
1. Comparison of FX(+/-) Intercross and FX(-/ F) Intercross	83

List of Illustrations

1. Illustration of the Coagulation Cascade	5
1. Illustration of the Prothrombinase Complex	6
1. Construction of the 5' and 3' FX Targeting Arms	14
1. Construction of the FX Socket-Targeting Vector	15
1. Targeted Disruption of FX Gene	17
1. PCR Analysis of ES Cell DNA.....	26
1. PCR Analysis of Mouse Genomic DNA	27
1. Southern Blot Analysis of ES Cell DNA	28
1. Southern Blot Analysis of Genomic DNA	28
1. Phenotypic Comparison of FX(+/+) and FX(-/-) Neonates	31
1. Kaplan-Meier Survival Curve of Homozygous FX Knock-Out Mice.....	31
1. Subcutaneous Bleeding in a FX(-/-) Mouse	32
1. RT-PCR Analysis of FX Transcript from FX(+/+) and FX(-/-) Neonates	35
1. Northern Blot Analysis of Total RNA from FX(+/+), FX(+/-) and FX(-/-) Livers	36
1. Western Blot Analysis of Plasma from FX(+/+), FX(+/-) and FX(-/-) Mice	37
1. Western Blot Analysis of Cell Lysates from FX(+/+), FX(+/-) and FX(-/-) Livers	38
1. Immuno-Staining of E13.5 Embryo Sections for PECAM-1 and ICAM-2	40
1. Construction of the FX Plug-Targeting Vector.....	51
1. Targeted Knock-In of FX-Friuli.....	58
1. PCR and Restriction Enzyme Digest (<i>BanI</i>).....	60
1. PCR Analysis to Differentiate FX(+/+) , FX(F/F), and FX(-/+) Mice	61

1. Southern Blot Analysis of DNA from HAT-Resistant ES Clones	62
1. Sequencing Analysis of PCR Products	64
1. Western Blot Analysis of Plasma	66
1. Examination of E10.5, E11.5 and E12.5 FX-Deficient Littermates from FX(-/F) Mothers	72
1. Examination of E13.5 FX-Deficient Littermates from a FX (+/-) Mother	73
1. Histological Analysis of the Heart Tissues from FX-Deficient Mice	75
1. Co-Localization of Iron Deposits and Fibrosis.....	76
1. Histological Analysis of the Spleen Tissues from FX-Deficient Mice.....	77
1. Whole-Mount <i>In Situ</i> Hybridization of E9 Embryos	97
1. Whole-Mount <i>In Situ</i> Hybridization of an E10.5 Embryo	97
1. Whole-Mount <i>In Situ</i> Hybridization of E11.5 Embryos	98
1. Whole-Mount <i>In Situ</i> Hybridization of E12.5 Embryos	98
1. <i>In Situ</i> Hybridization of E13.5 Wild-Type Paraffin-Embedded Embryo Sections	100
35. <i>In Situ</i> Hybridization of E14.5 Wild-Type Paraffin-Embedded Embryo Sections.....	101
36. <i>In Situ</i> Hybridization of E15.5 Wild-Type Paraffin-Embedded Embryo Sections.....	102
37. FX Expression in E12.5 Embryos.....	103
38. FX Expression in E14.5 Embryos.....	104
39. FX Expression in E15.5 Embryos.....	105

Abstract
A Genetic Approach toward Defining the Role of Factor X
in Development and Coagulation
Shing Jen Tai
Katherine A. High, MD.

Activated Factor X (FX) is a vitamin K-dependent serine protease that plays a crucial role in blood coagulation by converting prothrombin to thrombin. There are no humans with complete deficiency of FX. The overall objective of this study is to investigate the role of FX in development and coagulation by generating FX-deficient mouse models and determining the embryonic pattern of FX expression. First, a FX knock-out mouse model was engineered by eliminating FX exon 8 and its 3' flanking sequence; this resulted in embryonic or perinatal lethality in FX $-/-$ mice. Approximately 50% of FX $-/-$ embryos died between days 10-12 of development. Fatal bleeding in the remaining FX($-/-$) animals occurred soon after birth. The cause of embryonic lethality remains unclear. Next, a viable mouse model of FX deficiency was generated. These mice expressed a FX variant with normal antigen levels but a low level of activity (4-9% in humans carrying the analogous defect, Pro³⁴³→Ser, termed FX Friuli). Homozygous mice had FX coagulation activity of ~5.5% of normal, which was sufficient to rescue both embryonic and perinatal lethality. To generate mice with even lower FX activity, FX(F/F) and FX(+/-) mice were crossed. Their offspring, FX(-/F) mice, indeed had even lower FX activity (1-3% of normal) and nonetheless also showed complete rescue of embryonic and perinatal lethality. Therefore, while complete absence of FX is incompatible with murine and

human survival, minimum FX activity as low as 1% demonstrates sufficiency in rescue of FX knockout mice from lethality. FX(-/F) mice provided an opportunity to assess the relative contributions of maternal and embryonic FX as well as FX activity and antigen to embryonic survival. FX(-/F) mice also facilitated investigation into a developmental role of FX by allowing for examination of FX(-/-) embryos born to mothers with minimal levels of FX activity. Furthermore, FX expression in multiple embryonic tissues was detected by *in situ* hybridization and immunostaining. Combined, these results represent an initial investigation into defining the role of FX in development.

1. Introduction

A powerful genetic tool to unveil important biological functions of a gene product is the generation of an animal model lacking a functional copy of the respective gene. Generation and detailed characterization of mouse models with deficiencies in various hemostasis-related components have enabled investigators to gain unparalleled insights into their roles not only in maintaining a critical balance in hemostasis, but also in supporting embryonic development and survival. Murine models for deficiencies of various clotting factors and hemostatic components can be approximately divided into two groups. Thus far, it has been learned that mice with deficiencies in factor VII (FVII), factor VIII (FVIII), factor IX (FIX), factor XI (FXI), fibrinogen, platelets, protein C (PC), or protein Z (PZ) completed embryogenesis and exhibited variable neonatal phenotypes ranging from nearly normal prognosis to hemostatic defects of various severities (Table 1).¹⁻⁹ While absence of any of the above mentioned hemostasis-related components did not impede embryonic development, deficiencies in factor V (FV), prothrombin (FII), tissue factor (TF), tissue factor pathway inhibitor (TFPI), or thrombomodulin (TM) invariably resulted in embryonic lethality of variable penetrance (Table 1).¹⁰⁻¹⁷ Table 1 below summarizes the mouse models of thrombosis and hemostasis.

Table 1. Mouse models of thrombosis and hemostasis (kindly provided by Dr. R. Camire, University of Pennsylvania).

Knockout	Strain	Viable	Embryonic Development/Survival	Phenotype	Reference
Thrombomodulin	129Sv	No	Lethal/E9.5	Growth retardation/ Defect in parietal endoderm	Healy, et al., 1995
Factor VIII	129Sv	Yes	Normal	Severe bleeding following trauma	Bi, et al., 1995
Fibrinogen	129/CF-1	Yes	Develop to term/Variable long-term survival	Signs of bleeding but control blood loss	Suh, et al., 1995
Tissue Factor	Several	No	Lethal/E8.5-11.5	Growth retarded/Defective yolk sac vessel development	Bugge, et al., 1996 Carmeliet et al., 1996 Toomey, et al., 1996
Factor V	C57BL/6J	No	50% Die E9-10/Remaining die following birth	Developmental delay/ Abnormal yolk sac	Cui, et al., 1996
TFPI	C57BL/6	No	Lethal/E9.5-11.5	Abnormal yolk sac vasculature/ Consumptive coagulopathy	Huang, et al., 1997
Factor VII	C57B16/J	Yes	Develop normally/ die perinatally	Fatal intra-abdominal bleeding/ Intracranial hemorrhage	Rosen, et al., 1997
Factor IX	C57BL/6	Yes	Normal	Severe bleeding following trauma	Lin, et al., 1997 Kundu, et al., 1998
Factor XI	C57BL/6	Yes	Normal	Normal; aPTT prolonged	Gailani, et al., 1997
Prothrombin	C57BL6/NIH BS	No	50% Die E9.5-11.5/Remaining die following birth	Abnormal yolk sac vasculature/ Fatal hemorrhage	Xue, et al., 1998 Sun, et al., 1998
Protein C	Swiss	No	Develop normally/Did not survive beyond 24 hr	Microvascular thrombosis/ Consumptive coagulopathy	Jalbert, et al., 1998
Protein Z	C57BL/6	Yes	Normal	Normal/Increases thrombotic phenotype in FV ^{L-riden} mice	Yin, et al., 2000

The murine and human factor X (FX) genes are similar in several aspects. As it is in humans, murine FX is located immediately downstream of the FVII gene in a head to tail orientation.^{18,19} Murine FX (20-kb) and human FX (26-kb) have an identical exon-intron organization; each gene is comprised of 8 exons and 7 introns; furthermore, with the exceptions of exon 6 and exon 8, each exon in murine FX is identical in length to the analogous exon in human FX.²⁰⁻²² Striking similarities were also noted in the relationship between domain structure of the FX protein and specific exons of the FX gene. For both murine and human FX genes, exon 1 encodes the signal peptide; exon 2, the propeptide and the Gla domain; exon 3, a short stack of aromatic amino acids;

exons 4 and 5, the EGF-1 (epidermal growth factor –1) and EGF-2 (epidermal growth factor –2) domains, respectively; exon 6, the activation peptide; and exons 7 and 8, the catalytic domain. Moreover, the organization of gene to structural domain observed in murine and human FX is conserved by other vitamin-K dependent clotting factors including FVII, FIX, and PC.²²⁻²⁵ The murine FX cDNA is 1.4-kb in length; it encodes a precursor protein of 481 amino acid residues with a molecular weight of approximately 54-kDa.^{26,27}

Based on sequence and structural homology with human FX protein, it is likely that murine FX undergoes similarly complex post-translational modifications before secretion.^{26,28-30} The essential modifications undergone by human FX precursor protein include proteolytic removal of the 40-amino acid pre-pro leader sequence (also evident in mouse FX precursor), vitamin K-dependent γ -carboxylation of the first 11 glutamic acid residues in the Gla domain, β -hydroxylation of aspartic acid residue 63, and removal of a specific tripeptide (Arg 140-Lys-Arg 142) to generate a 59-kDa FX zymogen, consisting of a heavy and light chain linked by a disulfide bond.^{26,31-34}

Activation of both murine and human FX is accomplished by cleavage of a specific Arg-Ile bond in the heavy chain, resulting in the removal of the heavily glycosylated 49-amino acid and 52-amino acid activation peptides, respectively.^{26,35} As serine proteases, murine and human FX contain a catalytic triad (His 233/236, Asp279/282, and Ser376/379) respectively in the active site.^{26,36} The amino acid sequence of mouse FX is over 70% conserved with

that of human FX; the highest conservation (>80%) is found in the catalytic domain.²⁶

Blood coagulation FX is a vitamin K-dependent, two-chain plasma protein that occupies a pivotal role in the coagulation cascade (Figure 1). Under physiological conditions and in the presence of calcium and on a phospholipid membrane surface, activation of FX to FXa, a serine protease of the prothrombinase complex (Figure 2), is initiated following vascular injury. Activation of FX to FXa is achieved by the Factor VIIa/Tissue Factor (FVIIa/TF) complex in the extrinsic pathway and maintained by the Factor IXa/Factor VIIIa (FIXa/FVIIIa) complex in the intrinsic pathway (Figure 1).³⁵ Activation of FX by either complex involves a cleavage of the same specific arginine-isoleucine bond found near the amino-terminal end of the heavy chain of FX.²⁶

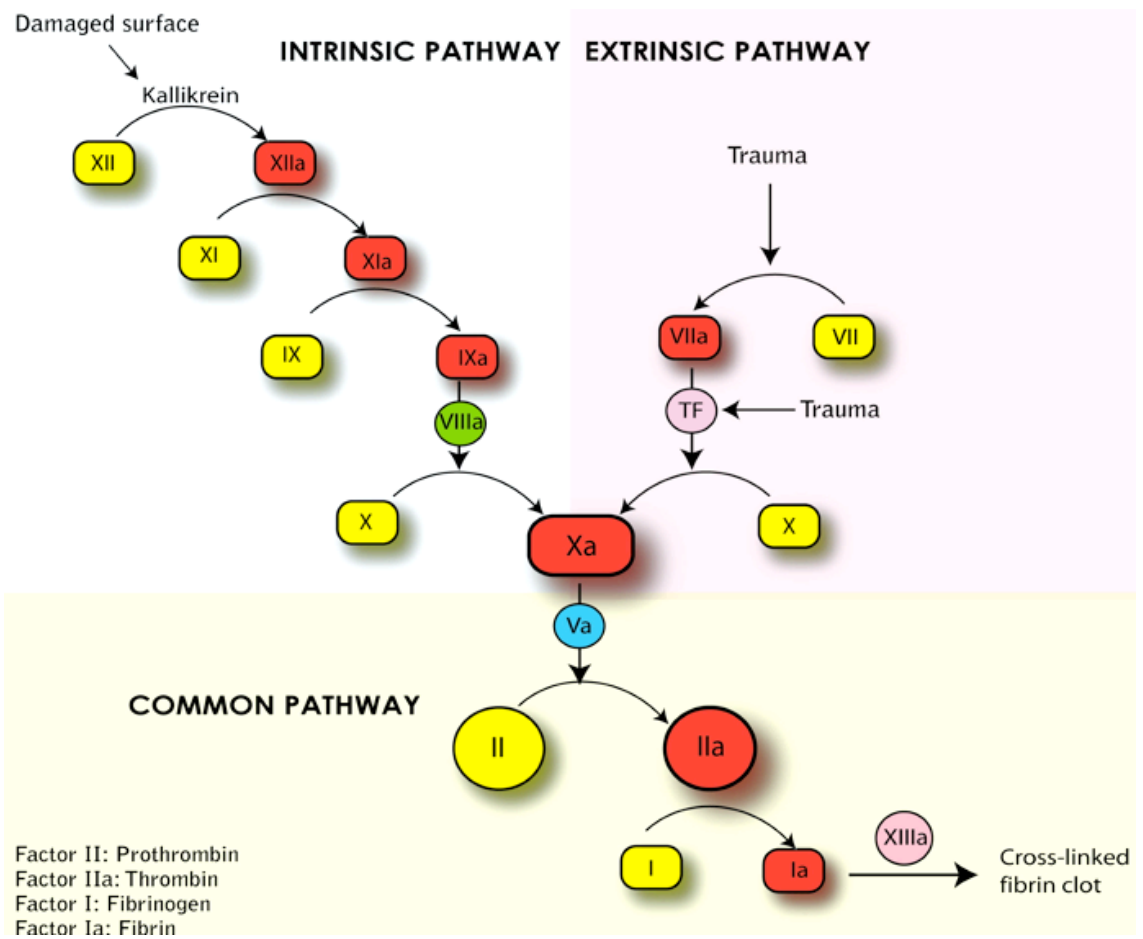


Figure 1. Illustration of the coagulation cascade (kindly provided by Dr. F. Khazi, Children's Hospital of Philadelphia)

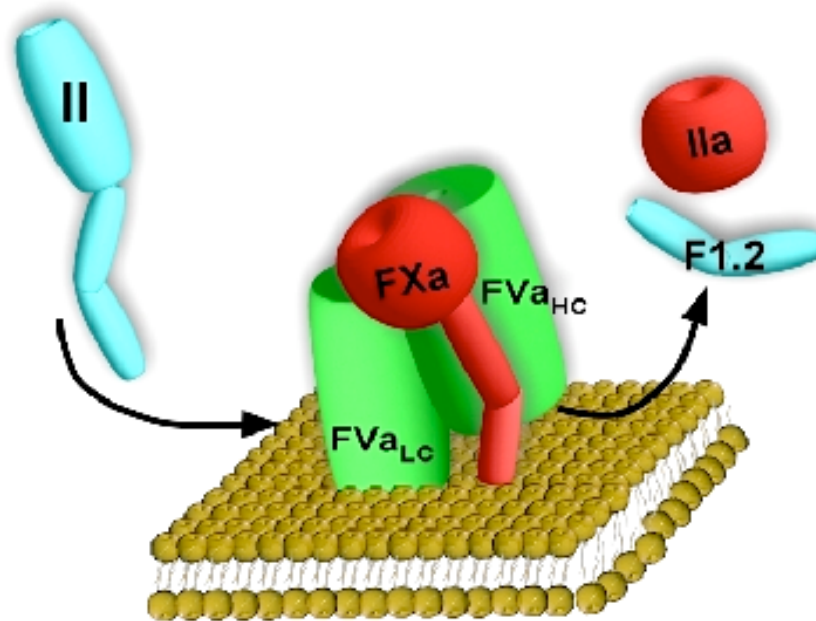


Figure 2. Illustration of the Prothrombinase complex (Kindly provided by Dr. R. Camire).

In association with its activated nonproteolytic cofactor, factor Va (FVa), activated FXa assembles on phospholipid membrane surfaces in the presence of Ca^{2+} to convert prothrombin to thrombin by cleavage of two peptide bonds (Figure 2).^{37,38} FXa is the only known physiological enzyme that catalyzes the conversion of prothrombin (FII) to thrombin (FIIa). In addition to its function of generating thrombin required for fibrin clot formation and platelet activation, FXa can also catalyze the activation of FV, FVII, FVIII, and protein C *in vitro*.³⁹⁻⁴² To maintain hemostasis, the procoagulant activities of FXa are counter-balanced by its inhibitors. Some plasma protease inhibitors of FXa activity include antithrombin III (ATIII), α 1 antitrypsin, and α 2-macroglobulin.⁴³⁻⁴⁵ Furthermore,

binding of tissue factor pathway inhibitor (TFPI) to FXa results in an inhibition of the procoagulant activity of the FVIIa/TF complex.⁴⁶

Several lines of evidence suggest that FX may have functions other than hemostasis. For example, in contrast to the closely related vitamin-K dependent proteins FVII and FIX, expressed only in the liver, FX in adult humans is also expressed in the stomach, lungs, skeletal muscle, ovary, testis, and other tissues.⁴⁷ In addition to its defined role in blood coagulation, FX/FXa has been shown to elicit a wide range of biological responses both *in vitro* and *in vivo*.⁴⁸⁻⁵⁴ These include stimulation of mitogenic activity in cultured rat aortic smooth muscle cells, induction of cytokine production and expression of adhesion molecules by human umbilical vein endothelial cells, up-regulation of transcription factor, *egr-1*, in a keratinocyte cell line, and others.^{48,49,53} It is important to note that for some FX/FXa induced responses, catalytic activity of FXa is required, but for others, it is not required.⁴⁸⁻⁵⁴ In light of these findings, an interesting investigation will be to determine whether a catalytically active FXa is required for embryonic survival. Additional evidence suggesting a non-hemostatic role for FX during development includes expression of mouse FX transcript as early as E7.5 prior to the formation of a functional circulatory system.⁵⁵ Given these findings, it is not unreasonable to hypothesize that FX, beyond its critically defined role in blood coagulation, may exert other biological influences that determine embryonic survival.

In this study, the overall objective is to investigate the role of FX in development and coagulation by generating and characterizing FX-deficient mouse models and by determining the embryonic pattern of FX expression.

2. Generation and characterization of FX knock-out mice

2.1 Introduction

Over the years, a number of hemostasis-related knock-out mouse models have been generated and characterized. Some of the mouse models showed an interesting phenomenon of variable embryonic lethality and postnatal mortality. For example, as noted earlier, both FV and prothrombin (FII) deficiencies resulted in partial embryonic loss and perinatal lethality.¹⁰⁻¹² Given that FVa is the cofactor of FXa in the prothrombinase complex, and prothrombin (FII) is the substrate of FXa, the expectation here is that FX is likely to play a crucial role in both embryonic and postnatal survival. If true, this may reflect both coagulation-dependent and coagulation-independent functions of FX.

As a matter of fact, no humans with complete deficiency of FX have been reported. Instead, all of the described mutations are either missense mutations or compound heterozygotes with a deletion or stop codon on one allele and a missense mutation on the other, suggesting that complete deficiency of FX is incompatible with life. Since it is likely that homozygous deletion of even a single exon of FX would result in lethality, it seems prudent to generate a FX knock-out mouse model using a plug-and-socket targeting strategy. This strategy enables repeated modification or rescue of a disrupted locus, if necessary.⁵⁶

The plug-and-socket targeting strategy provides several advantages that are critical to the overall design of the study presented here. First, this strategy enables targeted disruption of any specific locus, using an appropriately

designed socket construct. A socket construct consisting of a selectable marker *Neo* (neomycin resistance gene) and a partial *HPRT* (hypoxanthine phosphoribosyl transferase) sequence is introduced into an *HPRT*-negative murine ES (embryonic stem) cell line. Upon homologous recombination, the socket vector targets a specific region of a gene for replacement with a *Neo/ΔHPRT* cassette. This targeted disruption of a gene effectively abolishes the function of its gene product. Thus, any effect resulting from complete absence of a gene product can be accordingly investigated. Second, this strategy also facilitates repeated modification (or rescue) of a specific locus previously disrupted by a socket vector. This particular feature of the strategy is highly desirable in the event that complete deficiency of a gene product is lethal, precluding further use of such a mouse model. In the rescue experiment, the second “plug” construct supplying the portion of *HPRT* sequence missing in the socket vector is introduced into the ES cell line previously targeted by the socket vector. Upon homologous recombination, the *Neo* gene is eliminated by restoration of a further modified gene sequence, and the full-length *HPRT* sequence is reconstituted for positive selection of ES cells by growth on HAT (hypoxanthine aminopterin thymidine) medium. The requirement for reconstitution of the *HPRT* sequence is predicted to increase the percent of correctly targeted clones identified after the second targeting event (unpublished observation made by Dr. O. Smithies). The use of the plug-and-socket constructs affords an additional advantage. Expression of the gene of interest is driven under the control of the endogenous promoter, a particularly

desirable feature in the case of a gene like FX, which is expressed in a variety of tissues, and in which the cause of the lethality in humans is still unclear.⁴⁷

This added advantage ensures that the expression of any variant FX gene will parallel that of the wild-type gene in both levels and sites of FX expression.

The choice of specific FX sequences to disrupt in the FX coding region was based on several considerations. First, since it was uncertain what level of FX expression would be required to rescue lethality, should lethality also occur in a mouse model of complete FX deficiency, a region of the FX gene that encodes variants with a range of FX activities and FX antigen levels was targeted for disruption. Since nearly half of the reported patients with FX deficiency have mutations in exon 8, deletion of the exon 8 sequences would afford a wide range of activity and antigen levels for “knock-in” or rescue. Mutations described for the human FX gene can be found on

http://www.med.unc.edu/isth/mutations-databases/Factor_X.htm. Second, since exon 8 encodes the last two residues (Asp^{279/282} and Ser^{376/379}) of the catalytic triad, one can potentially generate a FX variant (with complete absence of activity but normal antigen levels) by making a substitution at either of these residues (in fact, such a substitution has been described in a patient heterozygous for a FX mutation, termed FX Stockton).⁵⁷ Any influence on embryonic survival of a catalytically inactive FXa molecule can then be assessed.

In this chapter, the objectives are 1) to generate a FX knock-out mouse model with deletion of exon 8 and its 3' flanking sequence using the plug-and-

socket targeting strategy, 2) to characterize FX knock-out mice with respect to the role of FX in coagulation and development.

2.2 Materials and methods

2.2.1 Isolation of murine FX genomic DNA

Designed from sequences in exon 8 of the murine FX cDNA sequence, the forward primer (5'-GCCGAGTCCACACTGATGACA-3') and reverse primer (5'-CCCTGTCAATCCACTT-3') PCR-amplified a 350-bp fragment from 129/SvJ mouse genomic DNA (Stratagene, La Jolla, CA).²⁶ After DNA sequencing to confirm the identity of the fragment, the PCR-amplified mouse FX exon 8 sequence was used as a probe to screen a bacterial artificial chromosome (BAC) library derived from *Hind*III, partially digested ES 129/SvJ DNA. Two BAC clones were found to hybridize with the 350-bp exon 8 probe; one of these was further analyzed by restriction enzyme digest, field inversion gel electrophoresis (FIGE), and Southern blot hybridization with the same PCR-amplified probe as described above. Subsequently, a 7-kb *Nhe*I digested fragment was recovered. PCR analysis and DNA sequencing of the isolated fragment indicated that it contains exons 6, 7, and 8, the intervening introns, and the flanking region downstream of exon 8. Once the identity of the recovered fragment was confirmed as the 3' portion of the murine FX gene, it provided a basis for the design and construction of the FX socket vector.

2.2.2 Construction of the FX socket-targeting vector

The 7-kb *Nhe*I FX fragment was first cloned into a pCI vector (Promega, Madison, WI); this resulted in a 11-kb plasmid vector (pCI-mFX-3') (Figure 3A).

To generate the 2.8-kb 5' FX targeting arm, the *Bam*HI and *Sph*I digested fragment from pCI-mFX-3' was cloned into a pCI vector. The resulting plasmid vector is called pCI-5' arm (Figures 3B and 4B). To generate the 1.6-kb 3' FX targeting arm, the *Eco*RI and *Nhe*I digested fragment also from the pCI-mFX-3' vector was ligated into a pCI vector at the *Eco*RI and *Xba*I sites. The resulting plasmid vector is called pCI-3' arm (Figures 3C and 4A).

Engineered in the pPD20 plasmid vector (provided by Dr. Randy Thresher, UNC Chapel Hill), the final FX socket construct (pPD20-mFX socket) consists of 5' and 3' homologous sequences flanking a functional *Neo* gene and a partially deleted, non-functional *HPRT* minigene (Figure 4C). The 2.8-kb 5' FX-targeting arm cloned into the *Not*I site in the pPD20 plasmid vector included exon 6, intron 6, exon 7, and part of intron 7 of the murine FX gene (Figure 4C). The 1.6-kb 3' FX-targeting arm cloned into the *Sal*I site in the vector contained sequence downstream of the putative polyadenylation signal (ATTAAA) and the overlapping termination codon (TAA) of the FX gene. The whole targeting construct spanned about 16.2-kb and was linearized with *Sac*II at the 5' terminus of the 5' targeting arm (Figure 4C) before it was introduced into E14TG2a *HPRT*-deficient ES cells (provided by Dr. Maeda).

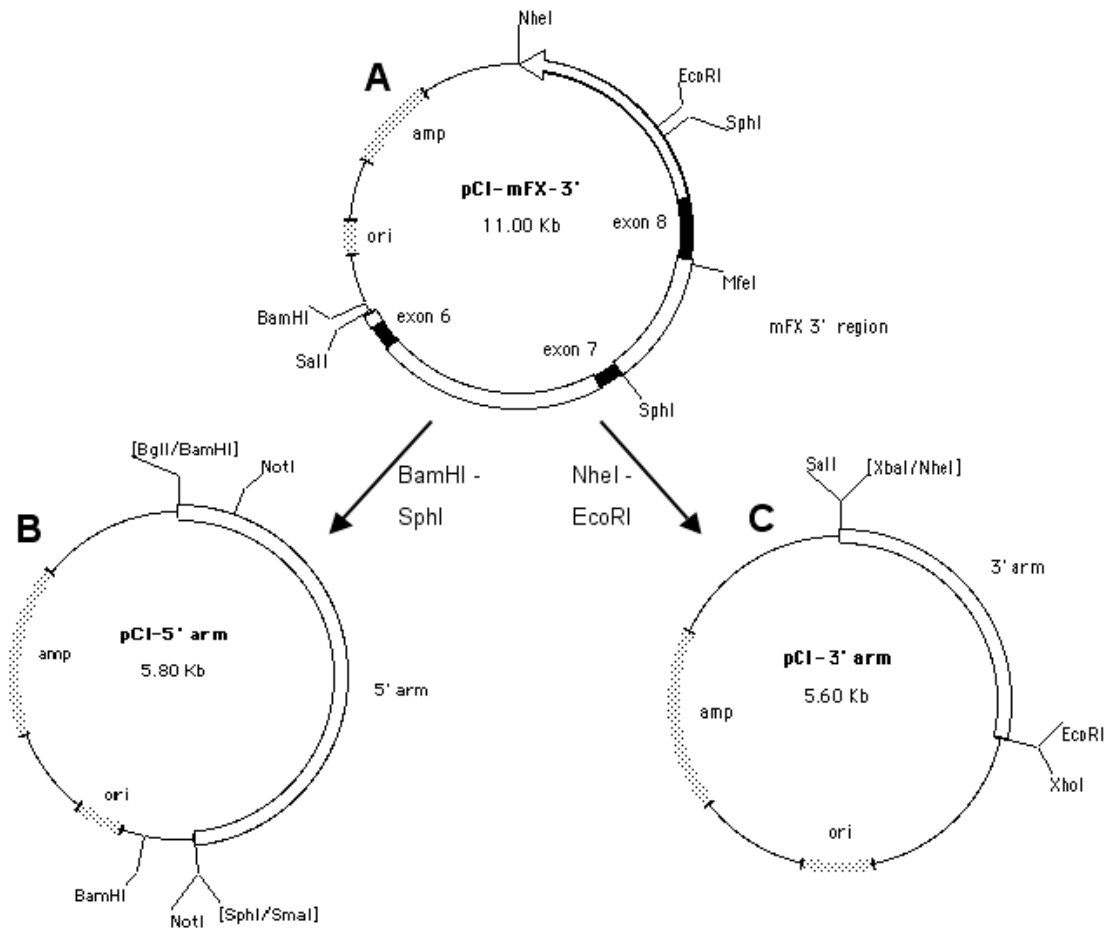


Figure 3. Construction of the 5' and 3' FX targeting arms. Shown in (A) is the pCI-mFX-3' vector containing the 7-kb *NheI* FX insert. Shown in (B) is the pCI-5' arm vector containing the 2.8-kb 5' targeting arm. Shown in (C) is the pCI-3' arm vector containing the 1.6-kb 3' targeting arm.

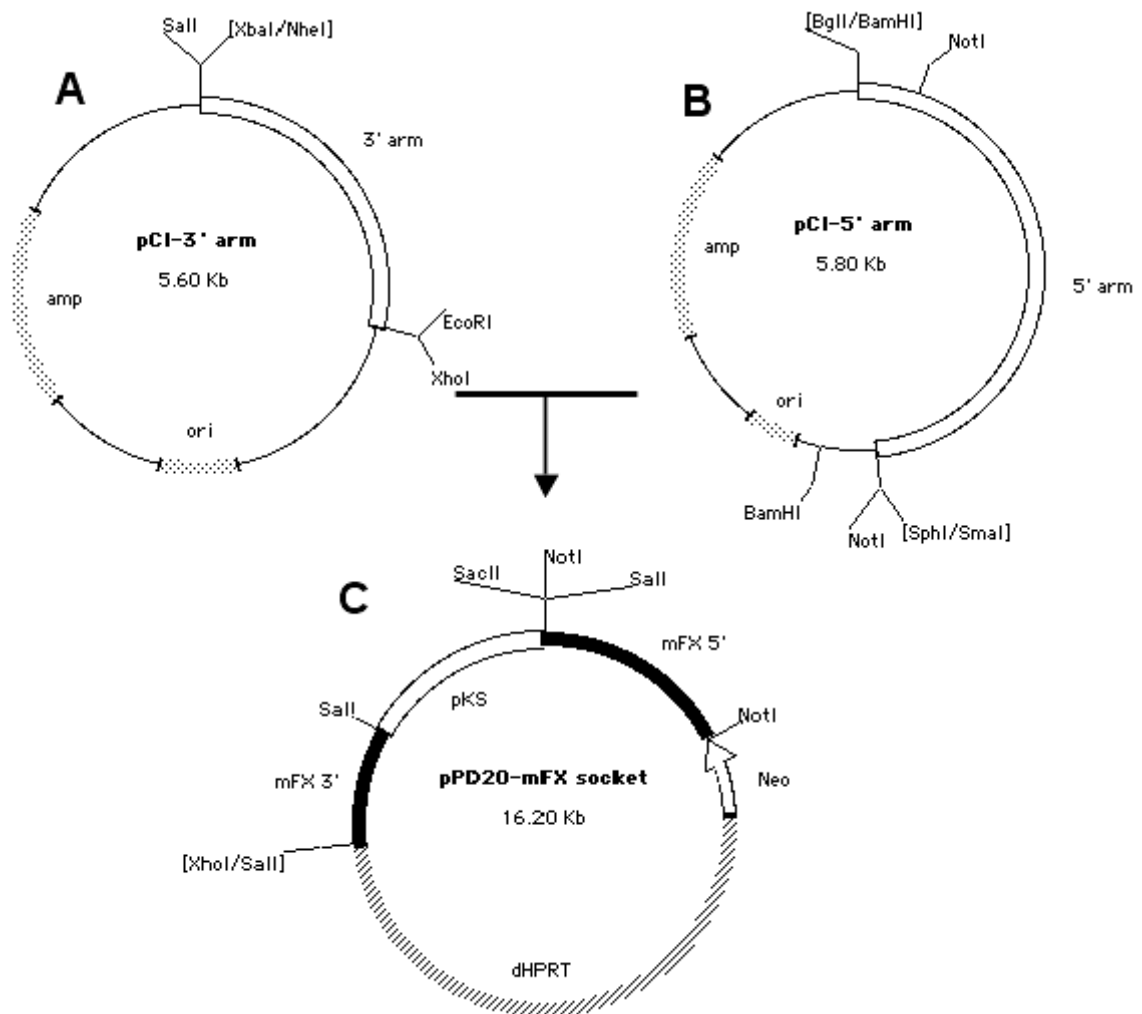


Figure 4. Construction of the FX socket-targeting vector. Shown in (A) is the pCI-3' arm containing the 1.6-kb 3' targeting arm. Shown in (B) is the pCI-5' arm containing the 2.8-kb 5' targeting arm. Shown in (C) is the final FX socket-targeting vector (pPD20-mFX socket) before linearization and electroporation.

2.2.3 Electroporation and selection of Neo-resistant ES cell clones

HPRT-deficient murine ES cells (E14TG2a) were grown on irradiated murine embryonic fibroblast feeder layers (MEFs) in HEPES buffered (10 mM)

Dulbecco's modified Eagle's medium (DMEM), supplemented with 15% fetal calf serum (FCS), 0.1 mM non-essential amino acids, 2 mM L-glutamine, 0.1

mM β -mercaptoethanol, 1000 U/ml leukemia inhibitory factor (LIF), and 50

$\mu\text{g/ml}$ of Gentamycin.⁵⁸ The electroporation of ES cells was performed as follows: the murine E14TG2a cells ($2\text{-}5 \times 10^7$ ES cells) were electroporated (800V, $3\mu\text{F}$) with $100 \mu\text{g}$ of *SacII* linearized FX socket-targeting vector (Figure 4C) for ~ 1 sec at room temperature. Twenty-four hours after electroporation, transfected ES cells seeded on *Neo*-resistant feeder layers were plated in G418 selection medium ($300 \mu\text{g/ml}$). Individual transfected clones that survived the G418 selection for 7-10 days were isolated and expanded in 96-well and 24-well plates to obtain DNA for further analyses by PCR and Southern hybridization before blastocyst injection.

2.2.4 Homologous recombination between the FX socket construct and FX locus

Following homologous recombination between the FX socket construct (Figure 5A) and FX locus (Figure 5B) in the *HPRT*-negative ES cell line (E14TG2a), exon 8 encoding the catalytic domain of the FX protein is deleted and replaced with a functional *Neo* gene and a partially deleted, non-functional 3' *HPRT* sequence (Figure 5C).

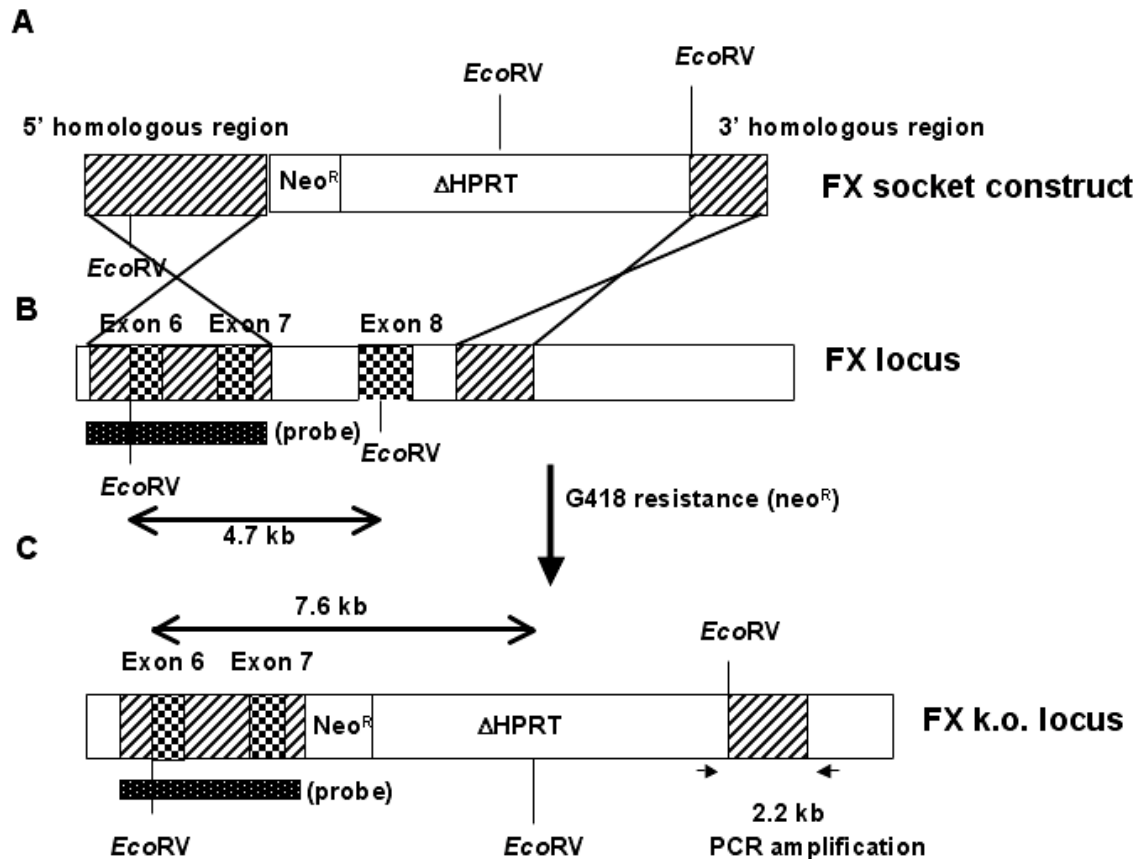


Figure 5. Targeted disruption of FX gene. (A) FX knock-out (socket) construct consists of a 2.8 kb 5' and 1.6 kb 3' homologous regions flanking a functional *Neo* gene and a partially deleted *HPRT* minigene. The relevant *EcoRV* sites are indicated. (B) The 3' end of the wild-type FX locus shows exons 6, 7, and 8, introns and the downstream flanking region. The darkened bar below exons 6 and 7 indicates the position of the probe used in Southern blot analysis. Relevant *EcoRV* sites are also shown. The distance between the two adjacent *EcoRV* sites in the wild-type FX locus is approximately 4.7-kb (C) After homologous recombination between the FX socket construct (A) and FX locus (B), exon 8 is replaced with the *Neo* gene and *HPRT* minigene (C). The resulting distance between the two adjacent *EcoRV* in the FX knock-out locus is now approximately 7.6-kb. The little arrows (under the 3' arm) indicate the location of a primer pair used in PCR analysis. Presence of a 2.2-kb PCR amplification product from the 3' end of the FX knock-out locus indicates correct recombination at the 3' site.

2.2.5 Isolation of ES cell DNA and mouse genomic DNA

To analyze G418-resistant E14TG2a ES cell clones for presence of a FX knock-out allele, DNA was isolated using the Easy DNA Kit (Invitrogen,

Carlsbad, CA). Both quantity and quality of the purified ES cell DNA were adequate for subsequent PCR and Southern blot analyses. For neonates, genomic DNA was isolated from liver tissues of the sacrificed pups using the same kit. For adult mice (4 weeks-old), genomic DNA was extracted from blood samples collected from the retro-orbital plexus into heparin-containing micro-capillaries and subsequently purified using the QIAamp DNA Blood Mini Kit (Qiagen, Valencia, CA).

2.2.6 PCR analysis on ES cell DNA and mouse genomic DNA

To demonstrate correct homologous recombination in E14TG2a cells between the FX locus and the introduced FX socket construct at the 3' targeting arm, two primers as indicated in Figure 5C (a forward primer 5'-CCTTTGGGCGGATTGTTGTT-3' annealing to a sequence at the 3' terminus of Δ HPRT minigene and a reverse primer 5'-CATAAAGCCTTGCCCCGATAGATA-3' annealing to a sequence downstream from the 1.6-kb FX homologous region) were used to PCR-amplify a 2.2-kb fragment from the purified ES cell DNA. Presence of a 2.2-kb PCR amplification product allowed rapid identification of those ES cell clones potentially containing the FX exon 8-deleted allele. This PCR reaction and a second PCR reaction to amplify a 350-bp fragment from exon 8 (previously used to screen the BAC library) were used in separate PCR reactions to differentiate FX(+/+), FX(+/-), and FX(-/-) mice.

2.2.7 Southern blot analysis on ES cell DNA and mouse genomic DNA

DNA from G418-resistant E14TG2a cell clones (identified by PCR to have been correctly targeted by the electroporated FX socket-targeting construct at the 3' homologous region), and DNA obtained from mice of heterozygous FX(+/-) cross were subjected to further analysis by Southern hybridization to ensure correct targeting at the FX 5' homologous region. Both ES cell DNA and mouse genomic DNA were digested with *EcoRV*, separated by electrophoresis on a 0.7% agarose gel, transferred onto Hybond-N+ positively charged nylon membrane (Amersham Life Science, Arlington Heights, IL), fixed by alkali treatment, and hybridized with a [³²P- α]dCTP labeled probe in a standard Southern hybridization. Corresponding to the 5' targeting arm of the FX socket-targeting construct (Figures 5B and C), the probe was radio-labeled by [³²P- α]dCTP in a random primer annealing reaction (Random primer labeling kit, Stratagene, La Jolla, CA) and purified from non-incorporated nucleotides using G-50 Sephadex columns (Roche, Indianapolis, IN).

2.2.8 Generation of FX-deficient mice

The correctly targeted FX(+/-) E14TG2a cell clones were expanded for production of chimeric mice performed by the Transgenic & Chimeric Mouse Facility of the University of Pennsylvania. One correctly targeted and expanded FX(+/-) cell clone was micro-injected into C57/BL6 blastocysts, and implanted into the uterine horns of pseudo-pregnant mice. Chimeric males were mated with wild-type C57/BL6 females to generate heterozygous FX (+/-) offspring, which were intercrossed to obtain homozygous FX(-/-) knock-out mice.

2.2.9 Reverse transcriptase-polymerase chain reaction (RT-PCR) on total RNA isolated from liver tissues

Total RNA was isolated from livers of FX(+/+) and FX(-/-) newborn mice using Trizol reagent (GIBCO/BRL), and reverse transcribed into first-strand cDNA using oligo(dT) primers (SuperScript Preamplification System, GIBCO/BRL). Following the cDNA synthesis, two pairs of primers designed from FX cDNA sequence 5' to exon 8 sequence (first pair: forward 5'-AGCCCGGTGCAACTCAGC-3' and reverse 5'-TTCCCGGCCACCCACAAT-3'; second pair: forward 5'-TGCGCCAGCGGTTACTTC-3' and reverse 5'-TCGCCTGGCCTGATGGA-3') were used in separate PCR reactions to amplify a 705-bp fragment (from exons 1 to 6) and a 390-bp fragment (from exons 5 to 7), respectively. To PCR-amplify FX exon 8 from cDNA, the two primers yielding the 350-bp amplification product (as described above) were used. In a control reaction, two additional primers (forward 5'-CCTTCCTGTGCATGGAGTCCT-3' and reverse 5'-GGAGCAATGATCTTGATCTTC-3') were used to amplify a 202-bp β -actin cDNA sequence.

2.2.10 Northern blot analysis on total RNA

For Northern blot analysis, total RNA (20 μ g) isolated from liver tissues of neonates was electrophoresed on a 1% agarose gel under denaturing conditions (2.2M formaldehyde), transferred onto a Hybond-N+ positively charged nylon membrane, fixed by UV cross-linking, and hybridized with a denatured FX cDNA fragment (705-bp) corresponding to exons 1-6. The 705-

bp FX cDNA fragment was amplified by RT-PCR and labeled with [³²P-α]dCTP as described above. Subsequently, the same blot was stripped and probed with a 202-b β-actin cDNA probe.

2.2.11 Western blot analysis on plasma and extracts isolated from liver tissues

To detect FX protein in circulation, plasma samples were obtained from FX(+/+), FX(+/-), and FX(-/-) neonates and from FX(+/+) and FX(+/-) adult mice. Blood samples from neonates were collected and combined with one-tenth volume of 3.8% sodium citrate in Eppendorf tubes; blood samples from adult mice were drawn into heparin-containing micro-capillaries and transferred into Eppendorf tubes. Collected samples were immediately centrifuged at 9000 rpm for 10 minutes at 4°C to obtain plasma. Furthermore, to show absence of FX protein in liver extracts isolated from FX(-/-) pups, protein samples precipitated from phenol-ethanol supernatants (obtained during isolation of total RNA using GIBCO/BRL reagents) were also analyzed by Western blotting. Both plasma samples (1:20 dilution) and protein samples 10 ng from liver tissues were separated by electrophoresis in 10% SDS/12% Tris-HCL polyacrylamide gels (Bio-Rad, Hercules, CA) under denaturing conditions, and transferred onto Hybond ECL nitrocellulose membranes (Amersham Pharmacia Biotech, Piscataway, NJ). After blocking, FX antigen from plasma was immunodetected with a horseradish-peroxidase conjugated rabbit anti-human FX polyclonal antibody (1:300 dilution) (Cedarlane, Ontario, Canada). FX antigen from protein samples derived from liver extracts was immunodetected

by an affinity-purified sheep anti-human FX polyclonal antibody (1:250 dilution) (Cedarlane, Ontario, Canada), and a horseradish-peroxidase conjugated rabbit anti-sheep immunoglobulin (1:1000 dilution) (Dako, Carpinteria, CA). Both primary antibodies raised against human FX antigen were previously shown to cross-react strongly with mouse FX protein (results not shown). In both cases, FX protein complex was then detected by applying chemiluminescence reagents (Amersham Life Science, Piscataway, NJ).

2.2.12 Activated partial thromboplastin time (aPTT) and prothrombin time (PT) FX assays

Blood collected from neonates and adult mice (4 to 6 weeks-old) was combined with one-tenth volume of 3.8% sodium citrate and centrifuged as described above to obtain plasma for measurement of FX coagulation activities by aPTT (activated partial thromboplastin time) and PT (prothrombin time) assays. To measure FX coagulation activity by aPTT, 50 μ l of plasma sample diluted (1:40) in imidazole buffer (Hedwin, Baltimore, MD) was mixed with 50 μ l of human FX-deficient plasma (Biomerieux, Durham, NC) and 50 μ l of aPTT reagent (Biomerieux); the mixture was incubated at 37° C for 3 minutes before the addition of 50 μ l of 25 mM CaCl₂ to initiate clot formation. To measure FX coagulation activity by PT, 50 μ l of plasma sample diluted (1:80) in imidazole buffer was combined with 50 μ l of human FX-deficient plasma, and incubated at 37° C for 3 minutes before the addition of 100 μ l pre-warmed thromboplastin reagent (Biomerieux). Time elapsed in seconds before each clot formation was determined by a fibrometer (Fibrosystem; BBL, Cockeysville, MD). Specific

dilution for each clotting assay was determined to maximize differences in clotting times between the wild-type and heterozygous plasma. In both clotting assays, standard curves were generated based on values derived from pooled normal mouse plasma.

2.2.13 Timed mating experiment

Timed mating of heterozygous FX(+/-) mice was set up. FX-null embryos along with their wild-type and heterozygous littermates were examined at different time points during development. After gross examination, genotype of each embryo was determined from DNA extracted from the yolk sac.

2.2.14 Immunohistochemical staining for PECAM-1 and ICAM-2

To conduct immunohistochemical staining for PECAM-1 (platelet endothelial cell adhesion molecules) and ICAM-2 (intercellular adhesion molecule-2), E13.5 embryos (FX-null embryos and their wild-type littermates) were harvested, fixed in 4% paraformaldehyde at 4°C overnight, and processed for paraffin-embedded sagittal sections (0.5 µm). Following deparaffinization and rehydration, tissue sections were incubated with 10 µg/ml primary antibody, either rat anti-mouse CD31(PECAM-1) or rat anti-mouse CD102 (ICAM-2) (PharMingen, San Jose, CA). Thereafter, sections were incubated with 5 µg/ml mouse adsorbed, biotinylated rabbit anti-rat IgG (Vector Laboratories, Burlingame, CA). Vectastain ABC-AP kit (Vector laboratories) containing alkaline phosphatase was used to amplify the complex formed between primary and secondary antibodies. Alkaline phosphatase activity on tissue sections was then visualized with addition of Vector Blue (Vector Laboratories). Negative

control included omission of either rat anti-mouse CD31 or rat anti-mouse CD102 in the experimental procedure.

2.3 Results

2.3.1 Construction of the FX socket-targeting vector

With the expectation that a deletion of murine FX would result in lethality, which would then require rescue to produce a viable FX-deficient mouse model, we chose to use the “plug-and-socket” targeting strategy originally described by Detloff and colleagues.⁵⁶ Screening of a 129/SvJ strain mouse genomic DNA library with a 350-bp PCR-amplified mouse FX exon 8-specific probe identified two BAC clones, each containing the 3' portion of the murine FX gene. Further investigation of one isolated BAC clone by restriction enzyme digests, gel electrophoresis, and Southern blotting yielded a 7-kb *NheI* digested fragment, which (by PCR analysis) contained exons 6, 7, and 8, the intervening introns, and the 3' flanking sequence of the murine FX gene (data not shown). Sequencing analysis of the same fragment confirmed PCR results (data not shown). The 7-kb FX fragment with the exclusion of exon 8 and the polyadenylation signal sequence (based on considerations discussed earlier) was used for the construction of the 5' and 3' targeting arms. The final 16.2-kb FX socket-targeting vector was comprised of a 2.8-kb 5' and a 1.6-kb 3' FX homologous sequences flanking a functional *Neo* gene and a partially deleted, non-functional *HPRT* gene ($\Delta HPRT$) (Figures 4C and 5A). The 2.8-kb 5' targeting arm contained exon 6, intron 6, exon 7, and part of intron 7 and the

1.6-kb 3' targeting arm contained genomic sequence downstream of the FX stop codon and its overlapping polyadenylation signal sequence.

2.3.2 Targeted disruption of FX exon 8

FX socket construct designed to delete exon 8 and its 3' flanking sequence was electroporated into HPRT-deficient murine ES cells (E14TG2a) as described above. Homologous recombination between FX locus (Figure 5B) and the FX knock-out vector (Figure 5A) resulted in targeted disruption of the FX gene by replacing exon 8 encoding the catalytic domain of the serine protease with a *Neo* and Δ *HPRT* cassette (Figure 5C). This disruption effectively inactivates FX function by completely abolishing the catalytic activity of the protein. Following transfection and selection in G418 medium, 192 G418-resistant ES clones were isolated and analyzed for correct targeting by PCR.

2.3.3 PCR results

To identify correctly targeted *Neo*-resistant ES clones, DNA was first analyzed by PCR using two specific primers as indicated in Figure 5C. In this PCR analysis, DNA from the correctly targeted ES clones yielded a 2.2-kb PCR amplification product from the 3' end of the FX-disrupted locus (Figure 6, *lanes 1, 6 and 7*), whereas DNA isolated from incorrectly targeted *Neo*-selected ES clones failed to show a PCR product of any length (Figure 6, *lanes 2, 3, 4, 5, 8 and 9*). Among the 192 G418-resistant ES clones analyzed by PCR, 8 individual clones demonstrated successful targeting at the 3' homologous region. This PCR reaction using the primer pair indicated in Figure 5C and a second PCR reaction using a primer pair to amplify the 350-bp exon 8 fragment

were carried out to genotype offspring resulting from heterozygous FX(+/-) intercross. Figure 7 shows the PCR results from the three expected genotypes. While the 350-bp PCR fragment from exon 8 is shown in the wild-type and heterozygous samples (Figure 7, *lanes 2, 4, 6, and 8*), it is absent in the FX knock-out samples (Figure 7, *lanes 10 and 12*). Likewise, the 2.2-kb PCR product amplified from the 3' end of the FX knock-out locus is present in the heterozygous and FX knock-out samples (Figure 7, *lanes 5, 7, 9 and 11*), and absent in the wild-type samples (Figure 7, *lanes 1 and 3*).

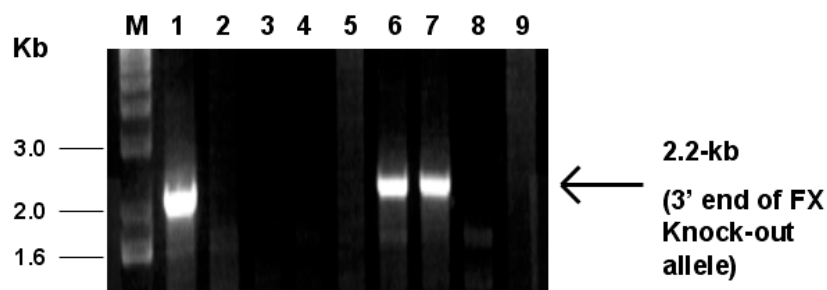


Figure 6. PCR analysis of ES cell DNA. ES cell clones correctly targeted at the 3' recombination site were identified by presence of a 2.2-kb PCR product (*lanes 1, 6 and 7*). Incorrectly targeted ES cell clones did not yield any PCR product (*lanes 2, 3, 4, 5, 8 and 9*) with the primer pair indicated in Figure 5C.

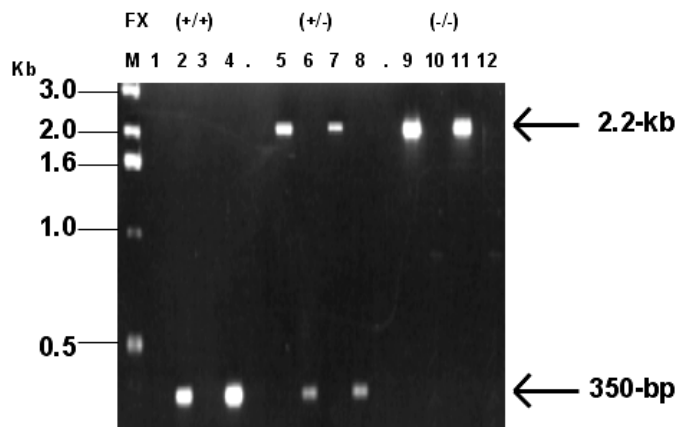


Figure 7. PCR analysis of mouse genomic DNA. Shown are PCR amplification products of the three genotypes from heterozygous FX(+/-) intercross. A 350-bp PCR fragment from exon 8 is present in the wild-type and heterozygous samples (*lanes 2, 4, 6 and 8*) and absent in the knock-out samples (*lanes 10 and 12*). Conversely, a 2.2-kb PCR product is present in the heterozygous and knock-out samples (*lanes 5, 7, 9 and 11*) and absent in the wild-type samples (*lanes 1 and 3*).

2.3.4 Southern blot results

To ensure correct targeting at the 5' recombination site, *EcoRV* digested DNA (from 8 PCR positive out of 192 ES clones analyzed) was hybridized with a 2.8-kb FX probe, corresponding to the 5' targeting arm (Figures 5B and C). *EcoRV* digested genomic DNA (from blood cells of mice) was also hybridized the 2.8-kb FX probe. Regardless of its origin (ES cells or blood cells), wild-type DNA uniformly showed a 4.7-kb fragment (Figure 8, *control lane*); heterozygous DNA yielded a 4.7-kb fragment and an additional 7.6-kb fragment (Figure 8, *lanes 1-8* and Figure 9, *lane 1*); homozygous FX knock-out DNA showed exclusively the 7.6-kb fragment (Figure 9, *lanes 2 and 3*). These results are consistent with the design of the FX socket vector; the FX knock-out locus (when digested with *EcoRV* and hybridized with the 2.8-kb probe) yielded a

fragment 2.9-kb longer than that produced by the wild-type locus in the same Southern blot analysis.

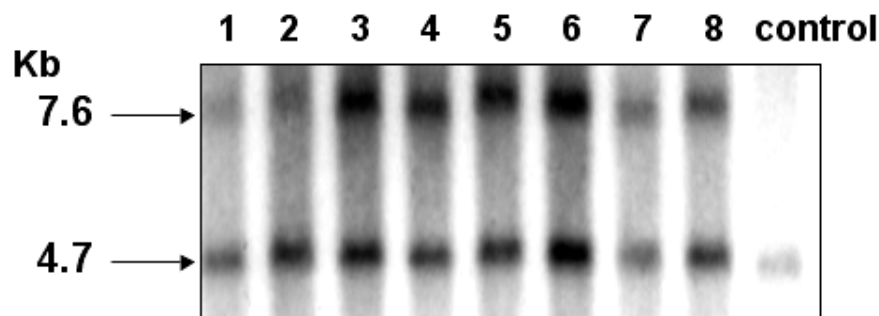


Figure 8. Southern blot analysis of ES cell DNA. Eight correctly targeted ES clones identified by PCR analysis were also confirmed by Southern hybridization using a 2.8-kb FX probe (Figures 5B and C). As predicted, *EcoRV* digested FX knock-out locus yielded a fragment 2.9-kb longer than that produced by the *EcoRV* digested FX wild-type locus. DNA samples from the eight correctly targeted ES clones contain a 4.7-kb wild-type fragment and a 7.6-kb knock-out fragment (*lanes 1-8*). The *control lane* containing DNA sample from a wild-type ES clone shows only the 4.7-kb wild-type band.

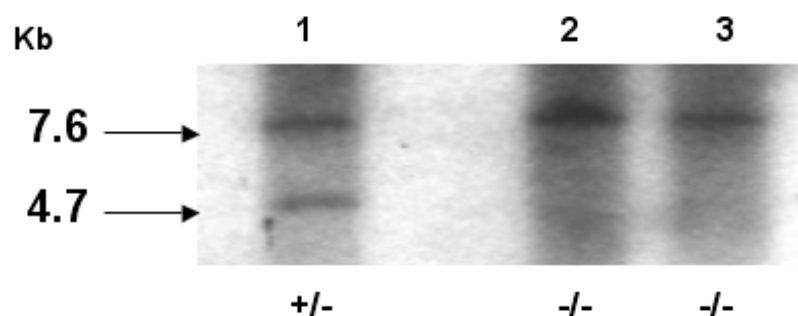


Figure 9. Southern blot analysis of genomic DNA. Genomic DNA isolated from blood cells of mice was digested with *EcoRV* and hybridized with a 2.8-kb FX probe (Figures 5B and C). Shown here is a Southern blot analysis of DNA from heterozygous FX(+/-) and FX(-/-) mice. As expected, DNA from heterozygous mice yielded a 4.7-kb wild-type fragment and an additional 7.6-kb knock-out fragment (*lane 1*), whereas DNA from FX knock-out mice showed only the 7.6-kb band (*lanes 2 and 3*).

2.3.5 Targeting frequency

Of the 192 G418-resistant ES clones isolated and analyzed by PCR, 8 were correctly targeted, showing a 2.2-kb PCR amplification product from the 3' end of the FX knock-out locus (Figure 6). Subsequently, Southern blot analysis of all 8 PCR-positive ES clones confirmed correct targeting at the 5' recombination site (Figure 8). Therefore, the overall targeting frequency achieved by the FX socket vector in E14TG2a cells was 4% (8/192).

2.3.6 Production of FX knock-out mice

Heterozygous FX(+/-) ES clones were expanded, and one expanded clone was micro-injected into C57/BL6 blastocysts for implantation into the uterine horns of pseudo-pregnant mice. Two weeks after the procedure, fifteen animals were born and seven showed chimerism by their coat color ranging from 75% to 100%. All chimeric males were mated with wild-type C57/BL6 females; 2 were fertile and gave rise to F1 offspring. PCR and Southern blot analyses of DNA obtained from F1 progeny revealed germline transmission of the FX knock-out allele from the chimeric fathers (results not shown). Furthermore, 50% of the F1 offspring were heterozygous for the FX-disrupted allele. Taken together, these results showed not only germline transmission, but also autosomal inheritance of the affected allele. Following their identification, heterozygous FX(+/-) mice were intercrossed to obtain homozygous FX(-/-) offspring for characterization of the phenotype induced by complete FX deficiency.

2.3.7 Phenotypic characterization of FX knock-out neonates

While no phenotypic difference was observed between FX(+/+) and FX(+/-) neonates, 26 homozygous FX(-/-) neonates examined were readily distinguished from their normal littermates by rapid development of an overall pale appearance shortly after birth. A closer inspection of FX-null pups revealed an obvious accumulation of blood in the abdominal cavity (Figure 10). The majority of homozygous FX(-/-) neonates (23 out of 26) developed severe intra-abdominal hemorrhage within hours of birth and died within 24 hours after delivery (Figure 11). In the absence of a more commonly observed intra-abdominal hemorrhage, 3 FX knock-out pups from 3 different litters instead manifested subcutaneous bleeding mostly over the head, back, neck area, and the limbs (Figure 12). Those few were able to survive for 2-4 days (Figure 11). Interestingly, FX-null pups were indistinguishable from their normal littermates at birth. Only after development of a hemorrhagic phenotype within a few hours of birth, were they readily identified by their pale appearance. By gross examination, FX knock-out mice appeared normal, showing no obvious signs of anatomical defects that would prevent post-natal survival.

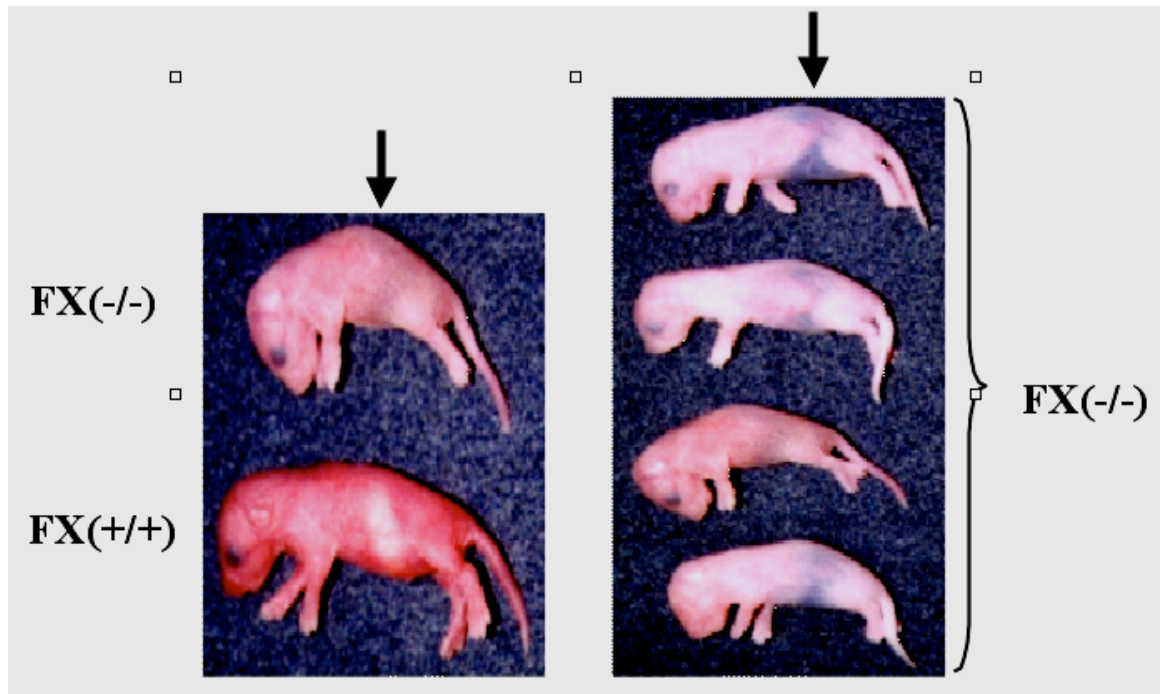


Figure 10. Phenotypic comparison of FX(+/+) and FX(-/-) neonates. The majority of FX knock-out pups developed severe intra-abdominal hemorrhage (arrows) and succumbed within 24 hours of birth.

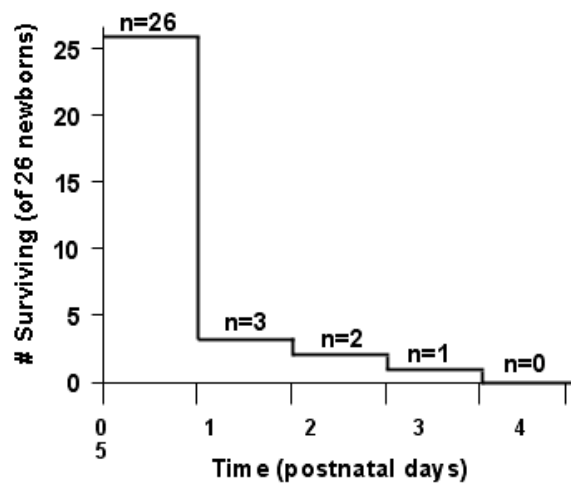


Figure 11. Kaplan-Meier survival curve of homozygous FX knock-out mice. 23/26 mice died within 24 hrs of birth and the remaining 3 suffering from subcutaneous bleeding also succumbed within the next three days.



Figure 12. Subcutaneous bleeding in a FX(-/-) mouse. As shown here, few FX knock-out mice showed subcutaneous bleeding mostly over the head, back, neck area, and the limbs.

2.3.8 Genotype analysis of the offspring from heterozygous FX(+/-) intercross

DNA analysis of the full-term offspring (n=213) resulting from mating of heterozygous FX (+/-) mice identified 76 (36%) FX (+/+), 111 (52%) FX (+/-), and 26 (12%) FX(-/-) (Table 2). Representation by the FX(-/-) mice (12%) was significantly smaller ($p < 0.001$) than the expected percentage (25%) derived from the Mendelian law of an autosomal inheritance. These results suggested that some FX knock-out mice might have suffered embryonic lethality.

Table 2. Genotype distribution among offspring from heterozygous FX(+/-) intercross.

	+/+	+/-	-/-	n	p
Full-term	76 (36%)	111 (52%)	26 (12%)	213	< 0.001

2.3.9 Evaluation of embryonic lethality and phenotype of FX knock-out mice

To verify intrauterine lethality, FX-null embryos from mating of heterozygous FX(+/-) mice were examined at various time points during development (Table 3). It was noted that as early as E10.5, viable FX(-/-) embryos accounted for only 14% of the total progeny (n=84) (Table 3). Data were similar at E11.5 (Table 3) with FX-null embryos also representing 14% ($p < 0.05$) of the total progeny (n=104). In the later stages of development, there was little change in the survival of FX(-/-) embryos, leading to FX knock-out mice representing 12% of the offspring (n=213) at birth or approximately 50% of the expected number of FX-null mice (Tables 2 and 3). Interestingly, at various stages of development, viable FX knock-out embryos were indistinguishable by gross examination from their wild-type and heterozygous littermates. Furthermore, no evidence of obvious bleeding was found with either viable or reabsorbed FX knock-out embryos at various developmental stages. For those FX knock-out mice that survived to term, 23 out of 26 died within 24 hours from intra-abdominal hemorrhage, and the remaining 3 suffered from fatal subcutaneous bleeding within four days of birth (Figure 11).

Table 3. Genotype distribution among offspring of heterozygous FX(+/-) parents

	+/+	+/-	-/-	n	p
E10.5	22 (26%)	50 (60%)	12 (14%)	84	< 0.1
E11.5	34 (33%)	55 (53%)	15 (14%)	104	< 0.05
E14.5	11 (32%)	18 (53%)	5 (15%)	34	> 0.2
E16.5 or older	21 (34%)	33 (54%)	7 (11%)	61	< 0.05
Full-term	76 (36%)	111 (52%)	26 (12%)	213	< 0.001

2.3.10 Detection of a partial transcript in FX knock-out mice

Since exon 8 was the only coding sequence eliminated in the design of the FX socket-targeting vector (Figure 5A), one might expect the presence of a partial transcript in FX-null mice. This expectation was confirmed by the results of RT-PCR (Figure 13): two pairs of upstream primers (all 5' to exon 8 sequence) yielded a 705-bp fragment (from exons 1 to 6) and a 390-bp fragment (from exons 5 to 7) for both wild-type and FX knock-out samples (Figure 13, *lanes 1-4*). However, when amplified with exon 8-specific primers, only the wild-type sample and not the knock-out sample gave rise to the expected 350-bp PCR product (Figure 13, *lanes 5 and 6*). Regardless of the genotype, the control primers yielded a 202-bp β -actin PCR product in all samples (Figure 13, *lanes 7 and 8*). Thus, consistent with the overall design of the FX socket vector, RT-PCR results revealed a partial transcript in FX knock-out mice.

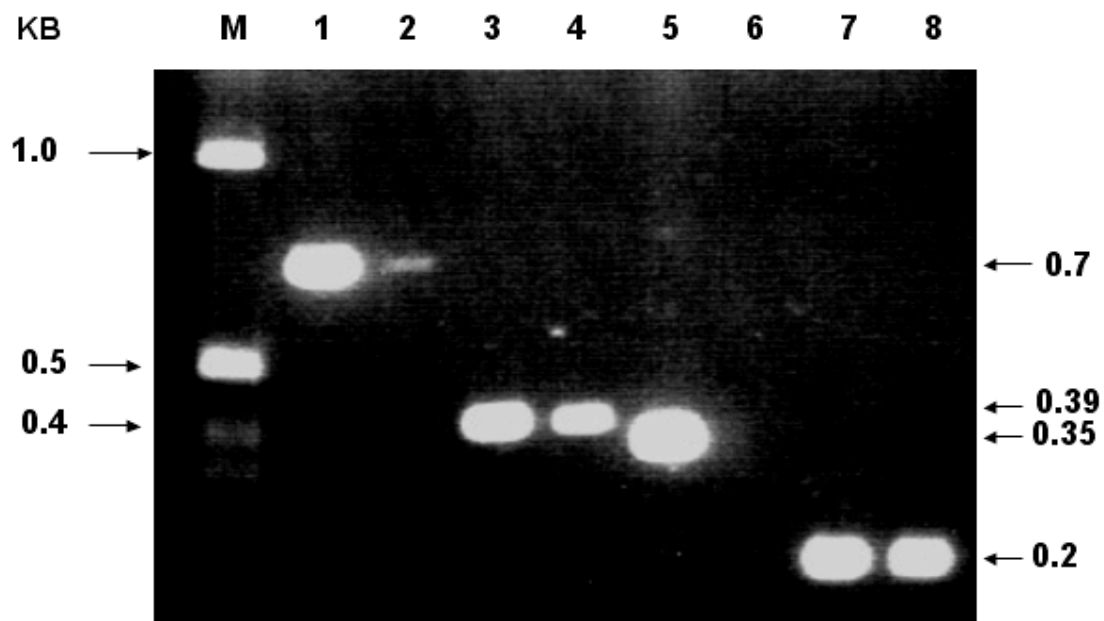


Figure 13. RT-PCR analysis of FX transcript from FX(+/+) and FX(-/-) neonates. The odd-numbered *lanes* contain RT-PCR products from a FX(+/+) neonate and the even-numbered *lanes* contain RT-PCR products from a FX(-/-) pup. In *lanes 1-4*, RT-PCR products were amplified, using two pairs of primers specific for sequences 5' to the deleted exon 8 sequence. In *lanes 5 and 6*, RT-PCR product was amplified, using FX exon 8 specific primers. Note the absence of an amplification product in *lane 6* containing sample from the FX knock-out pup. *Lanes 7 and 8* show RT-PCR products for the beta-actin transcript.

Northern blot analysis on total RNA extracted from liver revealed an expected 1.4-kb FX transcript in wild-type neonates, the same signal of less intensity in heterozygous mice, and absence of this signal in the homozygous FX knock-out mice (Figure 14). Instead, a faintly discernible 2-kb transcript was noted in the total RNA of the homozygous FX(-/-) neonates (Figure 14). The low signal of the 2-kb band is likely due to the targeted replacement and thus absence of the putative FX polyadenylation signal sequence (ATTAAA) in the knock-out allele. The authenticity of the weak 2-kb signal from the targeted allele is supported by its presence in RNA from heterozygous mice and its

absence in RNA from wild-type samples. The amount and quality of the RNA samples analyzed on Northern blot were similar based on the signal intensities of a 1.9-kb β -actin control (results not shown).

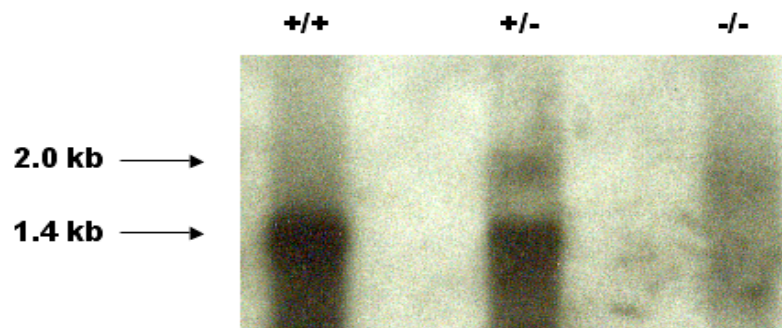


Figure 14. Northern blot analysis of total RNA from FX(+/+) , FX(+/-) and FX(-/-) livers. While an expected 1.4-kb FX transcript was detected in wild-type and heterozygous samples, it was clearly absent in the knock-out sample. Instead, a faintly discernible 2-kb signal was noted in the knock-out sample; Authenticity of the signal is supported by its presence in an heterozygous sample and its absence in a wild-type sample.

2.3.11 Absence of FX antigen in FX(-/-) neonates

To determine whether a protein was synthesized from the partial FX transcript, Western blot analysis was performed on plasma from wild-type, heterozygous, and homozygous FX knock-out mice. All primary antibodies used in Western blot analysis were previously tested and shown to cross-react with a 54-kDa signal corresponding to the mouse FX protein (results not shown). Despite detection of low levels of a partial transcript in FX knock-out pups, the 54-kDa mouse FX protein present in both wild-type and heterozygous mice is clearly absent in the knock-out newborn mice (Figure 15). Consistent with the

genotypes of mice, the noted 54-kDa band intensity is respectively reduced in the heterozygotes compared to wild-type for both adult and newborn mice (Figure 15). This result suggests that, if a protein is synthesized at all from the partial FX transcript, it is either unstable or not secreted into the circulation. To address the question of whether a protein is synthesized but not secreted, cell lysates were prepared from liver tissue of FX(+/+), FX(+/-), and FX(-/-) neonates and analyzed on a Western blot; this analysis again failed to disclose a FX signal in the FX(-/-) samples (Figure 16). Low levels of a partial transcript (Figures 13 and 14) and the absence of a detectable protein in FX-null mice (Figures 15 and 16) confer generation of a mouse model with complete lack of FX.

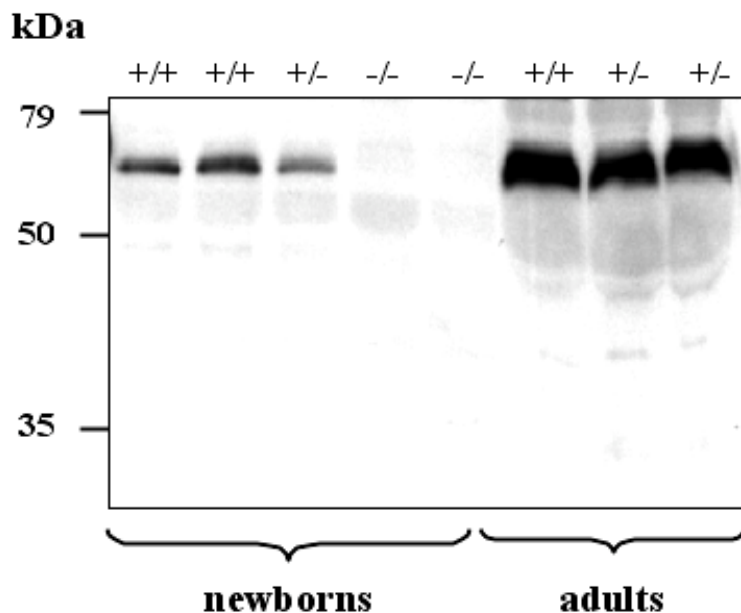


Figure 15. Western blot analysis of plasma from FX(+/+), FX(+/-) and FX(-/-) mice. Note the absence of a 54-kDa mouse FX protein in plasma of FX (-/-) newborn mice. This signal was readily detected in plasma of wild-type and heterozygous newborn and adult mice (FX knock-out mice did not survive into adulthood).

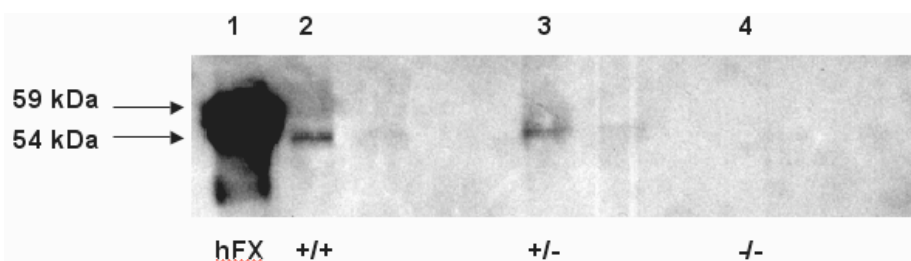


Figure 16. Western blot analysis of cell lysates from FX(+/+), FX(+/-) and FX(-/-) livers. A 54-kDa mouse FX protein is readily observed in the liver cell lysates of wild-type and heterozygous mice (*lanes 2 and 3*); this signal is absent in the sample from a FX knock-out mouse (*lane 4*). A 59-kDa human FX protein (Haematologic Technologies Inc.) is shown as positive control for this analysis (*lane 1*).

2.3.12 Coagulation activities of plasma from FX(-/-) newborn mice

In an aPTT-based assay, plasma from FX(+/+) and FX(+/-) neonates did not yield averaged clotting times statistically different from each other (Table 4) or from that of pooled normal mouse plasma (data not shown), while plasma from FX(-/-) pups revealed significantly reduced coagulation activities as demonstrated by a two-fold increase in averaged clotting time when compared to that of wild-type plasma (Table 4). Likewise, a PT-based assay revealed lack of a remarkable difference in averaged clotting times between wild-type and heterozygous plasma, but demonstrated complete failure of homozygous FX knock-out plasma to form a fibrin clot; no clot formation was detected within a reasonable length of time (Table 4).

Table 4. Coagulation times in seconds of FX(+/+), FX(+/-), and FX(-/-) newborn plasma. (aPTT=1:40 dilution; PT=1:80 dilution)

FX allele	+/+	+/-	-/-
aPTT (sec)	54.5±7.5	61.9±9.3	107.7±15.8
n	19	31	6
PT (sec)	99.4±15.9	140±22	>225
n	10	16	7

2.3.13 Immuno-staining of E13.5 embryo sections for PECAM-1 and ICAM-2

PECAM-1 is expressed on endothelial cells and mediates cell-to-cell interactions in angiogenesis.^{59,60} ICAM-2 is a cell surface glycoprotein that is expressed on endothelial cells, T cells, and B cells.^{61,62} Paraffin-embedded sections from E13.5 wild-type and FX knock-out embryos were immuno-stained for the two endothelial cell-associated markers, PECAM-1 and ICAM-2 (Figure 17). For both markers, no obvious difference in the staining pattern was observed between the FX knock-out and wild-type embryos at this stage of development.

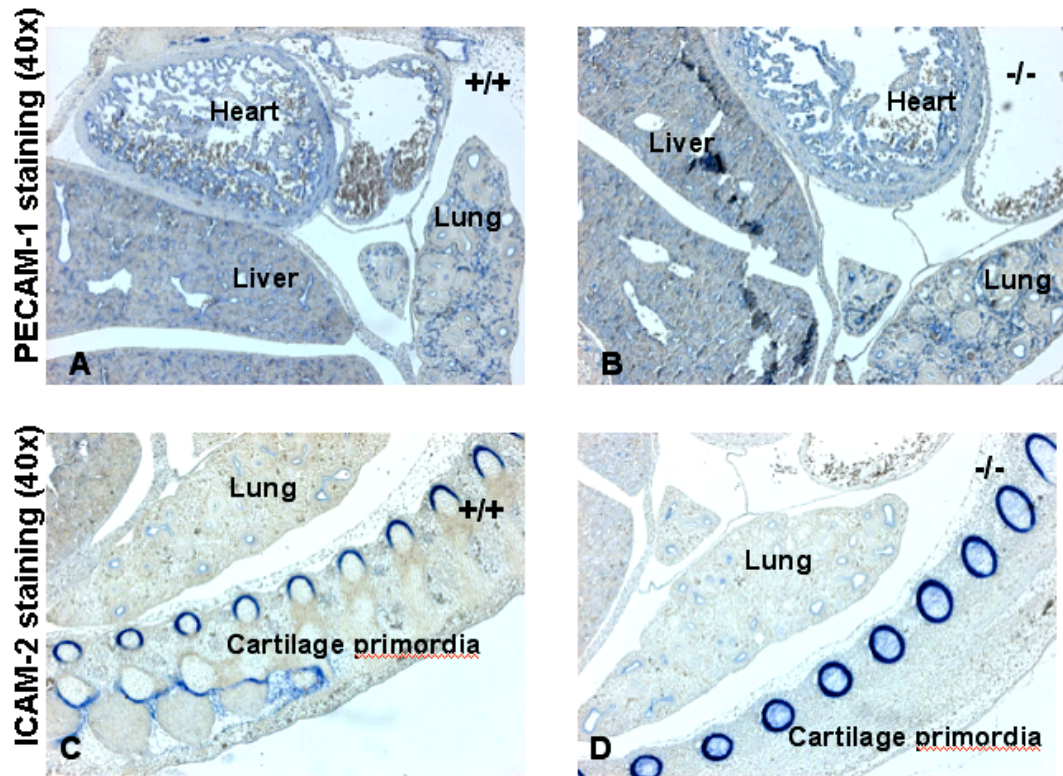


Figure 17. Immunostaining of E13.5 embryo sections for PECAM-1 and ICAM-2. The upper panels show PECAM-1 staining of paraffin-embedded sections from a wild-type (A) and a FX knock-out embryo (B). The lower panels show ICAM-2 staining of paraffin-embedded sections from a wild-type (C) and a FX knock-out embryo (D). For both markers, no remarkable difference in the staining pattern was noted between E13.5 wild-type and FX knock-out embryos.

2.4 Discussion

Despite a more selective deletion (deletion of exon 8 only), FX knock-out mice generated in this study showed a phenotype similar to that of a previously reported FX knock-out mouse model, in which exons 2 to 8 had been eliminated.⁶³ Similar to the other model, our model of complete FX deficiency resulted in embryonic lethality in approximately 50% of FX-null mice and fatal perinatal bleeding in the remaining half that survived to term, although the proportion of FX-null mice at birth, and the length of postnatal survival were not

identical in the two models. These minor variations might be attributed to different strains of ES cells and mice used to generate the two mouse models. Whereas the other model was generated on 50/50 R1 129/Swiss mixed genetic background,⁶³ our model was engineered on E14TG2a (derived from 129/Ola Hsd), C57/BL6, and SvJ 129 mixed genetic background. Although both models of complete FX deficiency result in similar phenotypes, use of the plug-and-socket targeting strategy here readily facilitates rescue of FX-null mice.

The data presented here show that approximately half of the expected numbers of FX-null mice were accounted for at birth (Table 2), and 100% of these FX-null mice died within four days of birth; the majority of these mice (~90%) succumbed within 24 hours of birth from intra-abdominal hemorrhage (Figure 11). Among the 26 FX-null mice examined, 3 manifested subcutaneous bleeding and survived up to 4 days following birth. With the exception of the bleeding diathesis described above, FX-null mice appeared otherwise normal by gross examination. No phenotypic differences were noted between wild-type and heterozygous FX mice.

Approximately 50% of FX knock-out mice suffered embryonic death. Timed mating of heterozygous FX(+/-) mice and analysis of their offspring disclosed that as early as E11.5 (Table 3), viable FX-null embryos were significantly under-represented, accounting for 14% rather than the expected 25% of the total progeny ($p < 0.05$). Presumably, death of FX knock-out embryos had occurred earlier at E10.5 or before. Thereafter, there was little change in the survival of FX(-/-) embryos, with FX knock-out mice representing

12% of the offspring at birth. These findings are consistent with data presented in the other study, in which it was shown that 17% and 15% of the progeny were respectively viable FX-null embryos at E12.5 and FX knock-out mice at birth.⁶³ Thus, this investigation together with the other report helps to define a critical period in development (~E10.5 to E12.5), in which FX plays an important yet elusive role in embryonic survival.

While perinatal lethality of FX knock-out mice is thought to be due to defective hemostasis (i.e. failure in thrombin generation), the underlying cause of embryonic lethality occurring in the absence of obvious evidence of bleeding remains to be investigated. Although several hypotheses have been offered to explain the cause(s) of embryonic lethality observed for deficiencies in a number of hemostatic components, no definitive data have been provided. The complex nature of the observed phenomenon can be better understood with consideration of the following example in FX deficiency. On the one hand, one can conjecture that the failure of FX knock-out mice to generate thrombin is embryonically lethal since it impairs not only platelet activation, but also soluble fibrin clot formation. If true, this would reasonably explain why mice lacking either FV (recall that FXa and FVa work in concert to generate thrombin) or prothrombin (FII) (prothrombin is the catalytically inactive zymogen of thrombin) showed a parallel pattern of embryonic loss, whereas mice deficient in fibrinogen completed embryonic development and were born at the expected Mendelian frequency, presumably because these mice still had catalytically active thrombin that is able to achieve minimal platelet activation.^{6,10-12} On the

other hand, consideration of additional evidence and observation brings into question this explanation for embryonic death in FX knock-out mice. Upon examination, neither viable nor reabsorbed FX knock-out embryos showed evidence of bleeding (this observation was based on inspection of embryos at various stages of development). Specifically, absence of obvious bleeding in FX knock-out embryos harvested from a critically defined period of development (~E10.5 to E12.5) makes hemorrhage unlikely as the deciding cause of embryonic lethality. The timing of intrauterine lethality (E10.5 to E11.5) in FX-knockout mice also challenges defective hemostasis as the underlying cause since the liver organ is just forming at E10.5, and for this reason, there is likely little generation of catalytically active thrombin in E10-11 day embryos. Furthermore, FX protein synthesized between E10.5 and E11.5 is unlikely to have activity in thrombin generation due to the absence of a functional γ -glutamylcarboxylase enzyme system. Essential for the activity of all vitamin-K dependent coagulation factors including FX, this enzyme is not expected to be fully functional until later stage of mouse development as it is not expressed until E16.5 in rat liver (rat gestation = 22 days; mouse gestation = 19 days).⁶⁴ Finally, absence of intrauterine lethality in mice lacking FVII, a crucial factor in the initiation of blood coagulation, would also challenge defective hemostasis as the underlying cause of embryonic loss.¹ As a matter of fact, suggestions of an additional non-hemostatic role during development have already been made for several hemostatic components including FV, FII, TF, TM, and TFPI.¹⁰⁻¹⁷ Taken together, these observations suggest that embryonic lethality of FX-null

mice might be attributed, not to its impaired coagulation, but rather to a biological function of FX that is yet to be defined.

Still the observation of incomplete or partial block to embryonic survival cannot be readily reconciled by suggestion of a non-hemostatic or developmental role for some hemostasis-related factors including FX. Seemingly, the embryonic requirement for FX is not absolute, since approximately half of FX knock-out mice developed to term (although they all succumbed to fatal hemorrhage within a few days of birth). Conversely, it may be that the embryonic need for FX is indispensable, and developmental success of some FX knock-out embryos may be attributed to variable maternal transfer of FX, sufficient to support embryonic survival of some but not all FX-null embryos. Whether the partial embryonic lethality of FX-deficient mice is due to lack of an absolute requirement for FX or due to variable maternal transfer of indispensable FX remains to be deciphered.

3. Generation and characterization of FX knock-in mice

3.1 Introduction

As shown in the previous chapter, our mouse model of complete FX deficiency resulted in partial embryonic lethality and fatal perinatal bleeding. Namely, approximately 50% of the expected numbers of FX-null mice died during development with the remaining half progressing to term to succumb to fatal bleeding within a few days of birth. This finding in a mouse model of complete FX deficiency is consistent with the absence of humans homozygous for deletions in the FX gene. Furthermore, these results affirm the importance of FX in supporting both embryonic and postnatal survival.

Early mortality of FX knock-out mice precludes their use as a viable model of severe FX deficiency. Rescue of these mice would afford a myriad of analyses that are otherwise unfeasible. Generation of a viable mouse model of severe FX deficiency would provide unique opportunities 1) to decipher specific characteristics of a FX variant that are able to rescue either just the embryonic lethality or both embryonic and perinatal lethality, since the underlying cause of embryonic lethality may not be due to failure in thrombin generation, believed to be the cause of perinatal lethality; 2) to characterize specific phenotypes (morphological and pathological conditions) associated with expression of a specific FX variant; and 3) to examine the contribution of maternal FX during development. First, female mice rescued with minimal levels of FX activity can be utilized in a breeding experiment to generate offspring with even lower levels of FX activity. Second, these mice with further reduced FX activity can then be

assessed for their viability and furthermore be used to investigate any evidence for contribution of maternal FX to embryonic survival.

That being said, how can FX knock-out mice suffering from embryonic and perinatal lethality be rescued for further studies? Is full catalytic activity of FX required for rescue? Will FX-deficient mice overcome both embryonic and postnatal challenges with restoration of minimal levels of catalytically active FX? Conversely, can a catalytically inactive FX molecule created by elimination of a functional active site support embryonic development, even though full-term mice with such a severe molecular defect are expected to succumb to fatal hemorrhage due to their inability to generate thrombin? Nonetheless, the goal here is not to define the minimal characteristics of FX protein required for rescue (which is not feasible with study of a single FX variant), but to rescue FX knock-out mice from lethality and reveal those characteristics of a variant that are able to achieve rescue.

Recall exon 8 encoding the catalytic domain of the protein was the only coding region of the FX gene that was deleted in the design of the socket construct used to generate the FX knock-out mice. Hence, to re-establish any minimal levels of FX catalytic activity or FX antigen (FX knock-out mice generated here do not have any FX activity or antigen), exon 8 with a desired mutation must be restored in the previously knock-out FX locus, using an appropriately designed plug construct. As described earlier, this rescue of the FX locus is made convenient with the use of a plug-and-socket targeting strategy.

While no homozygous deletions of the FX gene in humans have ever been reported (this observation is reaffirmed by the lethal phenotype of FX knock-out mice), mutations in exon 8 alone (mostly missense mutations) account for more than 50% of all mutations described for the FX gene. This finding is not statistically surprising, considering that exon 8 is the largest exon in the FX gene. With respect to the rescue experiment presented here, only mutations found in exon 8 of the FX gene are relevant for consideration. For the purpose of illustration, Table 5 provides a small list of naturally occurring human FX variants with specific mutations in exon 8, their corresponding levels of FX activity and antigen, and their respective clinical phenotypes. Factor X mutations can be readily found on http://www.med.unc.edu/isth/mutations-databases/Factor_X.htm.

Table 5. A list of some naturally occurring human FX variants with mutations in exon 8.

Variant	Mutation	Codon	Exon	FX:C (%)	FX:Ag (%)	Clinical phenotype	Reference
Stuart	Val²⁹⁸→Met	GTG→ATG	8	<1	<1	Severe bleeding tendency	Denson (1969)
Marseille	Ser³³⁴→Pro	TCC →CCC	8	21-26	100	Asymptomatic	Bezeaud (1995)
Friuli	Pro³⁴³→Ser	CCC →TCC	8	4-9	100	Epistaxis, bleeding from gums	James (1991)
Unnamed	Thr³⁵⁸→Met	ACG →ATG	8	3	ND	Not reported	Odom, (1994)
Nottingham	Ala⁴⁰⁴→Thr	GCC→ACC	8	1	110	Menorrhagia	Deam (2001)

It is important to note that mouse and human FX proteins are over 70% similar in their amino acid sequences (with the highest conservation observed in the amino acid sequence for the catalytic domain).²⁶ Furthermore, exon 8 mutations shown in Table 5 occur at particular residues that are conserved for blood coagulation FX among several species, suggesting that an analogous mutation, when introduced into the mouse FX gene, will encode a FX variant that is likely to exhibit structural and functional characteristics similar to those described previously for the respective human FX mutation. However, with no knowledge of whether minimal FX catalytic activity or FX antigen (e.g. FX molecule that lacks any catalytic activity) is required to achieve minimally the embryonic rescue of FX-knockout mice, selection of a FX variant with normal antigen levels and reasonable levels of FX catalytic activity seems appropriate to attempt rescue of FX knock-out mice. For these reasons, a specific human FX variant (FX Friuli) with a mutation in exon 8 was selected to attempt rescue of FX-knockout mice. As indicated in Table 5, FX Friuli resulting from substitution of Serine (TCC) for Proline (CCC) at amino acid 343 shows 4-9% FX activity and normal antigen levels in humans.⁶⁵

First identified in a population of patients in the Friuli region of Italy, FX Friuli is associated with a homozygous point mutation (C to T transition at nucleotide position 19,297) that results in the substitution of serine for proline at amino acid position 343.⁶⁵ This change occurs at a highly conserved proline residue that is part of a 14 residue motif (L*****P*****C) found in at least 16 other members of the serine protease superfamily.⁶⁵ Patients who are homozygous

for this point mutation have demonstrated moderate bleeding tendency, and both prolonged prothrombin and partial thromboplastin times that correspond to FX activity levels of 4% to 9% of normal. However, these patients show normal levels of FX antigen in their plasma. As a result of C to T transition at nucleotide number 19,297, a *BanI* restriction site present in exon 8 of the wild-type FX gene is abolished in FX Friuli.⁶⁵ Accordingly, this base change is utilized in the design of a screening method to discriminate FX Friuli mice from wild-type mice.

The objectives of the work described in this chapter are 1) to rescue FX knock-out mice from lethality by generating a viable mouse model of FX deficiency, 2) to determine specific characteristics of a FX variant that are capable of effecting a rescue, 3) to delineate morphological and/or pathological conditions associated with expression of a specific FX variant, 4) to uncover additional evidence for a non-hemostatic role of FX in development, and 5) to assess contribution of maternal FX to embryonic survival.

3.2 Materials and methods

3.2.1 Construction of the FX plug-targeting vector

Plasmid vector pCI-mFX-3' containing the 7-kb 3' end of mouse FX genomic sequence (Figure 18A) was digested with *SphI* to release a 2.4-kb fragment. The resulting insert containing FX exon 8 sequence was then ligated with *SphI* digested pGEM-3Z plasmid vector (Progema) to produce a correctly oriented insert-to-vector template (pGEM-3Z-exon 8) (Figure 18B). In an *in vitro* site-directed mutagenesis reaction containing this plasmid template (QuikChange

Multi-Site Directed Mutagenesis kit, Stratagene), a pair of mutagenic primers (forward: 5'-CCTGAAGATGCTGGAGGTAT**CT**ACGTGGATCGCAACACC-3' and reverse: 5'-GGTGTTGCGATCCACGTAG**GG**ATACCTCCAGCATCTTCAGG-3') designed to make the desired substitution of TCC for CCC in exon 8 was used to generate the Friuli mutation. To obtain the rest of FX genomic sequence from pCI-mFX-3' that is upstream from the first *SphI* site, pCI-mFX-3' was digested sequentially with *MfeI* and *SaII* to release a ~4.1-kb FX fragment. This fragment was then subcloned into the *MfeI/SaII* digested pGEM-3Z-exon 8 plasmid, yielding a 8.1-kb plasmid (pGEM-3Z-mFX 3') (Figure 18C). Subsequently, to generate the final FX-plug construct (pBY9-mFX plug, Figure 18D) for the knock-in experiment, a 5.3-kb FX sequence (including exons 6, 7 and 8 mutated, and intron sequences) was removed from *SaII/HindIII* digested pGEM-3Z-mFX 3' plasmid, and cloned into the *XhoI/HindIII* digested pBy9 plug vector (provided by Dr. Randy Thresher, UNC Chapel Hill). Spanning about 10.2-kb in length, the final FX plug-targeting vector contains the identical 2.8-kb 5' targeting arm as the FX socket-targeting construct and a 1.4-kb 3' targeting arm (Figure 18D). Necessary for the reconstitution of *HPRT* sequence, the 3' arm provides a region of *HPRT* sequence that overlaps with that in the pPD20 plasmid (used to engineer the FX socket construct). The specific substitution to confer the Friuli mutation was confirmed with dideoxynucleotide sequencing before electroporation of the FX plug construct.

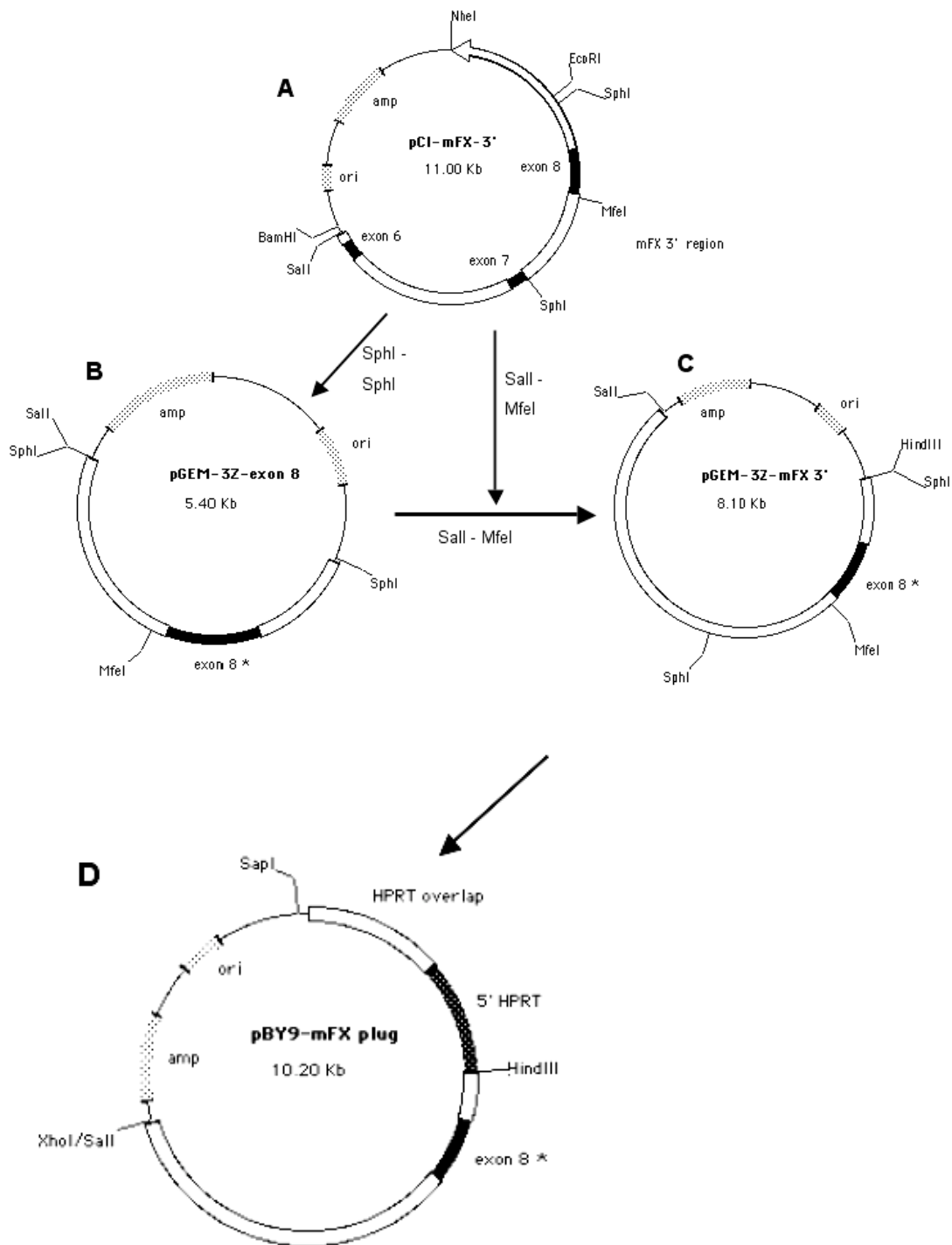


Figure 18. Construction of the FX plug-targeting vector. (A) pCI-mFX-3' contains the 7-kb 3' FX genomic sequence. (B) pGEM-3Z-exon 8 contains the Friuli mutation in exon 8 after an *in vitro* site-directed mutagenesis. (C) pGEM-3Z-mFX 3' contains the 3' FX sequence (with Friuli mutation) that is absent in the FX knock-out locus. (D) pBY9-mFX plug containing the Friuli mutation in exon 8 is the final FX plug-targeting vector used in the rescue experiment.

3.2.2 Electroporation and selection of HAT-resistant ES cell clones

ES cells were grown on irradiated murine embryonic fibroblasts (MEFs) in HEPES buffered (10 mM) Dulbecco's modified Eagle's medium (DMEM), supplemented with 15% fetal calf serum (FCS), 0.1 mM non-essential amino acids, 2 mM L-glutamine, 0.1 mM β -mercaptoethanol, 1000 U/ml leukemia inhibitory factor (LIF), and 50 μ g/ml of Gentamycin. *HPRT*-negative murine ES cells heterozygous for deletion of exon 8 (from the original targeting event) were electroporated with 100 μ g/ml of *SapI* linearized FX plug construct, using the same electroporation conditions as previously described in Chapter 2. Twenty-four hours after electroporation, transfected ES cells seeded on *HPRT*-positive feeder layers were grown in the culture medium supplemented with HAT (120 μ M hypoxanthine/0.4 μ M aminopterin/20 μ M thymidine). HAT selection lasted for 7-10 days before DNA isolated from the individual HAT-resistant ES clones (i.e. clones with reconstituted *HPRT* sequence) was analyzed by PCR and Southern hybridization.

3.2.3 Isolation of ES cell DNA and mouse genomic DNA

To analyze HAT-resistant ES cell clones for homologous recombination, DNA was isolated using the Easy DNA Kit (Invitrogen, Carlsbad, CA). To genotype for mice carrying the Friuli mutation, genomic DNA was extracted from blood samples collected from the retro-orbital plexus into heparin-containing micro-capillaries, and purified using the QIAamp DNA Blood Mini Kit (Qiagen, Valencia, CA).

3.2.4 PCR analyses on ES cell DNA and mouse genomic DNA

DNA from HAT-resistant ES clones was first subject to PCR analysis, using two specific primers (little arrows in Figure 19C) (forward primer: 5'-AGGCACCCCCAGGCTTTACAC-3' annealing to a *HPRT* sequence present only in the pBY9 vector and reverse primer: 5'-TCGAGGCTGCAGTGAGCAGTG-3' annealing to a downstream *HPRT* sequence unique in the pPD20 vector).⁶⁶ Presence of a 1.6-kb amplification product in DNA samples identified those HAT-resistant ES clones that not only contain the reconstituted *HPRT* sequence, but also demonstrate homologous recombination at the 3' end. DNA samples positively identified by the last PCR reaction were further analyzed for the absence of a *BanI* site in a 350-bp exon 8 PCR product amplified from the mutated FX allele. To differentiate FX(F/F), FX(+/F), and FX(+/+) mice by PCR analysis, the same 350-bp exon 8 PCR product (amplified with primers described above) was digested with *BanI* and analyzed on 2% TAE gel (note: presence of the Friuli mutation results in elimination of the *BanI* site within the 350-bp exon 8 PCR product).

3.2.5 Southern blot analysis on ES cell DNA and mouse genomic DNA

DNA from HAT-resistant ES clones and mice (positively identified by prior PCR analysis) was further examined by restriction enzyme digest with *EcoRV* and Southern hybridization. The 2.8-kb FX sequence that served as the 5' targeting arm in both FX socket and FX plug constructs was used as a probe labeled with ³²P-dCTP in a random priming reaction.

3.2.6 DNA sequencing to confirm substitution of TCC for CCC in FX exon 8

The 350-bp exon 8 PCR product amplified from DNA samples extracted from HAT-resistant ES clones (first identified by a separate PCR reaction and Southern hybridization) and the same 350-bp PCR product amplified from genomic DNA of mice (either offspring of chimeric mice or offspring of heterozygous FX(+F) mice) were subjected to dideoxynucleotide sequencing to confirm the substitution of TCC for CCC (corresponding to amino acid 340 in mouse FX) in exon 8 of FX gene.²⁶

3.2.7 Generation of homozygous FX-Friuli [FX(F/F)] mice

Production of all chimeric mice was performed by the Transgenic & Chimeric Mouse Facility of the University of Pennsylvania. Individual FX(+F) murine ES cell clones were expanded; one was micro-injected into C57/BL6 blastocysts for implantation into the uterine horns of pseudo-pregnant mice. Chimeric males were mated with wild-type C57/BL6 females to produce heterozygous FX(+F) offspring, which were intercrossed to obtain homozygous FX(F/F) mice for detailed characterization.

3.2.8 Western blot analysis of plasma

Collected from four weeks-old FX(+/+) and homozygous FX(F/F) mice, blood samples were processed as described above to obtain plasma for Western blot analysis. Plasma samples (1:5 and 1:20 dilutions) were separated by electrophoresis in 10% SDS/12% Tris-HCL polyacrylamide gels (Bio-Rad, Hercules, CA) under denaturing conditions, and transferred onto a Hybond ECL

nitrocellulose membrane (Amersham Pharmacia Biotech.). After blocking, FX antigen was incubated with and immunodetected by a horseradish-peroxidase conjugated rabbit anti-human FX polyclonal antibody (1:300 dilution) (Cedarlane, Ontario, Canada). Signals from the FX/antibody-HRP complex were visualized by applying the chemiluminescence reagents as instructed from the manufacturer (Amersham Pharmacia Biotech.).

3.2.9 Generation of FX(-/F) mice

To generate and characterize mice with even lower levels of FX activity, homozygous FX(F/F) female mice were mated with heterozygous FX(+/-) male mice. Note female rather than male FX(F/F) mice were selected in this breeding scheme to evaluate their reproductive fitness. Two distinct PCR reactions were used to ensure correct genotypic analysis of FX(-/F) and FX(+/F) offspring from this cross. From the first PCR reaction, a 350-bp exon 8 PCR product was subject to *BanI* restriction digest to differentiate mutated exon 8 (carrying the Friuli variant) from wild-type exon 8. Furthermore, to confirm presence of a *Neo* sequence in FX(-/F) mice and its absence in FX(+/F) mice, two specific primers (forward primer: 5'-GCCGCGCTGCCTCGTCCTG-3' annealing to a sequence in the *Neo* gene and reverse primer: 5'-CCAAACCCCGCCATTCCGTCCTC-3' annealing to a sequence in the 3'*HPRT* minigene) found only in the socket vector used to generate the knock-out FX allele were applied in a second PCR reaction. FX(-/F) offspring resulting from this mating were further characterized and compared with FX(+/) mice.

3.2.10 Activated partial thromboplastin time (aPTT) and prothrombin time (PT) FX assays

Blood samples collected from tails of 4 to 6 weeks-old adult mice [FX(+/+), FX(+/F), FX(F/F), and FX(-/F)] were combined with one-tenth volume of 3.8% sodium citrate and centrifuged at 9000 rpm for 10 minutes in 4°C to obtain plasma for measurement of FX coagulation activities by aPTT and PT assays. To measure FX clotting activities by aPTT, 50 µl of plasma sample diluted (1:2 to 1:80) with imidazole buffer (Hedwin, Baltimore, MD) was mixed with 50 µl of human FX-deficient plasma (Biomerieux, Durham, NC) and 50 µl of aPTT reagent (Biomerieux); the mixture was incubated at 37° C for 3 minutes before the addition of 50 µl of 25 mM CaCl₂ to initiate clot formation. To measure FX clotting activities by PT, 50 µl of plasma sample diluted (1:2 to 1:80) with imidazole buffer was combined with 50 µl of human FX-deficient plasma, and incubated at 37° C for 3 minutes before the addition of 100 µl pre-warmed thromboplastin reagent (Biomerieux). Time elapsed in seconds before each clot formation was determined with a fibrometer (Fibrosystem; BBL, Cockeysville, MD). Based on the values of pooled normal mouse plasma (1:10 to 1:200 dilutions), standard curves for the aPTT and PT FX assays were respectively generated to convert clotting times to percent normal FX activities.

3.2.11 Genotypic analysis of offspring from mating of FX(-/F) mice

Reproductive fitness of FX(-/F) mice, male and female, was evaluated and compared to that of their respective wild-type mice. Full-term offspring resulting from mating of FX(-/F) mice were genotyped according to the two PCR

screening strategies described earlier. For each expected genotype [FX(F/F), FX(-/F), and FX(-/-)], the numbers of offspring observed were compared to the numbers of offspring expected based on the Mendelian frequency of autosomal transmission. Numerical differences were analyzed by the chi square test.

3.2.12 Phenotypic analysis of embryos resulting from FX(-/F) mothers

To investigate the embryonic phenotypes of several FX-deficient genotypes as littermates, FX(-/F) females were mated with heterozygous FX(+/-) males.

From this mating scheme, four different FX-deficient genotypes [FX(+/-), FX(+/F), FX(-/F), and FX(-/-)] were possible for phenotypic characterization.

Timed mating was set up between FX(-/F) females and FX(+/-) males; embryos from the cross were harvested and analyzed at critical time points (E10.5, E11.5, and E12.5) during development. Subsequent to microscopic examination, the genotype of each embryo was confirmed by analysis of its yolk sac DNA.

3.2.13 Histological analysis of FX-deficient mice

Adult mice of various ages were sacrificed by CO₂ inhalation; organs were harvested, washed in PBS, and fixed in 10% formalin overnight at 4°C.

Tissues were embedded in paraffin, sectioned (5 μm in thickness), and stained with Prussian blue, or Masson's trichrome stain, using standard protocols.

3.3 Results

3.3.1 Homologous recombination between the FX plug-targeting vector and FX knock-out locus

Following homologous recombination between the FX plug construct (Figure 19B) and FX knock-out locus resulting from the first targeting experiment (Figure 19A), the *Neo* gene is replaced by exon 8 carrying the Friuli mutation, and concomitantly the *HPRT* minigene is reconstituted (Figure 19C) for HAT-resistance selection of ES cells. [Note as the result of this homologous recombination event, correctly targeted ES cells are G418-sensitive and HAT-resistant].

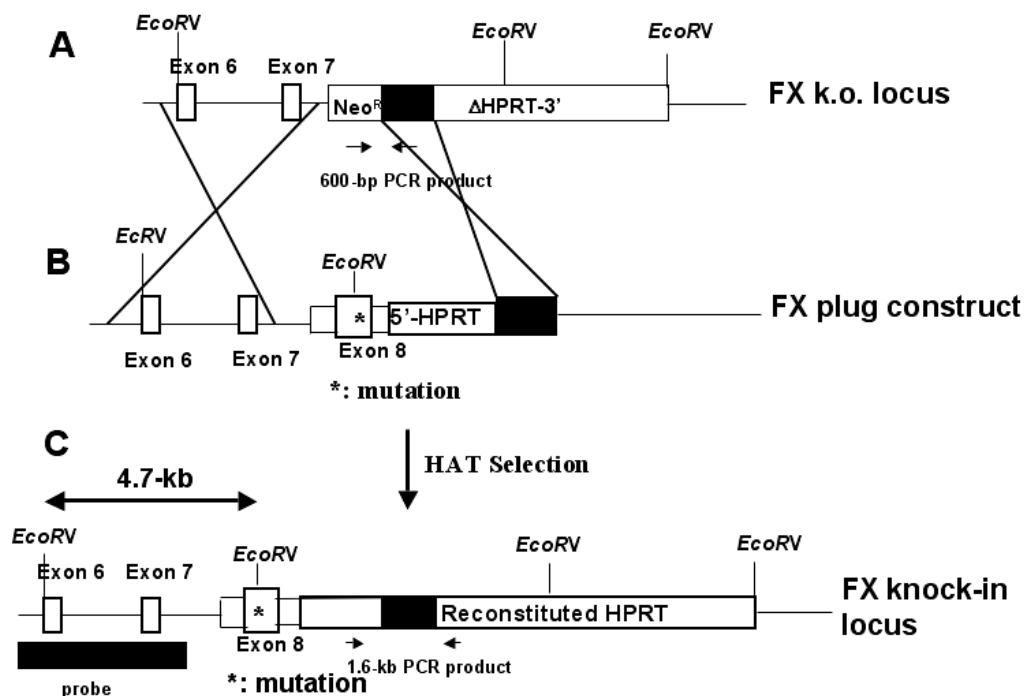
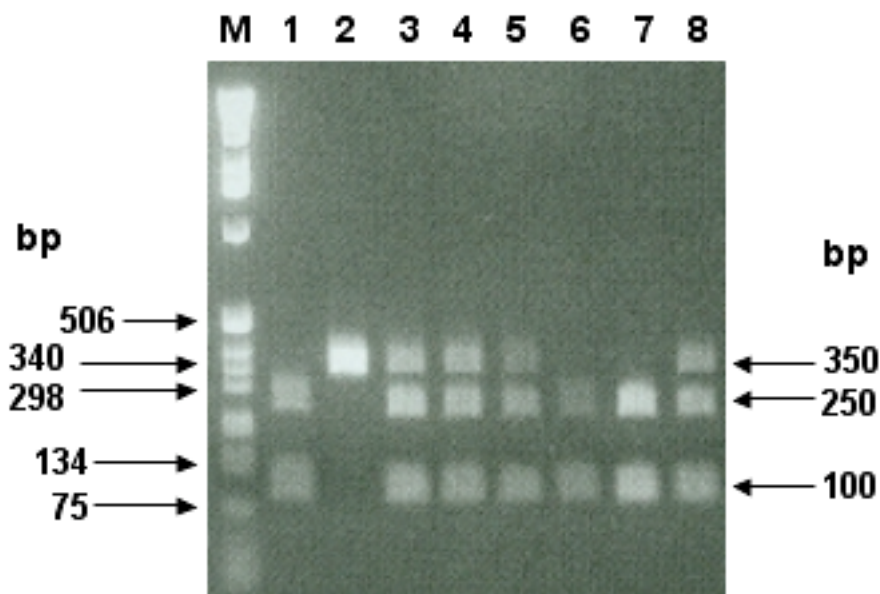


Figure 19. Targeted knock-in of FX-Friuli. (A) The 3' end of FX knock-out locus shows the deleted exon 8 replaced by *Neo* and partial *HPRT* minigene cassette. Figure 19 (continued)

The little arrows below the cassette indicate the location of a primer pair used in a PCR reaction to differentiate FX(-/F) mice from FX(F/F) mice. (B) FX plug construct contains the Friuli mutation in exon 8 (*) and supplies the missing 5' portion of an *HPRT* minigene. Its 5' targeting arm is the same 5' arm in the FX socket construct and its 3' targeting arm contains a 1.4-kb overlapping *HPRT* sequence with the FX socket construct. (C) Following homologous recombination, *Neo* gene is replaced by the mutated exon 8 and the *HPRT* minigene is reconstituted for HAT medium selection. The two arrows below the reconstituted *HPRT* sequence indicate the location of a primer pair used in a PCR reaction to identify correctly knock-in ES clones. The darkened bar below exons 6 and 7 represents a probe used in Southern hybridization. With knock-in of exon 8, the distance (4.7-kb) between two adjacent *EcoRV* sites at the 3' end of the FX gene is also restored as indicated by the length of a double-head arrow.

3.3.2 PCR results

Among the 48 HAT-resistant ES clones analyzed, clones that were correctly targeted by the FX plug construct revealed not only a 1.6-kb PCR product amplified from the reconstituted *HPRT* sequence (Figure 19C), but also a 350-bp exon 8 PCR product that is not subject to *BanI* restriction digest, in addition to the wild-type fragment that is subject to the restriction digest (results not shown). Genotypes of mice [FX(+/+), FX(+/F), and FX(F/F)] were revealed based on the results of *BanI* digest of the 350-bp exon 8 PCR product (Figure 20): wild-type samples (lanes 1, 6, and 7) yielded two fragments (250-bp and 100-bp), heterozygous FX(+/F) samples (lanes 3, 4, 5, and 8) showed three fragments (350-bp mutated exon 8, 250-bp, and 100-bp), and the only homozygous FX(F/F) sample (lane 2) showed a mutated and thus uncut 350-bp fragment.



Bands from *BanI* digest of PCR product:

350-bp (F)
 250-bp (WT)
 100-bp (WT)

Figure 20. PCR and restriction enzyme digest (*BanI*). To genotype FX(+/+), FX(+/F), and FX(F/F) mice, a 350-bp PCR product amplified across the region of exon 8 containing the Friuli mutation was digested with *BanI*. Presence of the Friuli mutation abolishes the *BanI* site. After *BanI* digest, wild-type exon 8 yields two fragments (*lanes 1, 6, and 7*), exon 8 heterozygous for the Friuli mutation shows three fragments (*lanes 3, 4, 5, and 8*), and exon 8 homozygous for the Friuli mutation fails to be digested as shown by a single fragment (*lane 2*).

Two PCR reactions were carried out to distinguish among FX(-/F), FX(F/F), and FX(+/F) mice. While *BanI* digest of the 350-bp exon 8 PCR product could be used to differentiate FX(F/F) and FX(-/F) mice from FX(+/F) mice, this PCR reaction itself was insufficient to make a distinction between FX(F/F) and

FX(-/F) mice since both genotypes gave rise to a single undigested fragment (Figure 21A). To differentiate FX(-/F) mice from FX(F/F) mice, a second PCR reaction using a primer pair shown in Figure 19A was carried; this reaction resulted in a 600-bp *Neo/ΔHPRT* PCR product that is present in FX(-/F) mice and absent in FX(F/F) mice (Figure 21B).

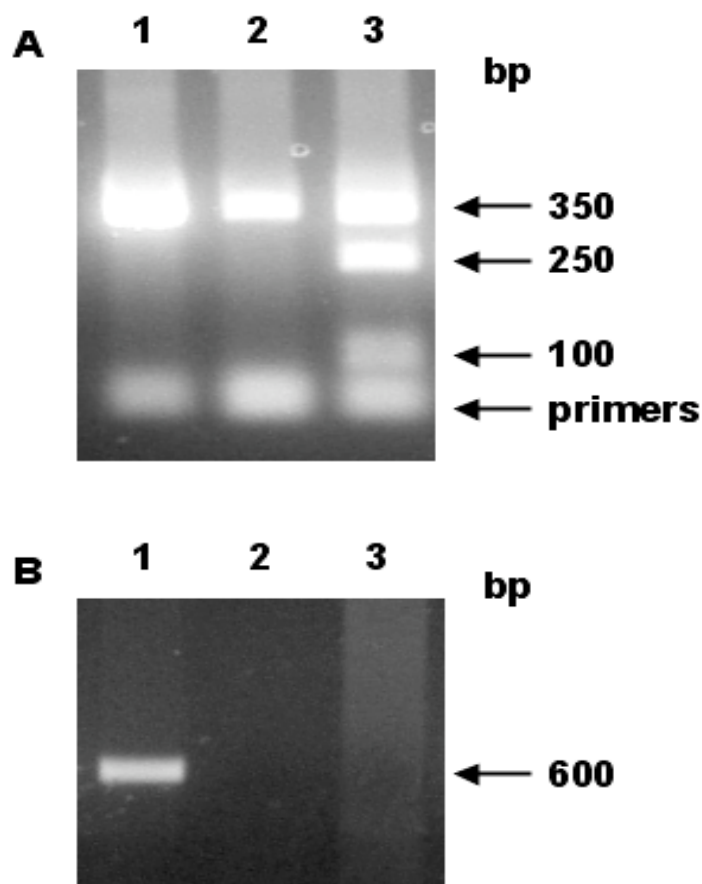


Figure 21. PCR analysis to differentiate FX(+/F), FX(F/F), and FX(-/F) mice.

Two simultaneous PCR reactions are required to differentiate FX(-/F) mice from FX(F/F) mice. (A) *Ban*I digest of the 350-bp exon 8 PCR product clearly identifies the FX(+/F) genotype (*lane 3*); however, it does not differentiate between the FX(-/F) and FX(F/F) genotypes (*lanes 1 and 2*). (B) Presence of a 600-bp PCR product amplified across a *Neo/ΔHPRT* sequence (Figure 19A) reveals the FX(-/F) genotype (*lane 1*) and its absence indicates the FX(F/F) genotype (*lane 2*).

3.3.3 Southern blot results

In a Southern hybridization with a 2.8-kb FX probe (Figure 19C), *EcoRV* digested DNA from correctly targeted HAT-resistant ES clones (previously identified by two separate PCR reactions) yielded a single 4.7-kb fragment (Figure 22, lanes 1-7) that is indistinguishable from a wild-type fragment (Figure 22, lane 8, lower band); *EcoRV* digested DNA from an heterozygous FX(+/-) ES clone was included as a marker control (Figure 22, lane 8). When hybridized with the same FX probe, *EcoRV* digested genomic DNA from mice [FX(F/F), FX(+/F), and FX(+/-)] revealed the same results (data not shown).

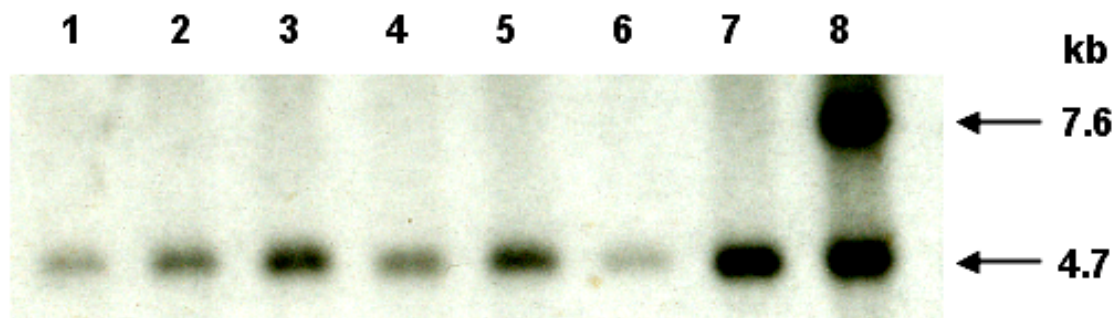


Figure 22. Southern blot analysis of DNA from HAT-resistant ES clones. DNA from HAT-resistant ES clones previously identified by PCR analysis were digested with *EcoRV* and hybridized with a 2.8-kb FX probe (Figure 19C). DNA from correctly knock-in clones yielded a 4.7-kb fragment (lanes 1-7) that is indistinguishable from a wild-type fragment (lane 8, lower band). *EcoRV* digested DNA from an heterozygous FX(+/-) ES clone resulting from the first targeting event was included as a marker control (lane 8).

3.3.4 Targeting frequency in the knock-in experiment

Electroporation of the FX plug-targeting construct to reconstitute the *HPRT* minigene for HAT selection resulted in a high targeting frequency of correctly retargeted ES cells. Among the 48 HAT-resistant ES clones isolated for further

analysis, 9 demonstrated correct targeting by both PCR and Southern hybridization (shown in Figure 22 are 7 of 9 correctly knock-in ES clones). Note that while 19% of ES clones analyzed after the second retargeting event were correctly targeted, only 4% of ES clones from the first, original targeting event were correctly targeted; note this increase is greater than four-fold.

3.3.5 DNA sequencing results

Dideoxynucleotide sequencing of a 350-bp exon 8 PCR product amplified from DNA samples of either HAT-resistant ES clones or of mice resulting from mating of heterozygous FX(+/F) parents confirmed the correct base substitution of TCC for CCC in exon 8. Shown in Figure 23 are the sequencing results of exon 8 PCR products derived from FX(+/F), and FX(F/F) mice, respectively.

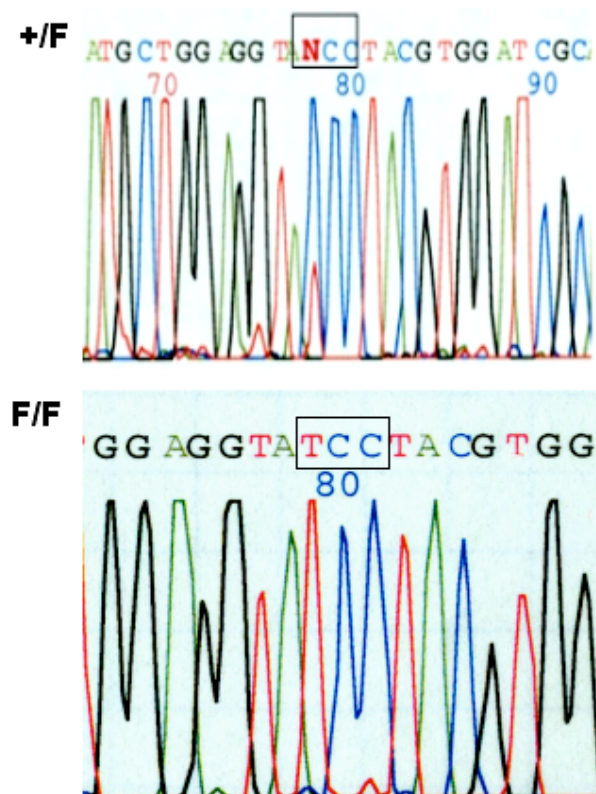


Figure 23. Sequencing analysis of PCR products. DNA Sequencing results of a 350-bp exon 8 PCR product confirm the correct base substitution of TCC for CCC in one allele of FX (+/F) mice (upper panel) and in both alleles of FX(F/F) mice (lower panel).

3.3.6 Production of homozygous FX(F/F) mice


One heterozygous FX(+/F) ES clone identified by PCR and Southern hybridization and confirmed by DNA sequencing was used to generate chimeric mice. After mating with C57/BL6 females, chimeric males transmitted the FX-Friuli allele to approximately half of their F1 offspring (n=24). Heterozygous FX(+/F) mice were intercrossed to generate homozygous FX(F/F) mice. The results of the intercross of FX(+/F) mice are highly informative and are summarized in Table 6. Representing 22% of the total progeny (n=298; $p>0.2$),

FX(F/F) mice were born at the expected frequency based on Mendelian inheritance. Unlike FX(-/-) neonates, FX(F/F) newborn mice showed no indication of any hemorrhagic condition. Furthermore, FX(F/F) mice have demonstrated normal survival; 80% of FX(F/F) mice have survived for at least 18 months whereas 100% of FX(-/-) mice have succumbed within 4 days. Taken together, these results show that expression of the Friuli variant is capable of rescuing FX knock-out mice from both embryonic and perinatal lethality. FX(F/F) mice (males and females) were also evaluated for their reproductive fitness; no discrepancies with wild-type mice were noted in terms of the frequencies of pregnancy and average size of littermates.

Table 6. Genotype distribution among offspring from heterozygous FX(+/F) intercross.

+/F		x		+/F	
+/+	+/F	F/F	n	p	
81 (27%)	153 (51%)	64 (22%)	298	> 0.2	

Survival: > 18 months



3.3.7 Levels of FX antigen in FX(F/F) mice

In Western blot analysis of two different dilutions of plasma (1:5 and 1:20), FX(F/F) mice demonstrated levels of FX antigen similar to that shown by FX(+/-) mice (Figure 24).

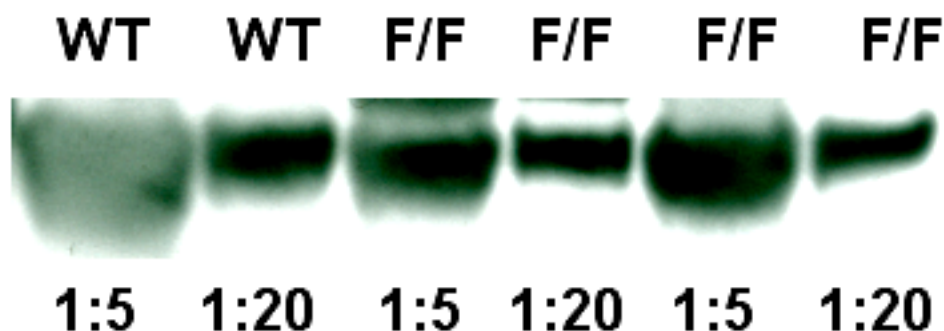


Figure 24. Western blot analysis of plasma. Homozygous FX (F/F) mice demonstrate levels of FX antigen similar to those shown by wild-type mice. Western blot analysis was performed at two different dilutions (1:5 and 1:20) to demonstrate similar FX antigen levels in FX (F/F) and FX (+/-) mice.

3.3.8 Levels of FX activity in FX(F/F) mice

Using clotting assays, levels of FX activity in FX(F/F) mice were measured (Table 7). While FX(+/-) mice showed levels of FX activity approximately half of those determined in wild-type mice (defined as 100%), FX(F/F) mice revealed FX activity levels of $5.5 \pm 1.8\%$ in an aPTT-based assay and $5.5 \pm 1.9\%$ in a PT-based assay. Thus, mouse model of FX-Friuli expresses levels of FX activity representative of those shown by humans carrying the analogous mutation.

Table 7. FX coagulation activity in FX(+/+), FX(+/ F) and FX(F/F) adult mice. Levels of FX activity are expressed in % normal. Level of FX activity from FX(+/+) mice was determined from pooled plasma (n=9).


FX allele	+/+	+/F	F/F
aPTT	100% (pooled)	49±3 % n=5	5.5±1.8 % n=4
PT	100% (pooled)	57.9±5 % n=3	5.5±1.9 % n=7

3.3.9 Generation of FX(-/ F) mice

Though useful and instructive as a viable model for FX deficiency, homozygous FX(F/F) mice nevertheless failed to define a lower limit of FX activity or FX antigen essential for survival, since these mice exhibited normal embryonic and postnatal survival. In order to generate and characterize mice with even lower levels of FX activity and antigen, FX(F/F) females were crossed with FX(+/-) males. Two different genotypes [FX(+/ F) and FX(-/ F)] were expected in the offspring of this cross. Genotype analysis of 97 offspring from such a mating revealed the expected distributions with 54% FX(+/ F) and 46% FX(-/ F) mice ($p>0.2$) (Table 8). Postnatal survival of FX(-/ F) mice has also been normal with 80% of FX(-/ F) mice surviving for longer than 15 months. FX(-/ F) mice are reproductively competent with frequencies of pregnancy comparable to those exhibited by wild-type mice (data not shown).

Table 8. Genotype distribution in offspring resulting from cross of FX(F/F) females and FX(+/-) males.

F/F		x	+/-				
♀			♂				
+/F	-/F	n	p				<i>FX alleles:</i>
52 (54%)	45 (46%)	97	> 0.2				<i>Friuli: F</i>
							<i>Wild-type: +</i>
							<i>Knock out: -</i>


Survival: > 15 months

3.3.10 Levels of FX activity in FX(-/F) mice

Recall no FX antigen was observed in FX knock-out mice and levels of FX antigen in homozygous FX(F/F) mice were similar to that of wild-type mice as determined by a series of Western blot analyses. Based on those observations, it was therefore expected that FX(-/F) mice would likely have levels of FX antigen approximately half of those in FX(F/F) mice (with protein synthesized only from the Friuli allele, but not from the knock-out allele in FX(-/F) mice). Next, FX activity of the FX(-/F) genotype was investigated. To determine levels of FX activity in FX(-/F) mice, aPTT and PT clotting assays were performed; FX(-/F) mice showed FX activity levels of $1.1 \pm 0.1\%$ in an aPTT-based assay and $2.9 \pm 0.2\%$ in a PT-based assay (Table 9). Based on these results, it can be concluded that FX activity levels of 1-3 % and FX antigen levels (~50%) are still adequate to rescue both embryonic and perinatal

lethality of FX knock-out mice showing complete absence of FX activity and antigen.

Table 9. FX Coagulation activity in FX(-/F) mice and age-matched wild-type adult mice. Levels of FX activity are expressed in % normal. Level of FX activity from FX(+/+) mice was determined from pooled plasma (n=9).

FX allele	+/+	-/F
aPTT	100% (pooled)	1.1±0.1 % n=8
PT	100% (pooled)	2.9±0.2 % n=8

3.3.11 Genotypic analysis of the offspring from FX(-/F) intercross

FX(-/F) mice with 1-3% FX activity and ~50% FX antigen levels were intercrossed to examine the genotypic representations of their offspring. Based on the results of the heterozygous FX(+/-) intercross (Table 2), no more than 12% of full-term progeny from FX(-/F) intercross are expected to be FX knock-out mice. However, genotype analysis of 89 full-term offspring resulting from the FX(-/F) intercross revealed that FX knock-out mice are represented at even further reduced proportion. Whereas 12% of progeny from the heterozygous FX(+/-) intercross were identified as FX(-/-) mice (Table 2), only 2% of progeny resulting from the FX(-/F) intercross were FX(-/-) mice (Table 10). Indicated by

the p value of less than 0.001, the observed 2% FX knock-out mice from the FX(-/F) intercross is statistically different from the expected 25% (Mendelian frequency).

Table 10. Genotype distribution among offspring from FX(-/F) intercross.

-/F x -/F			[FX activity: 1-3%] [FX antigen: ~50%]	
F/F	-/F	-/-	n	p
29 (33%)	58 (65%)	2 (2%)	89	< 0.001

3.3.12 Phenotypic analysis of embryos from FX(-/F) mothers

Embryonic phenotypes of FX-deficient offspring resulting from mating of FX(-/F) females and FX(+/-) males were characterized. Several anomalies were observed. First, gross examination of uterine horns derived from low FX mothers [FX(-/F) mothers with 1-3% FX activity and ~50% FX antigen] carrying E10.5, E11.5 or E12.5 embryos disclosed blood pools throughout the uteri (Figures 25A, D and G). The noted blood pools within uteri are likely maternal in origin based on several observations: 1) they are found outside the yolk sacs and in spaces between embryos; 2) no correlation was found between location of blood pools and specific genotype of embryos; 3) the overall volume of blood pools was far too great to be lost by a few FX(-/-) embryos in each litter. Based on the earlier results (Table 10), in which FX(-/F) mice were shown to survive

embryonic development in expected Mendelian frequency, FX(-/F) embryos are not expected to make any significant contribution, if at all, to the accumulation of blood pools observed in the uteri of low FX mothers. Second, the yolk sacs of E10.5, E11.5, and E12.5 FX knock-out embryos were completely lacking in visible vasculature and exhibited a rough, granular surface (Figure 25B, E and H); these observations were not noted for the yolk sacs of other genotypes (in the same E10.5, E11.5, and E12.5 litters) including the yolks sacs of FX(-/F) embryos, which clearly show a smooth, vascularized surface (Figures 25C, F and I). Third, in addition to demonstrating abnormalities in the yolk sac vasculature, it is also important to note that the FX knock-out embryos examined (E10.5, E11.5 and E12.5) have also reabsorbed or have begun to reabsorb (Figures 25B, E and H). Therefore, with these observations, the relationship between cause and effect is unclear.

Next, FX(+/-) females (these females have ~50% FX activity and ~50 FX antigen) were mated with FX(+/-) males. However, examination of the uteri of FX(+/-) mothers carrying E13.5 embryos did not reveal any evidence of blood pools (Figure 26A). This observation in FX(+/-) mothers provided an additional support for the belief that blood pools in the uteri of FX(-/F) mothers are maternal rather than embryonic in origin. Examination of these E13.5 embryos from FX(+/-) mothers (n=2) revealed one viable FX knock-out embryo (Figure 26B). Unlike the FX knock-out embryos born to FX(-/F) mothers (Figures 25B, E and H), this FX knock-out embryo born to FX(+/-) mother showed clearly visible vasculature in its yolk sac (Figure 26B) and is indistinguishable from a

wild-type littermate (Figure 26C). This finding is not completely unexpected, since approximately 50% of FX knock-out embryos have survived embryonic development (Table 2).

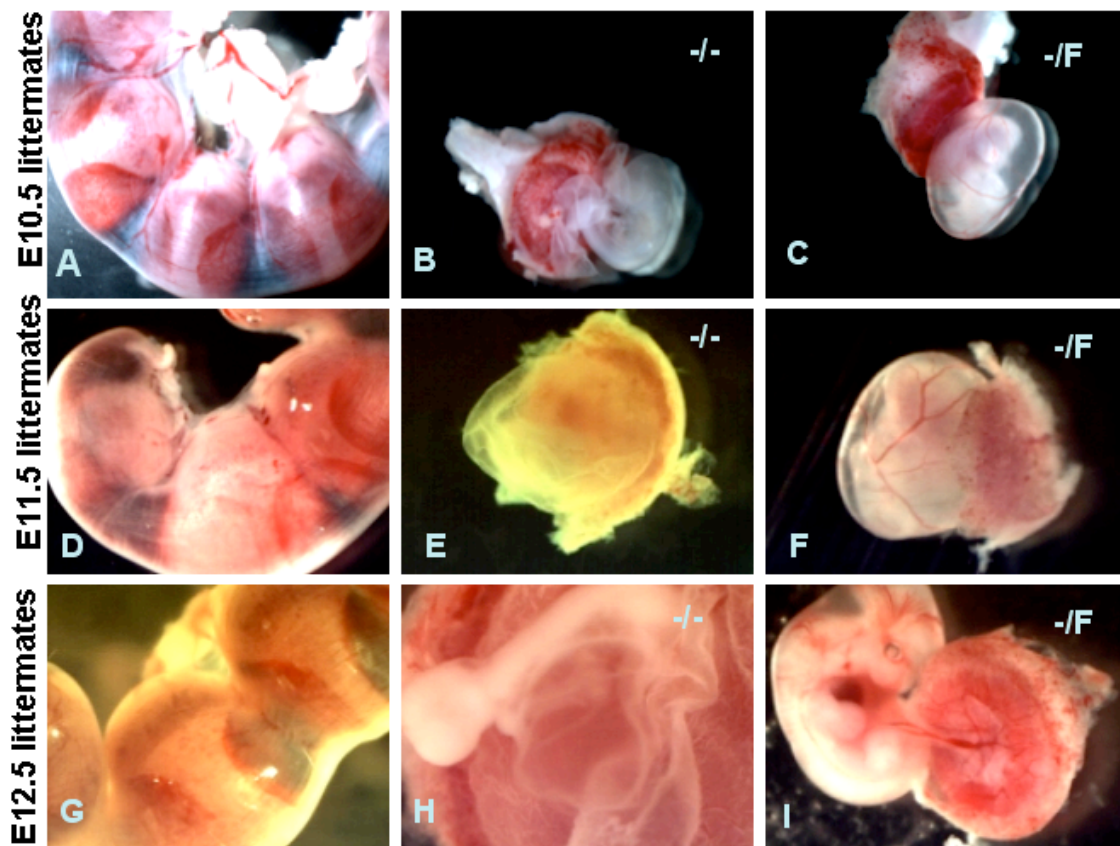


Figure 25. Examination of E10.5, E11.5 and E12.5 FX-deficient littermates from FX(-/F) mothers. During pregnancy, FX(-/F) mothers suffer severe but non-fatal intrauterine hemorrhage (A, D and G). While FX(-/F) embryos are viable and show clearly visible vasculature in their yolk sacs (C, F and I), FX knock-out littermates have reabsorbed and lack any vasculature in their yolk sacs (B, E and H).

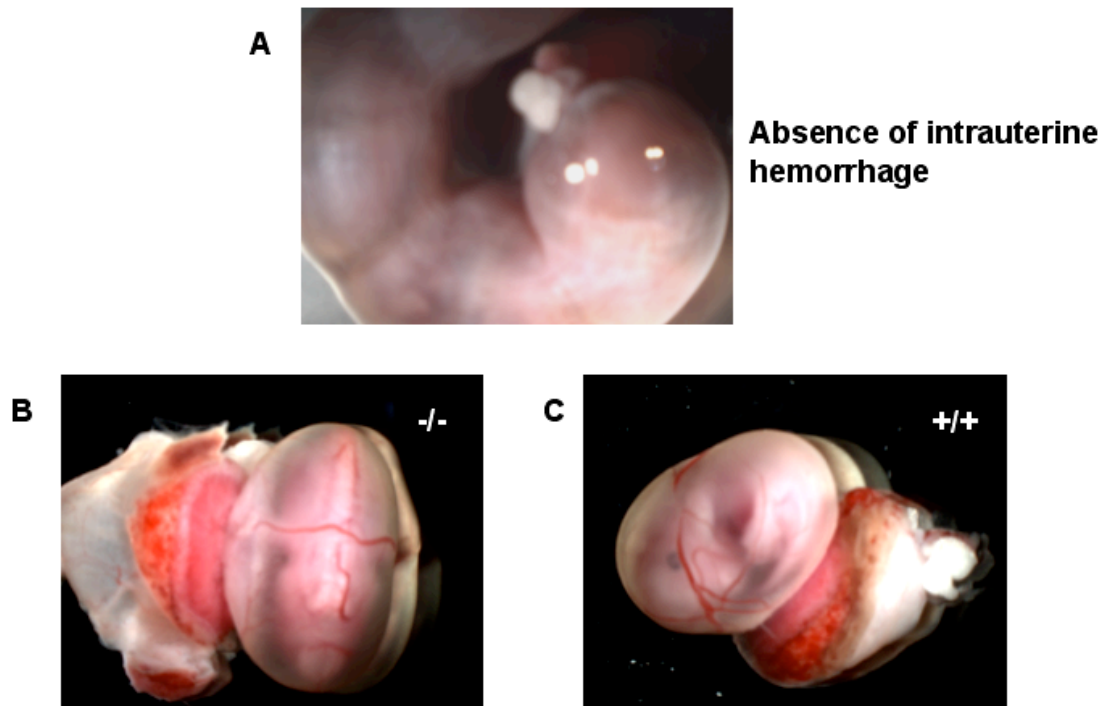


Figure 26. Examination of E13.5 FX-deficient littermates from a FX (+/-) mother. (A) During pregnancy, FX(+/-) mothers do not suffer from intrauterine hemorrhage (i.e. no blood pools are noted in the uteri of these mothers). (B) A viable FX knock-out embryo at E13.5 shows a clearly defined yolk sac vasculature that is indistinguishable from that of a wild-type littermate (C).

3.3.13 Histological analysis of FX-deficient mice

The FX(F/F) and FX(-/F) mice, both of a mixed background, have demonstrated normal survival through the postnatal period. However, a previous report documents that both low TF (~1%) and low FVII (~1%) mice exhibit cardiac fibrosis resulting from recurrent episodes of hemorrhaging into the myocardium from cardiac vessels.⁶⁷ Examination of cardiac tissues from 10 months-old FX (F/F) mice disclosed similar findings, i.e. Prussian blue staining revealed iron depositions in the myocardium, and Masson's trichrome staining also showed fibrosis localized to the same areas (Figures 27E-H and Figures 28A-F).

Cardiac tissue of the wild-type littermates examined at the same age did not show evidence of iron deposition nor cardiac fibrosis (Figures 27A-D). These findings are consistent with the observations made by Pawlinski and colleagues in low TF and low FVII mice.⁶⁷ Examination of FX(F/F) mice at 3 months of age failed to disclose evidence of iron deposition and cardiac fibrosis (data not shown). Interestingly, two FX (-/F) mice (with 1-3% FX activity) examined at 7-months of age did not show obvious signs of iron deposition or cardiac fibrosis (Figures 27I-L). Therefore, these results suggest that both genotype and age of mice are important determinants in the development of cardiac fibrosis in FX-deficient mice. Serial tissue sections from spleens of FX-deficient mice and wild-type littermates (10 months-old and 7 months-old) were also analyzed by Prussian blue and Masson's trichrome stains. No noticeable differences were detected by Masson's trichrome staining (Figures 29B, D and F). However, FX deficient mice [both 10 months-old FX(F/F) mice and 7 months-old FX(-/F) mice] showed elevated iron levels in their spleens (Figures 29A and C).

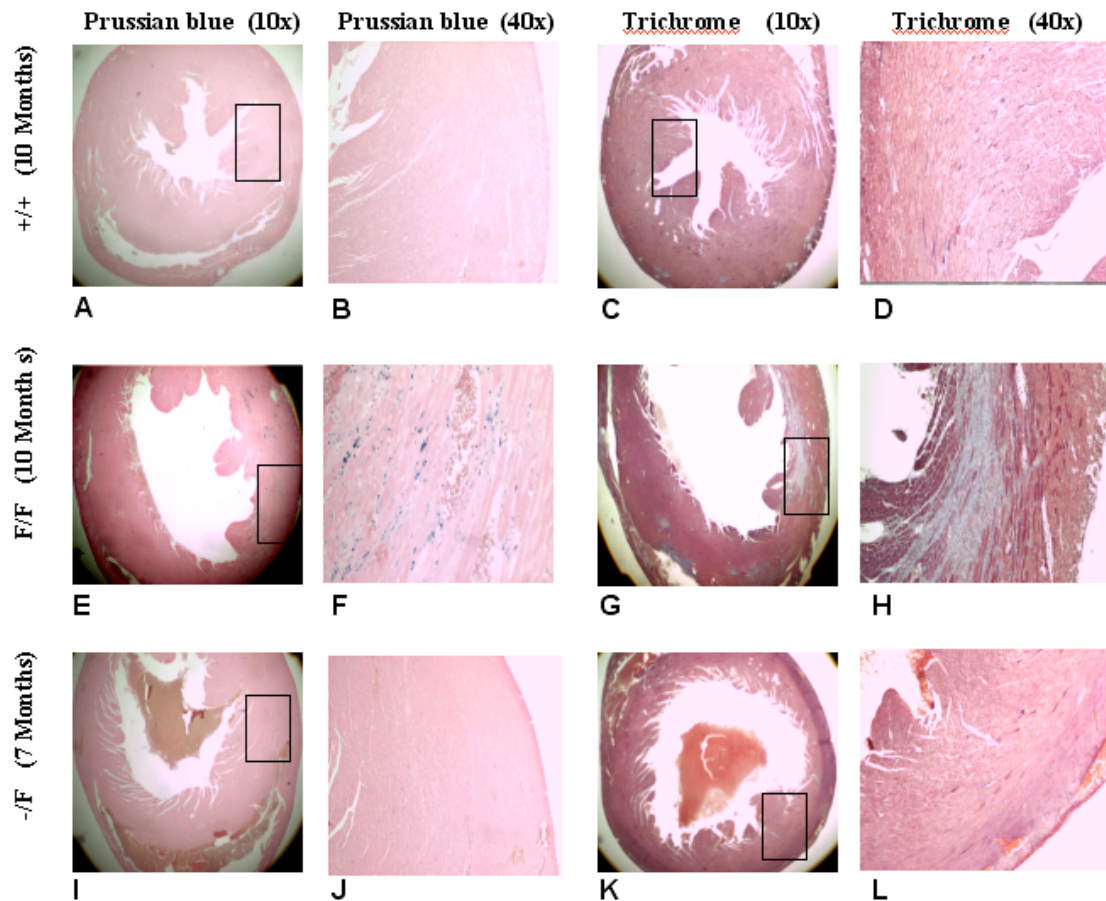


Figure 27. Histological analysis of the heart tissues from FX deficient mice. Iron deposition and fibrosis were found in the heart tissue of a 10 months-old FX(F/F) mouse (E-H), but not in that of a wild-type littermate examined at the same age (A-D). Interestingly, neither iron deposits nor fibrosis were found in the heart tissue of a 7 months-old FX(-/F) mouse (I-L).

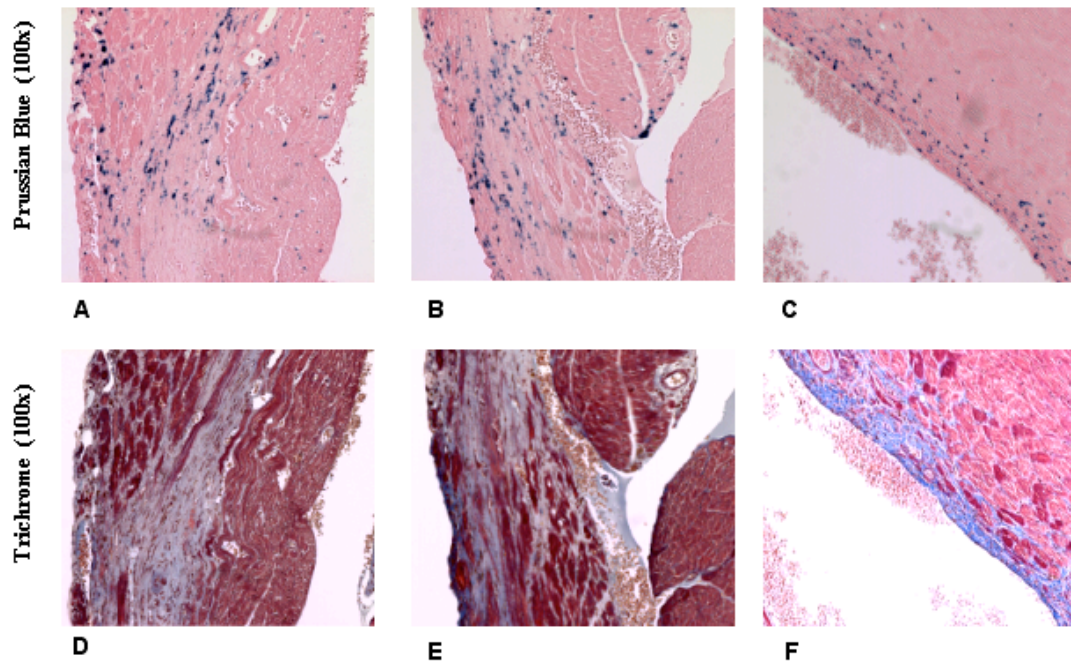


Figure 28. Co-localization of iron deposits and fibrosis. Further examination of the cardiac tissue from a 10 months-old mice FX(F/F) mouse revealed that fibrosis (D-F) had localized to the same areas as iron deposits (A-C).

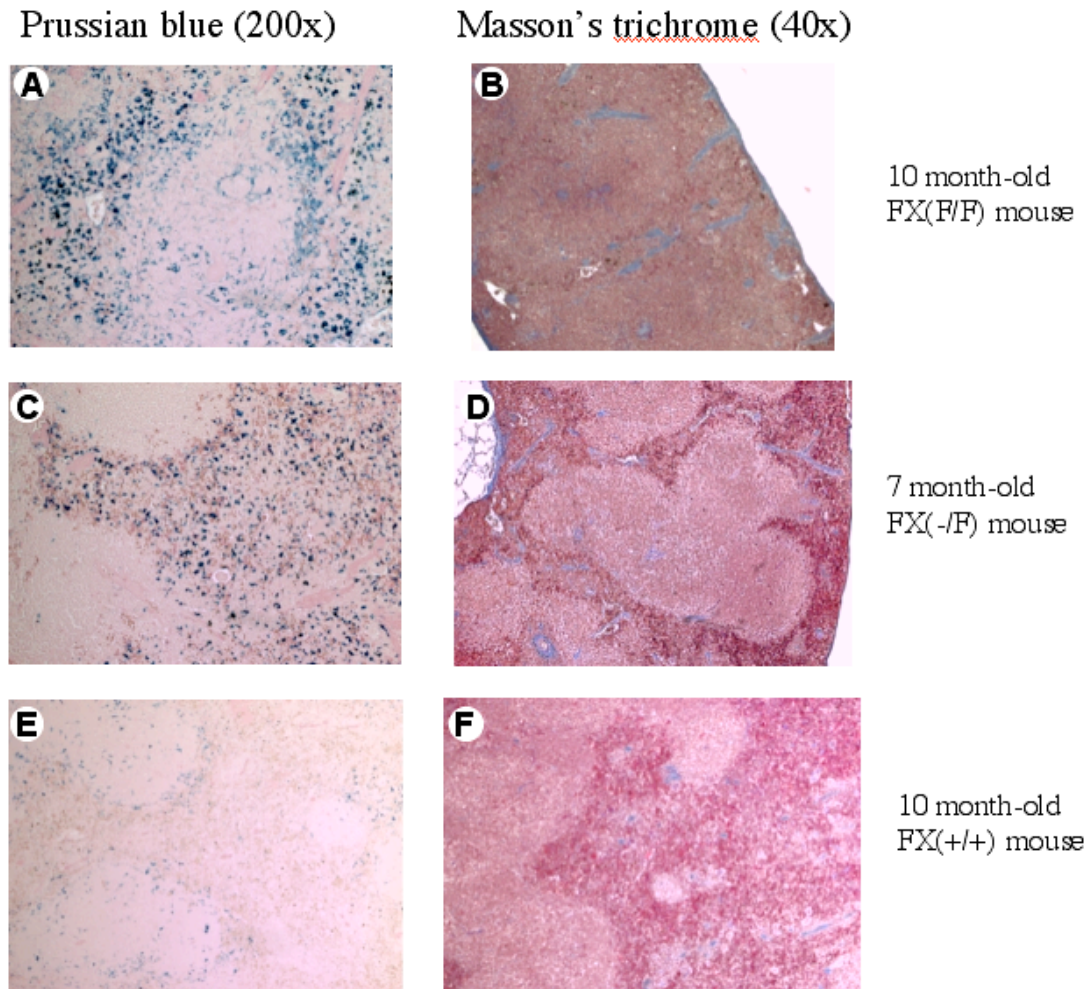


Figure 29. Histological analysis of the spleen tissues from FX-deficient mice. While spleen tissue from a 10 months-old FX(+/+) mouse showed a normal level of iron (E), the same tissue from both FX(F/F) and FX(-/F) mice (10 months-old and 7 months-old, respectively) demonstrated abnormally high levels of irons (blue spots in A and C). For all three genotypes examined, no obvious differences in fibrosis development were noted (B, D and F)

3.4 Discussion

As demonstrated in the previous chapter, complete FX deficiency (i.e. no FX catalytic activity and FX antigen) resulted in embryonic lethality of approximately half of the expected numbers of FX knock-out mice and fatal perinatal hemorrhage in the remaining half that survive to birth. Thus, one of

the highest priorities was to rescue FX knock-out mice from embryonic and perinatal lethality. Using the plug-and-socket sequential targeting strategy as detailed above, the first viable mouse model of FX deficiency was generated. Expression of the analogous mouse FX mutation was based on a naturally occurring human FX variant (FX-Friuli).

Expression of FX-Friuli in mice successfully resulted in complete rescue of the FX knock-out mice from both embryonic lethality and perinatal mortality. While FX knock-out mice represented only 12% of the full-term progeny resulting from the heterozygous FX(+/-) intercross (Table 11), genotype analysis of 298 full-term offspring resulting from the intercross of the heterozygous FX(+/F) mice identified 64 or 22% homozygous FX(F/F) mice (Table 11). The percentage of homozygous FX(F/F) mice is not statistically different from the expected 25% ($p>0.2$) in the absence of embryonic lethality, thus suggesting embryonic success of FX(F/F) mice. Unlike the FX knock-out mice that developed to term, FX(F/F) newborn mice did not show or develop any visible signs of hemorrhagic conditions and were indistinguishable in appearance from their wild-type littermates. The postnatal survival of homozygous FX(F/F) mice is also remarkable with 80% of these mice living longer than 18 months, whereas the survival of 26 FX knock-out mice developing to term was limited to 4 days (Table 11).

Table 11. Comparison of FX(+/-) intercross and FX(+/+) intercross.

+/F x +/F			Survival: > 18 months	
+/+	+/F	F/F	n	p
81 (27%)	153 (51%)	64 (22%)	298	> 0.2
+/+	+/-	-/-	n	p
76 (36%)	111 (52%)	26 (12%)	213	< 0.001
+/- x +/-			Survival: 0.5-4 days	

Detailed analysis of homozygous FX(F/F) mice revealed characteristics that mirror those exhibited by individuals homozygous for the analogous FX mutation. As reported for humans, mice expressing the FX Friuli variant also demonstrated 4-8% FX activity (as determined by both aPTT and PT clotting assays) and normal FX antigen levels (as judged by Western blot analysis). These similarities are not completely unexpected in light of the knowledge that the Friuli mutation occurs in a particular amino acid residue that is highly conserved among several species including human and mouse. Nevertheless, by the virtue of a viable FX-deficient mouse model with a set of specific characteristics, it is learned that expression of a FX variant with as low as 4-8%

FX activity and normal antigen level is readily able to support both embryonic and postnatal survival.

In an attempt to determine the lower limit of FX activity and FX antigen levels required to support embryonic and postnatal survival, FX(F/F) females were mated with FX(+/-) males to produce FX(+/F) and FX(-/F) offspring; the latter genotype is expected to generate FX-deficient mice associated with even lower FX activity and FX antigen levels than those shown by FX(F/F) mice. Genotype analysis of 97 full-term progeny resulting from such a mating identified 46% FX(-/F) mice (Table 8). No statistical difference was found between the observed representations of FX(-/F) mice (46%) and the expected representations (50%) in complete absence of embryonic lethality ($p>0.2$). This result suggests an absence of significant embryonic lethality in FX(-/F) mice. Despite the still lower FX activity and FX antigen levels, FX(-/F) mice demonstrated relatively normal postnatal survival; 80% of FX(-/F) mice have survived at least 15 months (note the average lifespan of mice is 24 months). While Western blot analysis of plasma from FX(-/F) mice was not performed, the relative levels of FX antigen in FX(-/F) mice are expected to be approximately half (~50%) of those in homozygous FX(F/F) mice, which demonstrate FX antigen levels similar to those in wild-type mice. Indeed, FX(-/F) mice present even lower FX activity (1-3%) compared to 4-8% in homozygous FX(F/F) mice (Tables 9 and 7). Taken together, these results suggest that while complete absence of FX activity and FX antigen is

incompatible with life, 1% FX activity and 50% FX antigen levels are nonetheless adequate to rescue both embryonic and perinatal mortality in FX knock-out mice. Furthermore, survival of mice at 1-3% FX activity is similar to observations made in humans, thus confirming utility of these low FX mice as model for human bleeding disorder. Due to normal embryonic and postnatal survival of FX(-/F) mice with 1-3% FX activity and 50% antigen levels, expression and characterization of a FX variant with less than 1% FX activity and antigen level (eg. FX-Stuart, see Table 5) may be necessary to unveil the lower limit of FX required for survival.^{68,69}

It is important to note that although both FX(F/F) and FX(-/F) mice have overcome embryonic and postnatal lethality, they are not completely normal compared to wild-type mice. First, 10 months-old FX(F/F) mice have developed cardiac fibrosis, contributed by both genotype and age (Figure 28). All FX-deficient [FX(F/F) and FX(-/F)] mice examined demonstrated significantly elevated levels of iron in their spleen tissues (Figure 29). Though not fatal, severe intrauterine hemorrhage is also observed in FX(-/F) mothers during pregnancy (Figure 25).

From the previous chapter, it was demonstrated that complete FX deficiency (complete absence of any FX catalytic activity and FX antigen) resulted in partial embryonic lethality and fatal perinatal bleeding. These observations give rise to the following questions. Why did partial embryonic lethality occur in place of complete embryonic lethality? Why was developmental success observed in some FX knock-out mice, but not in

others? Although several hypotheses have been described to explain partial embryonic lethality observed in some knock-out mouse models, including FV, FII (prothrombin), and FX knock-outs, no evidence has been provided to confirm any of the proposed hypotheses. Based on the data that approximately 50% of FX knock-out mice developed and survived to term, it seems that the embryonic requirement for FX is not absolute. On the other hand, the remaining 50% of FX knock-out mice failed to complete development; this would on the contrary suggest that embryonic requirement for FX is essential. One of the hypotheses offered to elucidate incomplete embryonic block describes the role of maternal transfer of some clotting factors during development.

FX(-/F) mice provided a rare opportunity to evaluate the contribution of maternal FX to embryonic survival of FX knock-out mice. It enabled a comparison of the FX(-/F) intercross with the FX(+/-) intercross; it specifically allowed for direct comparison of FX knock-out offspring resulting from FX(-/F) mothers (with 1-3% FX activity and ~50% FX antigen levels) with those resulting from FX(+/-) mothers (with ~50% FX activity and ~50% antigen levels). While genotype analysis of 213 full-term offspring from FX(+/-) intercross identified 12% FX(-/-) mice, the same analysis of 89 full-term offspring resulting from FX(-/F) intercross revealed only 2% FX(-/-) mice (Table 12). A statistical analysis (i.e. Fisher's exact test) confirms that 2% FX knock-out mice in the FX(-/F) intercross is significantly different from the 12% FX-null mice in the FX(+/-) intercross ($p=0.0045$).

Table 12. Comparison of FX(+/-) intercross and FX(-/F) intercross.

-/F x -/F			[FX activity: 1-3%] [FX antigen: ~50%]	
F/F	-/F	-/-	n	p
29 (33%)	58 (65%)	2 (2%)	89	< 0.001
+/- x +/-			[FX activity: ~50%] [FX antigen: ~50%]	
+/+	+/-	-/-	n	p
76 (36%)	111 (52%)	26 (12%)	213	< 0.001

} *P=0.0045*

A detailed comparison of these two intercrosses focusing specifically on the relationship between levels of FX activity in mothers and representation of FX knock-out mice at birth reveals insights and implications that were not previously possible with other crosses. First, the comparison shows an apparent correlation between levels of FX activity in mothers and representation of full-term FX knock-out mice with decreased levels of maternal FX activity resulting in increased embryonic lethality of FX(-/-) mice and thus their reduced representation at birth. Although the observed correlation between FX activity in mothers and representation of FX knock-out mice at birth can be attributed to variations in the mixed genetic backgrounds of mice used in the study (i.e. FX-deficient mice were not bred on a single, pure genetic background), results

summarized in Table 12 are nonetheless consistent with the hypothesis of maternal transfer of FX during embryonic development.

Taken together, these findings suggest that 1) there is a maternal transfer of FX during development; 2) the maternal contribution of FX is perhaps variable (levels of maternal FX activity represent the limiting factor); 3) maternal FX supports embryonic survival of FX knock-out mice. Furthermore, if the hypothesis of maternal transfer is indeed correct, it can then be concluded that partial embryonic lethality of FX(-/-) mice may be due to variable transfer of maternal FX adequate to support embryonic survival of some but not all FX-knock-out mice, and moreover that the embryonic requirement for FX is essential, evident in reduced maternal FX levels resulting in increased embryonic lethality of FX knock-out mice.

Second, the comparison of two intercrosses described above also reveals additional insight for determining whether it was the restoration of minimal FX catalytic activity or of FX antigen that enabled rescue of FX knockout mice from embryonic lethality. As shown earlier, FX knock-out mice did not show any FX activity or FX antigen. Expression of FX-Friuli with 4-8% FX activity and normal FX antigen levels was able to achieve complete rescue of FX knock-out mice from embryonic and perinatal lethality. While it is thought that catalytic function of FX is essential for perinatal survival, it is unclear whether catalytic activity of FX protein is required for embryonic survival. [Some studies have suggested that FX/FXa have the ability to induce biological responses in the absence of its catalytic activity].⁵²⁻⁵⁴ In other words, are FX

mice able to survive embryonic development on a catalytically inactive FX protein? Comparison of the two intercrosses above [FX(-/F) intercross and FX(+/-) intercross] (Table 12) suggests that embryonic survival of FX mice on a catalytically inactive FX protein is unlikely. While FX(-/F) and FX(+/-) mothers demonstrated distinct levels of FX activity (1-3% and ~50% respectively), they actually shared similar levels of FX antigen (~50%; FX protein synthesis is absent from the knock-out allele, but present at similar levels for the Friuli and wild-type alleles as demonstrated in Western blot analysis). Therefore, if the hypothesis of maternal transfer of FX is correct, an inference can be drawn; reduced representation of full-term FX knock-out mice (2% of total progeny) from FX(-/F) mothers compared to 12% full-term FX knock-out mice from FX(+/-) mothers is due to maternal transfer of reduced FX activity rather than of FX antigen (since FX(-/F) and FX(+/-) mothers have similar levels of FX antigen but distinct levels of FX activity). Furthermore, one can conclude that it was the restoration of minimal FX catalytic activity (not of FX antigen) with the expression of homozygous FX-Friuli that rescues FX knock-out mice from lethality.

Based on the conclusions made here, the following prediction is made. It can be hypothesized that an intercross of specific heterozygous FX mice (mice with one wild-type FX allele and one mutated FX allele; the second allele results in normal synthesis of catalytically inactive FX protein) should produce homozygous FX mutated mice that behave virtually as FX Knock-out mice in terms of their representations at birth (12%). Despite synthesizing normal

levels of FX antigen, these homozygous mice like FX knock-out mice will not have any FX catalytic activity, which was suggested earlier to be essential for embryonic survival. For these homozygous FX-mutated embryos, the only source of catalytically active FX protein will be the mothers (~50% FX activity) as it was for FX knock-out embryos resulting from FX(+/-) mothers (also ~50% FX activity).

Third, while relative embryonic survival of FX knock-out mice is directly dependent on the specific genotype of the mother (with specific levels of maternal FX activity), the embryonic success of FX(-/F) mice is completely independent of the mother's genotype. For instance, in both FX(F/F) X FX(+/-) cross and FX(-/F) intercross, FX(-/F) mice were born at expected frequencies with absence of embryonic lethality. Therefore, endogenous FX activity as low as 1% (shown by the FX(-/F) genotype) is sufficient to support both embryonic and postnatal survival, regardless of mother's genotype [FX(+/-), FX(+/F), FX(F/F), or FX(-/F)].

The underlying cause of embryonic lethality of FX knock-out mice is still unclear. Recall examination of yolk sacs of E10.5, E11.5 and E12.5 FX knock-out embryos from FX(-/F) mothers revealed complete absence of vasculature (Figure 25B, E and H), whereas normal vasculature development was clearly observed in the yolk sacs of FX(-/F) embryos respectively from the same litters (Figure 25C, F and I). At the same time, inspection of the FX knock-out embryos themselves also revealed that they have already reabsorbed or have begun to reabsorb. One hypothetical explanation may be that FX is either

directly or indirectly involved with the proper formation and/or development of vasculature in the yolk sac, and consequently in the absence of FX-related function, development of the yolk sac vasculature is impaired, leading to re-absorption and thus embryonic lethality of FX knock-out mice. Alternatively, it may be the death of FX knock-out embryo that leads to the observed abnormalities in the yolk sac vasculature. At this point, it is unclear which event occurs first or simultaneously. At the same time, it is important to note that FX transcript has been detected in both embryo and yolk sac as early as E7.5 in development.⁵⁵

Still a point of uncertainty is whether embryonic lethality and perinatal mortality share the same underlying cause. While failure to generate thrombin has been thought to be the cause of perinatal lethality in FX-knock-out mice, the underlying cause of embryonic lethality remains to be deciphered. In other words, it is unclear whether embryonic failure and perinatal mortality can be attributed to absence of a single function of FX; does FX have two distinct roles in development and postnatal survival?

In summary, the data presented in this chapter suggest that FX (catalytically active FX) is required for embryonic survival, whether it is embryonic or maternal in origin. If the FX source is embryonic, FX activity as low as 1% [as in FX(-/F) mice] is sufficient to support both embryonic and postnatal survival independent of the mother's genotype. However, if the only FX source is maternal as it is for FX knock-out embryos, the likelihood of embryonic survival of these mice is directly dependent on the specific genotype

of the mother. Reduced levels of maternal FX activity result in decreased embryonic survival of FX knock-out mice and their decreased representation at birth. Although these findings and observations do not define a specific developmental role for FX (as demonstration of its requirement does not necessarily reveal its essential function), they do support a role of maternal FX in embryonic success of FX knock-out embryos. Moreover, the data suggest that the maternal transfer of FX is perhaps variable (i.e. variable in distribution), sufficient to support embryonic survival of some but not all FX knock-out mice. Perhaps, it was variable transfer of maternal FX that results in partial embryonic lethality of FX-null mice. In light of data presented here, it is likely that partial embryonic lethality also observed in both FV and FII (prothrombin) knock-outs is due to limited maternal transfer of the respective hemostatic factors.

4. FX expression during development

4.1 Introduction

In contrast to other vitamin K-dependent clotting factors, FVII and FIX, which are expressed solely in liver, FX is expressed predominantly, but not exclusively in liver.^{47,70} Northern blot analysis of adult human tissues revealed FX mRNA in various tissues in addition to liver.⁴⁷ Functional study of the 5' flanking region of human FX gene revealed an interaction of a regulatory sequence (CCAAT) with an ubiquitous transcription factor, NF-Y.⁴⁷ Though the same regulatory sequence is found in the 5' flanking region of FIX gene, it interacts with a transcription factor, NF-1 that is structurally unrelated to the ubiquitously expressed NF-Y transcription factor.^{71,72} These observations may explain why FX is expressed in multiple tissues whereas expression of FIX is confined to liver. RT-PCR analysis of some cell lines derived from the central nervous system (human glioblastoma and human neuroblastoma) also demonstrated FX mRNA in those cells.⁷³

Additionally, RT-PCR analysis of RNA from various tissues of adult mouse showed FX transcript in multiple tissues including liver, stomach, intestine, kidney, skeletal muscle, ovary, testes, and spleen.⁷⁴ Though not identical, tissue distribution of FX expression in adult mouse is similar to that in adult human.⁴⁷ Despite what has been learned about the tissue distribution of FX in adult mouse, little is known about the embryonic expression pattern of FX. As a matter of fact, to date, spatial and temporal patterns of FX expression during mouse development have yet to be characterized. On the other hand,

characterization of various chick embryonic tissues at E13 revealed FX mRNA of various levels in liver, chorioallantois, allantoamnion, kidney, spleen, and intestine.⁷⁵ In light of this finding in chick embryonic tissues, it is of interest to determine whether FX expression during murine development is also observed in multiple tissues.

Thus far, the underlying cause of embryonic lethality of FX knock-out mice is still unclear. Could embryonic lethality observed in FX knock-out mice be attributed to a function of FX/FXa that is independent of its role in thrombin generation in blood coagulation? A previous study on embryonic expression of murine coagulation system components has reported early expression of some hemostasis-related genes (including FX) prior to the formation of a functional circulatory system.⁵⁵ This finding supports the concept that some coagulation factors may have additional non-hemostatic functions during development. Temporal and spatial delineation of FX expression may provide some clues to its function(s) during development. For example, a comparative analysis of the embryonic expression pattern of FX with that of a similarly expressed biological molecule (i.e. cellular receptor) may reveal developmentally crucial interactions that were previously overlooked. Furthermore, identification of FX expression in specific embryonic tissues may provide important knowledge to design an alternative rescue strategy for FX knock-out mice (i.e. tissue-specific rescue of FX knock-out mice). Therefore, the primary objective of the study presented in this chapter is to gain some insight into the embryonic pattern of murine FX

expression by carrying out both *in situ* hybridization and immunohistochemical study.

4.2 Materials and methods

4.2.1 Timed mating of heterozygous FX(+/-) mice

Conception was determined by observation of a coital plug. At various stages of embryonic development (e.g. E9, E10.5, E11.5, E12.5, E13.5, E14.5, and E15.5), pregnant females were sacrificed, and only viable (non-reabsorbed) embryos were harvested, fixed in 4% paraformaldehyde, and further processed for either *in situ hybridization* of whole mount embryos or of paraffin-embedded embryo sections (depending on the embryonic age). To prevent any discrepancy in treatment of samples, genotype of viable embryos was determined only after each hybridization experiment, using yolk sac DNA. Attempt to genotype reabsorbed embryos was also made; in DNA samples that were not yet completely degraded at the time of isolation, FX-knock-out genotype was recovered at greater than 90% frequency. Reabsorbed embryos were not treated for *in situ* hybridization because of degraded transcript.

4.2.2 Synthesis of FX riboprobes

Mouse FX cDNA (~1.1-kb) corresponding to exons 1 to 7 and FX cDNA (~340-bp) corresponding to exon 8 were cloned separately into a transcription vector (pBluescript II SK(+/-); Stratagene) at *EcoRI* / *EcoRV* sites and *EcoRV* / *HincII* sites, respectively. Before *in vitro* transcription using the DIG-labeling kit (Roche), two DNA templates were linearized by digestion with *EcoRI* or *EcoRV*, respectively. Following separate *in vitro* transcription reactions with

Digoxigenin-UTP and RNA polymerase T7, two Digoxigenin-labeled antisense FX RNA (ribo) probes were generated; a 1.1-kb anti-sense FX riboprobe and a 340-b anti-sense FX riboprobe. To generate the sense probes, two DNA templates were digested with *EcoRV* or *Drall*, respectively. Two separate *in vitro* transcription reactions were carried out using RNA polymerase T3 to generate the corresponding Digoxigenin-labeled sense FX riboprobes.

4.2.3 Whole-mount *in situ* hybridization (E9 to E12.5)

In situ hybridizations of whole-mount embryos were carried out based on a protocol (kindly provided by Dr. J. Golden, University of Pennsylvania). After re-hydration, embryos were bleached with 6% hydrogen peroxide, treated with 10 µg/ml proteinase K for 20 minutes, and washed with 2 mg/ml glycine solution for 10 minutes. Following post-fixation for 20 minutes with 4% paraformaldehyde and 0.2% glutaraldehyde solution, embryos were incubated in pre-hybridization solution (50% deionized formamide, 5x SSC (pH 4.5), 1% SDS, 50 µg/ml heparin, 50 µg/ml yeast RNA) for 1 hour at 70°C, and then in hybridization solution containing either the 1.1-kb anti-sense FX riboprobe or the 340-b anti-sense FX riboprobe (1 µg/ml) at 70°C overnight. After several washes, embryos were blocked with blocking solution (10% heated inactivated sheep serum, 2% blocking reagent, Roche, and 2 mM levamisole) for 2 hours, and incubated overnight at 4°C with 1:2000 pre-absorbed sheep anti-DIG, alkaline phosphatase conjugated Fab (Roche cat# 1093274) in solution containing 1% heat inactivated sheep serum, 2% blocking reagent (Roche), and 2 mM levamisole in TBST (50 mM Tris-HCl, pH7.5, 150 mM NaCl, 10 mM KCl,

and 0.1% Tween 20). After washes with TBST, embryos were washed 3x for 10 minutes each with NTMT (100 mM NaCl, 100 mM Tris, pH 9.5, 50 mM MgCl₂, 0.1% Tween, and 2 mM levamisole), and then incubated with BM purple (Roche) in darkness until sufficient signal intensity was developed (usually overnight at 4°C). After sufficient color development, embryos were washed 2x for 10 minutes each with NTMT and 2x for 10 minutes each in PBT (PBS, pH 5.5, 0.1% Tween 20), post-fixed with 4% paraformaldehyde, 0.1% glutaraldehyde in PBS for one hour at room temperature, further washed with PBT, and stored in PBT at 4°C until further microscopic analysis. When available, knock-out embryos were included in the same analysis. For other negative controls, corresponding DIG-labeled sense FX riboprobe was used in place of an anti-sense FX riboprobe.

4.2.4 *In situ* hybridization of paraffin-embedded embryo tissue sections (E13.5 to E15.5)

With some additions, the following protocol was also based on a protocol (kindly provided by Dr. J. Golden). To carry out *in situ* hybridizations of paraffin-embedded embryo tissue sections, sections were dewaxed in xylene and treated in a graded series of methanol/PBT solutions (from 100% methanol to 25% methanol/PBT). After wash in DEPC-treated PBS, sections were fixed in 4% paraformaldehyde (pH 7.2) for 20 minutes. After additional wash in DEPC-treated PBS, sections were treated with 10 µg/ml proteinase K in PBS (for 5-20 minutes depending on the age of embryo section). Following proteinase K treatment and PBS wash, tissue sections were post-fixed with 4%

paraformaldehyde (pH7.2) for 15 minutes. Following additional washes in DEPC-treated PBS, sections were acetylated; sections were incubated 2 x 5 minutes in 0.1 M triethanolamine (TEA) buffer, pH8.0 containing 0.25% (v/v) acetic anhydride (Sigma) in Coplin jars, which were rocked vigorously. Subsequently, sections were covered in pre-hybridization mix (50% deionized formamide, 5X SSC, 2% blocking powder (Roche), 0.1% Triton X-100, 0.1% CHAPS (Sigma), 1 mg/ml tRNA, 5 mM EDTA, and 50 µg/ml heparin). Before pre-hybridization, tissue sections were covered with a piece of parafilm, placed in a box containing tissue paper soaked in 50% formamide and 5X SSC, and incubated for one hour at 70°C. Next, sections were incubated with hybridization mix containing either the 1.1-kb DIG-labeled anti-sense FX riboprobe or the 340-b DIG-labeled anti-sense FX riboprobe (650 ng/ml) in 70°C overnight. Following overnight hybridization, slides were washed 3x for 15 minutes each in a solution (50% formamide, 5% SSC (pH4.5, 1% SDS) at 70°C, then 3x for 15 minutes each in another solution (50% formamide, 2X SSC, pH4.5) at 65°C, and then 3x for 5 minutes each in TBST at room temperature. Next, slides were blocked in 10% heat inactivated sheep serum/TBST for 30 minutes and incubated with a Sheep anti-DIG alkaline phosphatase conjugated Fab (Roche; 1:2000) in the blocking solution at 4°C overnight. Subsequently, slides were washed with TBST 3x for 10 minutes each and with NTMT 3x for 5 minutes each. For color development, slides were incubated in BM purple in darkness. When sufficient signal developed, color reaction was stopped by washing slides in PBT (pH5.5). After the wash, slides were dehydrated, cleared

with xylene, mounted in Permount and coverslipped before further analysis.

When available, tissue sections from FX knock-out embryos were included in the same analysis. For other negative controls, corresponding DIG-labeled sense FX riboprobe was used in place of an anti-sense FX riboprobe.

4.2.5 Immunohistochemical staining for FX antigen

The protocol used for immunohistochemical studies of FX protein expression was based on that provided by Vector Laboratories (Burlingame, CA). Paraffin-embedded embryo tissue sections were cleared in xylene and hydrated in a series of decreasing concentrations of alcohol solutions. Following the manufacturer's instructions to unmask antigen, slides were boiled in diluted antigen unmasking solution (Vector laboratories) for 1 minute. Slides were incubated with 0.3% hydrogen peroxide in ddH₂O for 30 minutes to quench possible endogenous peroxidase activity and washed in PBS. To block the sections, slides were treated with diluted normal blocking serum (1.5%.) for 30 minutes. After the wash, sections were incubated with an adsorbed sheep anti-human FX antibody (10 µg/ml; Cedarlane) for 30 minutes, washed in PBS, and incubated with diluted biotinylated secondary antibody (Vectastain Elite ABC kit with sheep IgG; Vector laboratories). To amplify signal, sections were incubated with Vectastain Elite ABC reagent for 30 minutes before the color reaction. To develop color signal, sections were incubated with peroxidase substrate solution (Vector NovaRED; Vector laboratories). After staining, sections were rinsed in ddH₂O, cleared with xylene, and mounted with Vecta Mount (Vector Laboratories) for further analysis. When available, tissue sections from FX

knock-out embryos were included in the same analysis. Other negative control included omission of the primary antibody in the staining procedure.

4.3 Results

4.3.1 Whole-mount *in situ* hybridization (E9 to E12.5)

Whole-mount *in situ* hybridization studies demonstrated FX mRNA in the midsection of E9 and E10.5 wild-type embryos (Figures 30 and 31).

Examination of an older (E11.5) embryos (hybridized with the DIG-labeled anti-sense FX 1.1-kb probe) yielded similar results; FX mRNA was detected in the midsection of a wild-type embryo, but not in a knock-out littermate (Figure 32).

No other prominent staining was noted in either. A comparison of a wild-type

E12.5 embryo with its FX knock-out littermate also revealed FX transcript in the liver area of the wild-type embryo, but its absence in the knock-out embryo

(Figure 33). This result is consistent with the use of DIG-labeled antisense FX

exon 8 riboprobe in the hybridization, demonstrating absence of a transcript

containing exon 8 in the knock-out embryo. More detailed inspection of the

wild-type E12.5 embryo revealed a punctate staining pattern in liver. This may

reflect areas of hepatocytes (positive staining) interspersed with blood forming

islands (negative staining for FX), since liver is still a major site of hematopoietic

activity at this stage of development.

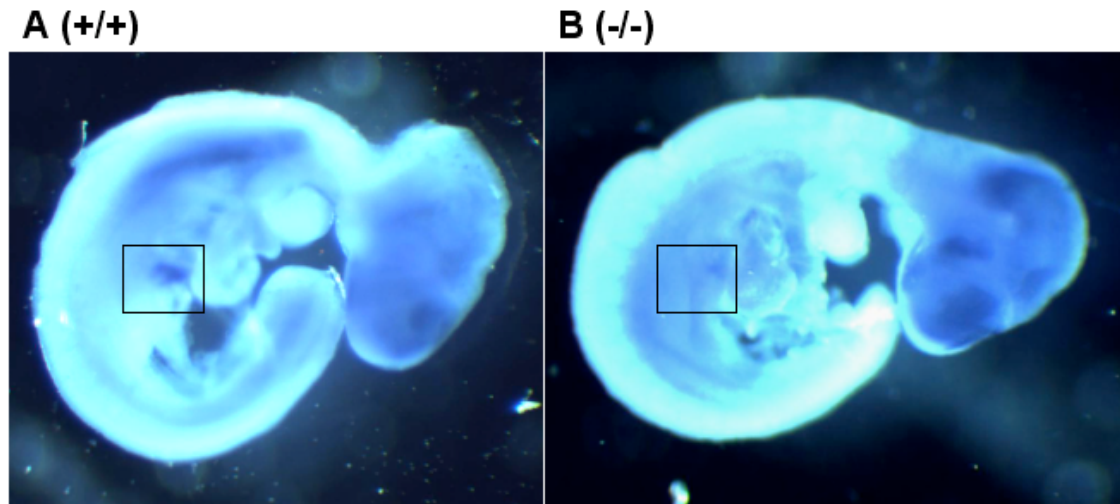


Figure 30. Whole-mount *in situ* hybridization of E9 embryos. E9 embryos were hybridized with a DIG-labeled antisense FX 1.1-kb probe. Note a hybridization signal (boxed area) in wild-type E9 embryo (A) and absence of the same signal in a FX knock-out littermate (B).

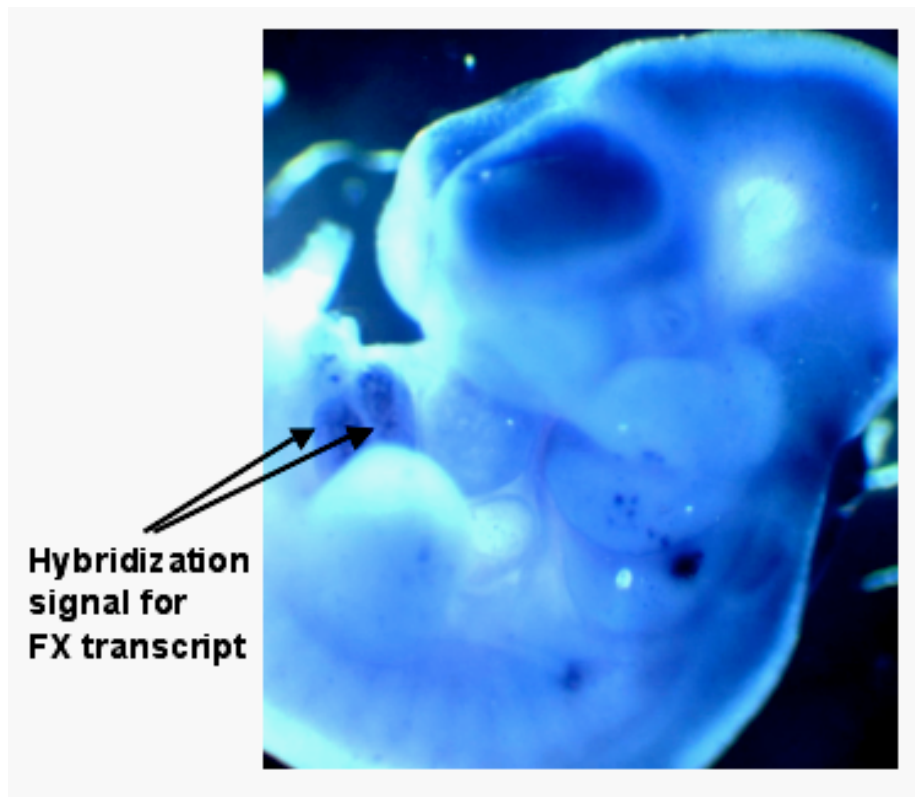


Figure 31. Whole-mount *in situ* hybridization of an E10.5 embryo. A wild-type E10.5 embryo was hybridized with a DIG-labeled antisense FX 1.1-kb probe. Positive signal was detected in the liver area. False-positive signals in other areas might be due to trapping of the probe.

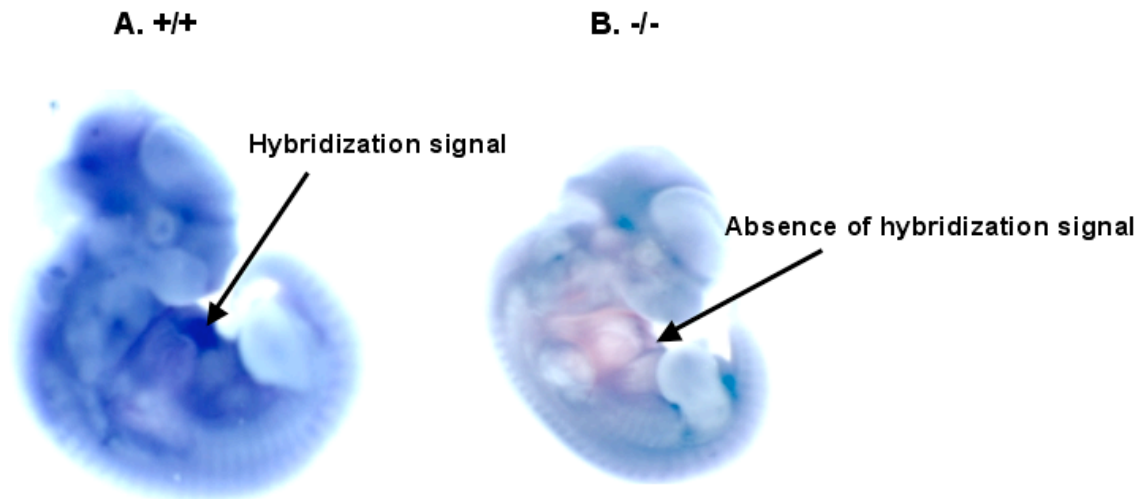


Figure 32. Whole-mount *in situ* hybridization of E11.5 embryos. Embryos were hybridized with a DIG-labeled antisense FX 1.1-kb probe. While a signal was observed in the liver area of a wild-type embryo (A), it was not detected in the same area of a FX knock-out littermate (B).

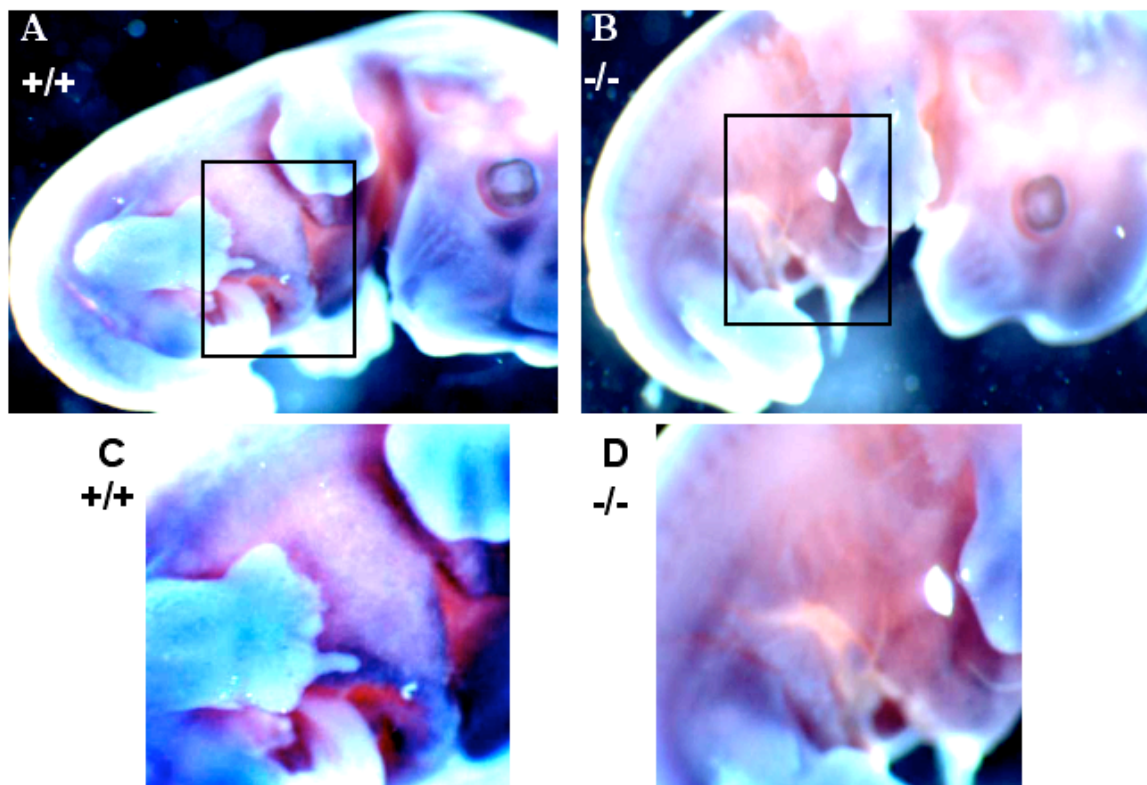


Figure 33. Whole-mount *in situ* hybridization of E12.5 embryos. Embryos were hybridized with a DIG-labeled antisense FX exon 8 probe. While a signal was observed in the liver area of a wild-type embryo (A and C), Figure 33 (*continued*),

it was not detected in the same area of a FX knock-out littermate (B and D). In this case, the signal is noted as a punctate staining pattern.

4.3.2 *In situ* hybridization of paraffin-embedded embryo tissue sections (E13.5 to E15.5)

In situ hybridizations of E13.5 wild-type paraffin-embedded tissue sections showed FX mRNA in liver when hybridized with the DIG-labeled anti-sense FX exon 8 riboprobe (Figures 34A and C) and absence of FX mRNA in the same tissues when hybridized with the corresponding sense riboprobe (Figures 34B and D). Tissue distribution of FX mRNA expression widened in further developed embryos. Examination of FX mRNA expression in E14.5 wild-type tissue sections indicated FX transcript in various tissues (liver, lung, brain, and kidney) after sections were hybridized with the DIG-labeled anti-sense FX 1.1-kb riboprobe (Figures 35A, C, E and G). However, when hybridized with the corresponding sense probe, tissue sections from the same embryo failed to demonstrate FX transcript in any of these tissues (Figures 35B, D, F and H). *In situ* hybridization of E15.5 wild-type tissue sections disclosed still further expansion of FX expression; when hybridized with the DIG-labeled anti-sense FX 1.1-kb riboprobe, embryo sections revealed FX transcript in multiple tissues including liver, lung, dorsal root ganglia, thymus, and anterior aspect of brain (Figure 36). There was little or no hybridization signal in GI tract (Figure 36).

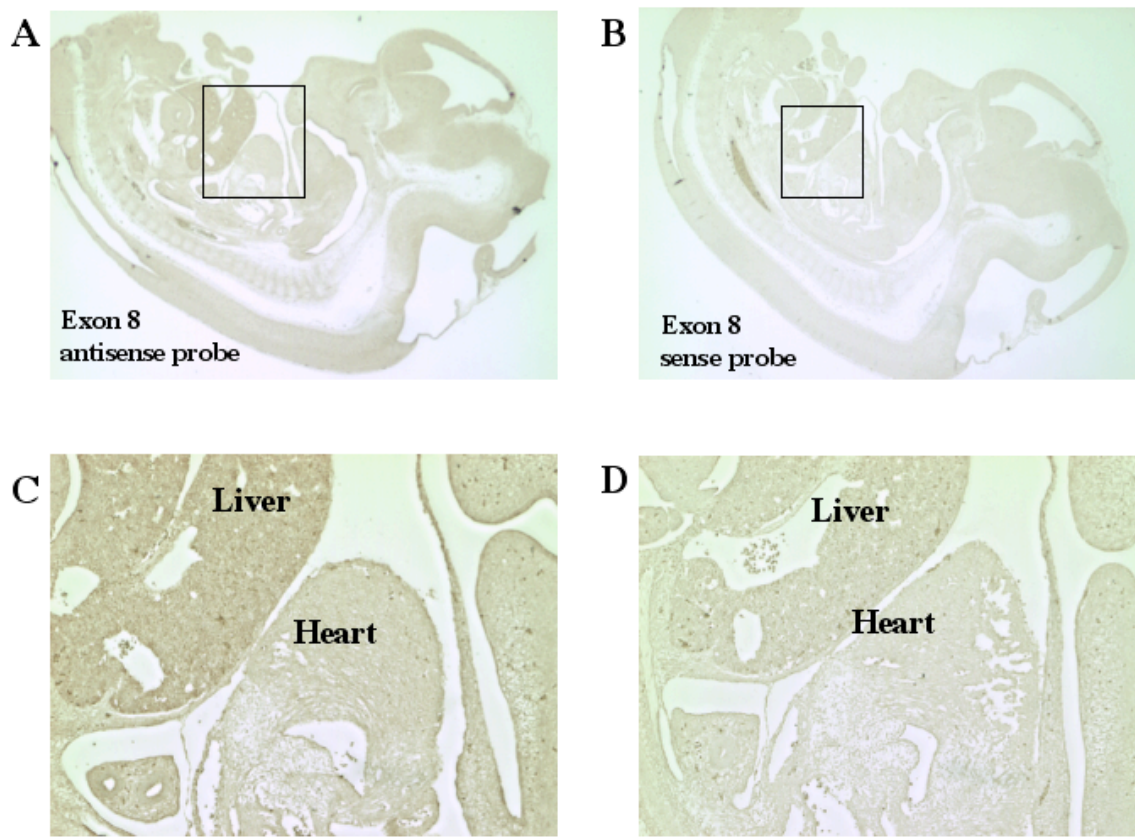


Figure 34. *In situ* hybridization of E13.5 wild-type paraffin-embedded embryo sections. Sections were hybridized with either DIG-labeled anti-sense FX exon 8 probe or the sense probe. Signal was detected in the liver of an embryo section hybridized with an anti-sense probe (A and C). No signal was observed in the liver of an embryo sections hybridized with a sense probe (B and D). No other prominent hybridization signals were noted (A-D).

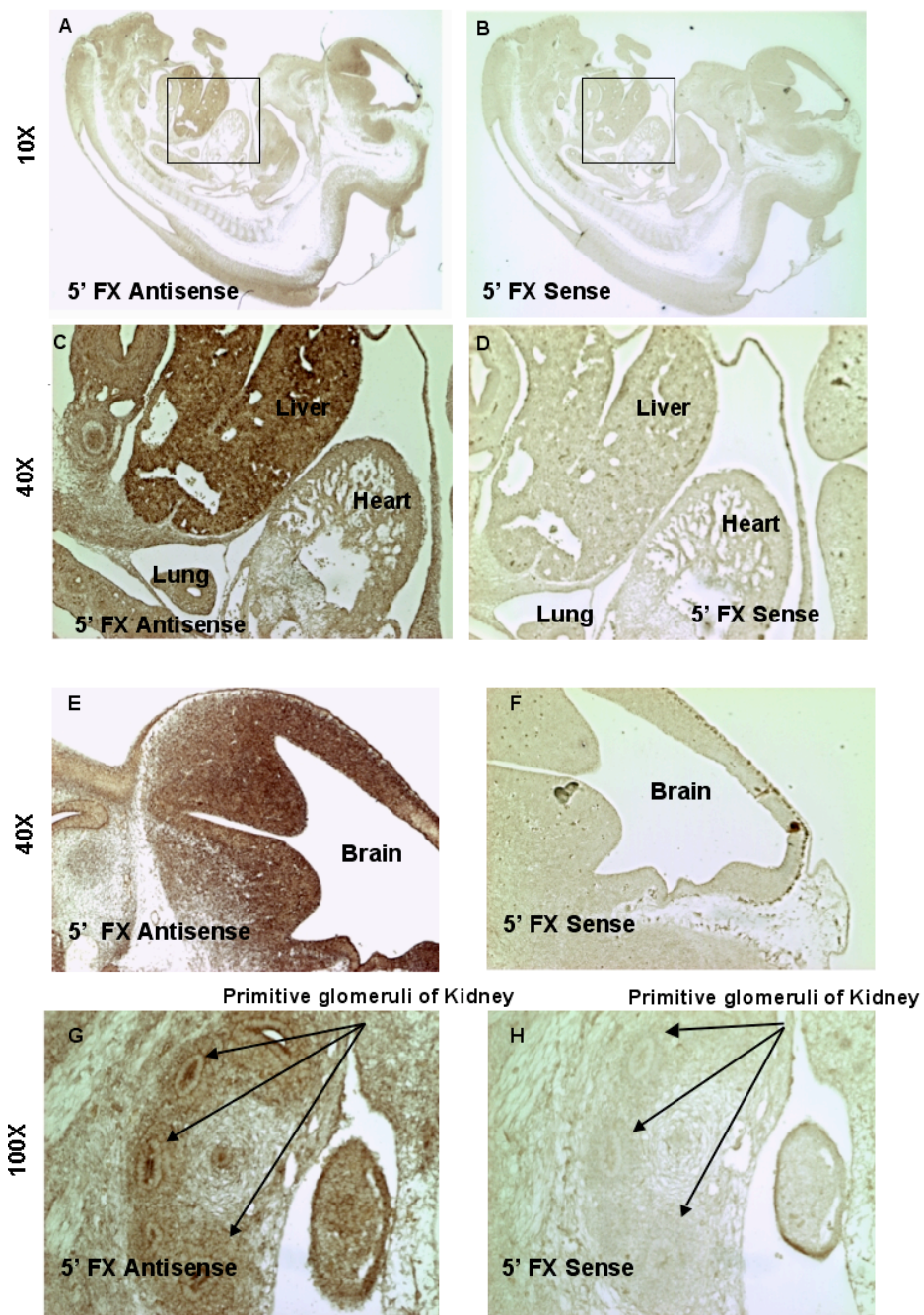


Figure 35. *In situ* hybridization of E14.5 wild-type paraffin-embedded embryo sections. Sections were hybridized with either DIG-labeled anti-sense FX 1.1-kb probe or the sense probe. FX signal was detected in multiple tissues when sections were hybridized with an anti-sense probe (A, C, E and G). No signal was noted in any tissue when sections were hybridized with a sense probe (B, D, F and H).

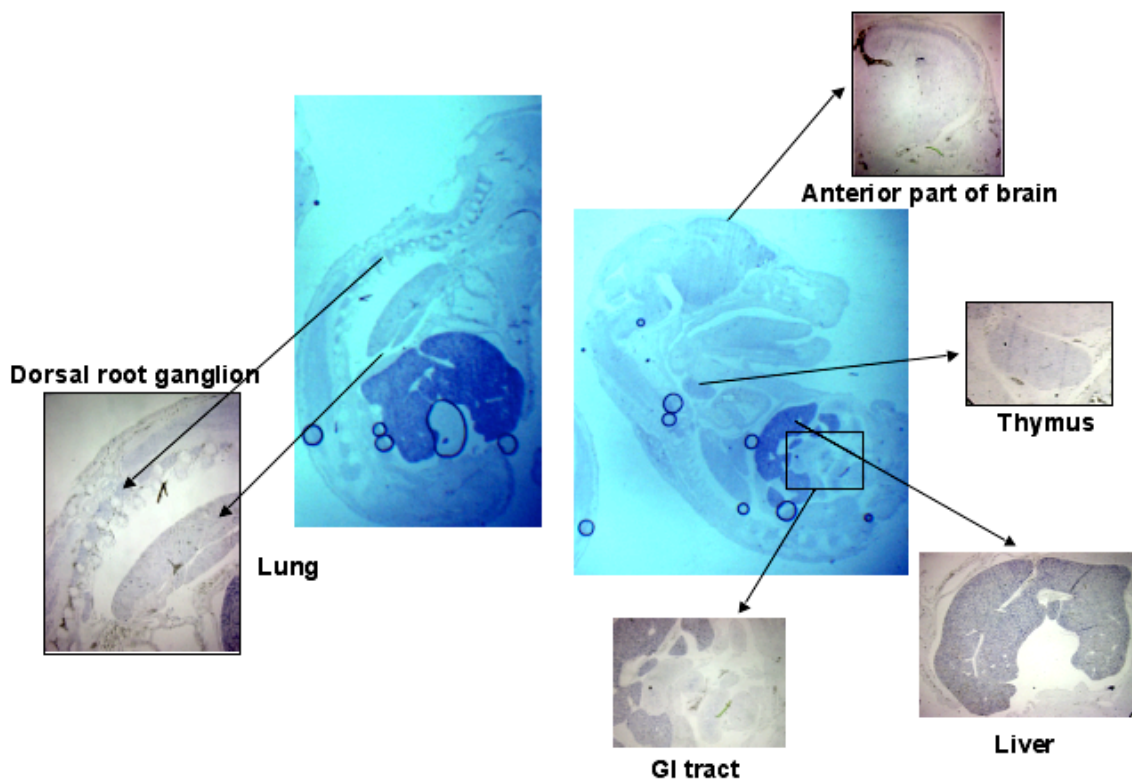


Figure 36. *In situ* hybridization of E15.5 wild-type paraffin-embedded embryo sections. Shown above are sections hybridized with a DIG-labeled anti-sense FX 1.1-kb probe. Hybridization signal was detected in multiple tissues including liver, dorsal root ganglia, lung, thymus, and anterior part of brain. Little or no signal was detected in GI tract.

4.3.3 Immunohistochemical staining for FX antigen

In the immunohistochemical study, a polyclonal antibody raised against human FX and showing cross-reactivity with mouse FX was adsorbed and used to investigate FX expression during mouse development. FX expression was observed in multiple tissues with its expression detected in more tissue types in the later stages of development than in an earlier stage. At E12.5, FX expression was noted not only in the liver, but also in the heart, and lung (Figures 37A and B). These findings are supported by the absence of FX

expression in the corresponding tissues in a FX knock-out littermate (Figures 37C and D). Although some background staining can be observed in the lung of the E12.5 FX knock-out embryo, its intensity is minimal compared to the strong signal intensity shown in the lung of a wild-type littermate.

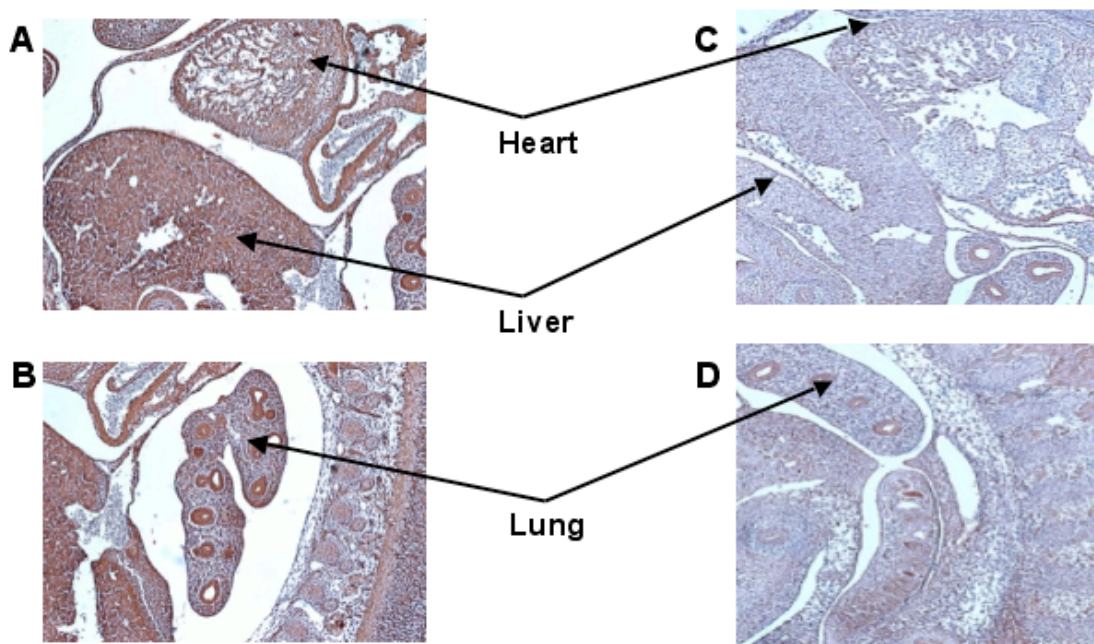


Figure 37. FX expression in E12.5 embryos. Paraffin-embedded sections from an E12.5 wild-type embryo (A and B) and from its knock-out littermate (C and D) were incubated with a adsorbed polyclonal sheep anti-human FX antibody. While signals were detected in wild-type tissues, no signal was observed in FX knock-out tissues.

At E14.5, FX expression widened to include expression in liver, lung, gastrointestinal tract, kidney, adrenal gland, dorsal root ganglia, thymus, and anterior aspect of brain (Figure 38). At this stage of development, the stronger staining for FX expression was located in liver, kidney, adrenal gland, dorsal root ganglia, and anterior area of brain with moderate and weaker staining

noted in thymus, lung, and gastrointestinal tract. Interestingly, no FX expression was detected in the heart as it was in E12.5 embryos.

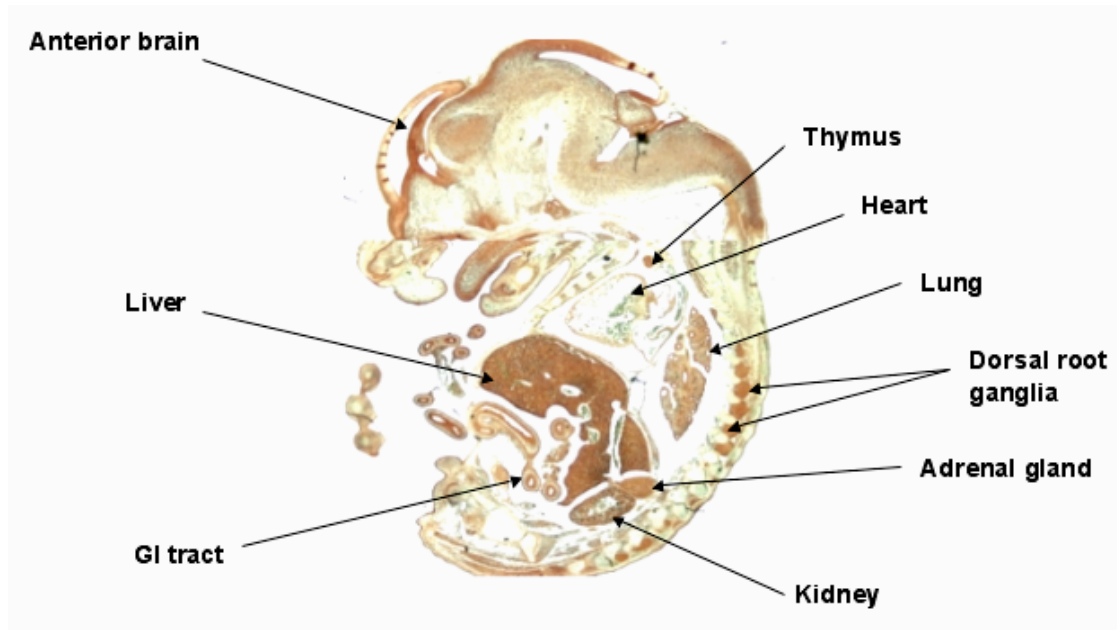


Figure 38. FX expression in E14.5 embryos. At this stage of development, FX expression was detected in multiple tissues in addition to liver.

At E15.5, FX expression persisted in all those tissues in which FX expression was observed in E14.5 embryos (Figure 38). Additionally, FX expression was seen in neopallial cortex and trigeminal ganglion (Figure 39). A weaker staining in the heart of an E15.5 embryo might be a false-positive staining 1) as it was absent in the left side of the same embryo, and 2) it was absent in the heart of E14.5 embryos, which showed very similar tissue distribution of FX expression.

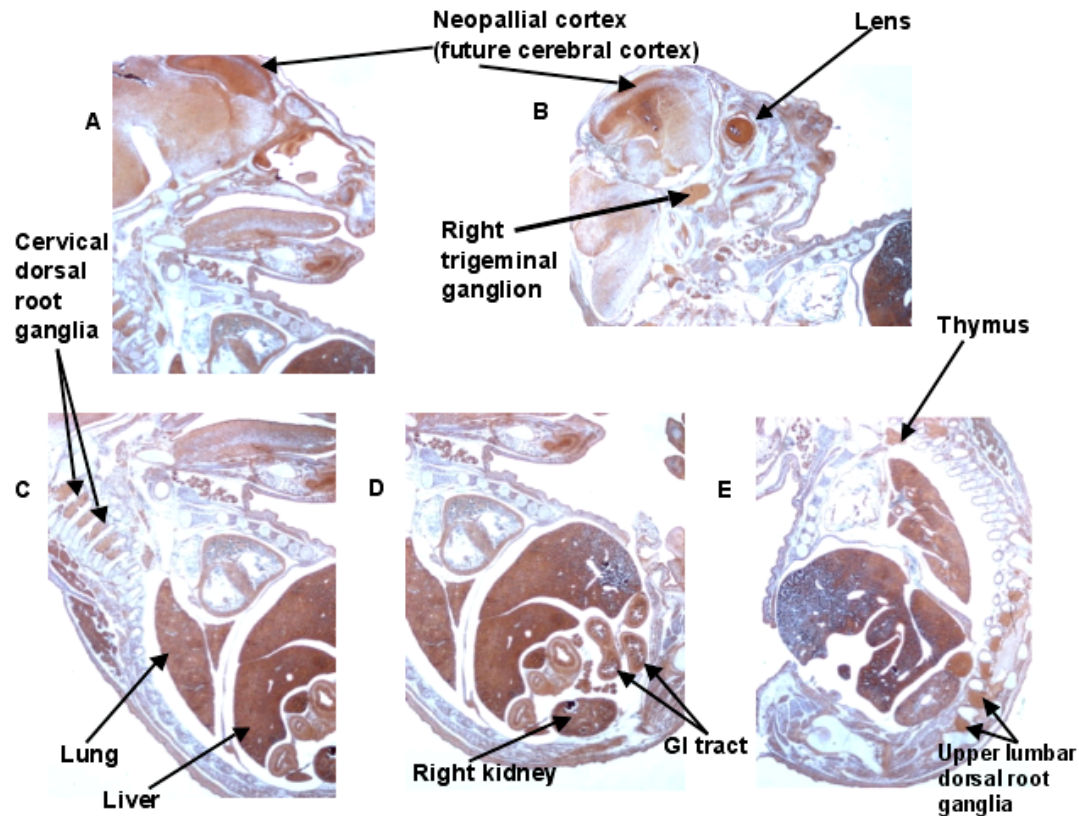


Figure 39. FX expression in E15.5 embryos. Likewise, FX expression was detected in multiple tissues in addition to liver.

4.4 Discussion

Although FX transcript is found in a number of adult tissues,⁷⁴ little is known about its spatial or temporal pattern of expression during mouse development.

The goal in this chapter is to investigate the embryonic expression pattern of FX at the tissue level, using both *in situ* hybridization and immunohistochemistry.

During the early stages of mouse development (E9-E12.5), FX expression is predominantly located in the abdominal region (i.e. liver) with no apparent expression found in other tissues (Figures 30-33). Separate *in situ*

hybridizations using the anti-sense FX 1.1-kb riboprobe or the anti-sense FX

exon 8 riboprobe indicated consistent absence of FX transcript in FX knock-out embryos. Taken together, these findings suggest the instability of exon 8-deleted FX transcript synthesized in the knock-out embryos.

According to the results of *in situ* hybridizations, embryonic distribution of the FX transcript directly correlates with the age of the embryo, with wider tissue distribution of the FX transcript in older than younger embryos. As expected, expression of FX transcript in the area of liver persisted throughout the duration of the embryonic ages examined (E9 to E15.5). At E14.5, FX transcript was also observed in kidney, lung, and certain areas of brain in addition to its already noted expression in liver (Figure 35). While expression of FX transcript was not noticeable in the kidney of E15.5 embryos, it was observed in other tissues including liver, lung, dorsal root ganglia, thymus, and the anterior aspect of the brain. Though not pinpointing the exact cell types responsible for FX transcription, these findings nevertheless demonstrate that FX expression is not confined to liver during development.

Some correlations were noted between *in situ* hybridization results and the immunostaining results for FX expression during mouse development. The strongest correlations between the two studies occurred in the older embryos (E14.5 and E15.5 embryos). Fewer correlations were observed in the younger E12.5 embryos. These observed discrepancies could be due to different abundance of the FX transcript in various developing tissues and to differences in the sensitivity of the two assays. The differential immunostaining pattern in E12.5 embryos from that observed in *in situ* hybridization is not likely due to

false-positive immunostaining considering the absence of the analogous staining pattern in E12.5 FX knock-out tissues.

An alternative strategy to delineate FX expression during development involves use of a previously described plug-and-socket targeting. A different FX plug construct containing a reporter gene (e.g. β -galactosidase or GFP) fused in frame with FX exon 8 sequences could be introduced into the HPRT-negative ES cells that were originally targeted by the FX socket construct. For example, determination of GFP expression pattern in heterozygous GFP embryos of various embryonic ages should accordingly reveal the spatial and temporal patterns of FX expression during development.

Understanding of the embryonic pattern of FX expression can be potentially useful in designing an alternative strategy for rescue of FX knock-out mice from embryonic lethality. In other words, rather than restoring minimal levels of FX activity as in the Friuli mice, is it possible to rescue FX knock-out embryos with tissue-specific restoration of FX expression? Is it possible to rescue FX knock-out embryos with hepatic-restricted expression of FX? In other words, is FX expression from tissues other than liver required to sustain embryonic development? These questions can be answered with the generation and subsequent breeding of two different mice to produce mice with hepatic-restricted expression of FX. To generate the first mouse, a FX plug construct containing three stop codons (flanked by loxP sites) upstream of exon 8 of FX gene, is introduced into the FX-null ES cells. Mice homozygous for the stop codons in FX gene will have similar phenotypes as those of FX knock-out

mice. Only the heterozygous mice will be viable and can be used for breeding. A second transgenic mouse expressing *cre* recombinase under the control of a liver-specific promoter will be generated. Crosses of these mice will ultimately generate mice that are homozygous for hepatic-restricted expression of FX. Homozygous mice can then be examined for their embryonic and postnatal survival. However, if hepatic-restricted expression of FX is insufficient to support embryonic survival, additional transgenic mice expressing FX in specific non-hepatic tissues can be generated and characterized. The choice of the specific non-hepatic tissue to attempt embryonic rescue will depend on the understanding of the embryonic pattern of FX expression.

Whether FX has a developmental-related role in addition to its function in thrombin generation remains to be elucidated. However, several studies and observations have together suggested a potential non-hemostatic role for FX. First, in contrast to closely related coagulation factors such as FVII and FIX, FX is expressed in multiple tissues in adult human, suggesting a likelihood of multiple functions.⁴⁷ RT-PCR analysis of adult mouse tissues has also demonstrated FX transcript in multiple tissues in addition to liver.⁷⁴ Other evidence supporting a non-hemostatic role for FX includes detection of FX transcript as early as E7.5 (i.e. prior to the formation of a functional circulatory system).⁵⁵ Still other studies have demonstrated the ability of FXa 1) to induce mitogenic activity in vascular smooth muscle cells both *in vitro* and *in vivo*, 2) to elicit enhanced release of endothelial cell mitogens independent of thrombin, and 3) to induce up-regulation of the *egr-1* transcription in human keratinocyte

cell line.^{50,52,76,77} Taken together, these findings suggest that FX may have biological role(s) other than thrombin generation that influence embryonic development and survival. Therefore, further understanding of the embryonic distribution of FX expression may unveil additional clues about its potential role(s) in mouse development.

5. Summary and future directions

In summary, the work presented here has shown that a mouse model of complete FX deficiency, constructed with a plug-and-socket targeting strategy, resulted in partial embryonic lethality, with FX-null mice born at ~50% expected number, and those surviving to term dying of bleeding complications within the first few days of birth. These findings and those of a previously described mouse model of FX deficiency⁶³ are consistent with data in humans in which complete FX deficiency is lethal. Timed matings suggested that embryonic lethality had occurred as early as E10.5 or even earlier. While the perinatal lethality in FX knock-out mice appears to be due to defective hemostasis, the exact cause of embryonic lethality is unclear, since it occurs in mid-gestation well before formation of a fully functional coagulation system, and furthermore, it occurs in the absence of obvious evidence for bleeding.

Expression of an analogous mouse mutation based on a naturally occurring human FX variant, FX-Friuli resulted in complete rescue of FX knock-out mice from both embryonic and perinatal lethality. Homozygous FX-Friuli mice FX(F/F) demonstrated a similar phenotype in terms of FX activity (averaging 5.5% in mice and 4-9% in humans), antigen (~100%), and survival as humans carrying the analogous mutation. Cross of homozygous FX(F/F) mice with heterozygous FX(+/-) mice produced FX(-/F) mice with even lower FX activity (1-3%) and 50% antigen levels. Normal survival of FX(-/F) mice demonstrated that as low as 1% FX activity and 50% antigen levels are nonetheless still sufficient to support both embryonic and postnatal survival.

Moreover, survival of FX(-/F) mice at 1-3% FX activity is similar to observations in humans, thus confirming utility of these mice as an accurate model for human bleeding disorders.

The value of FX(-/F) mice is not limited to their utility for studying and developing novel treatments for FX deficiency. FX(-/F) mice enable investigation into an elusive role of FX during development by allowing for examination of FX knock-out mice born to mothers with minimal levels of FX activity. In an important contrast to a viable FX knock-out embryo born to a FX(+/-) mother with 50% FX activity and antigen levels (Figure 26), some FX knock-out offspring of FX(-/F) mothers with 1-3% FX activity and 50% antigen levels clearly lack yolk sac vasculature and have reabsorbed in the absence of hemorrhage (Figure 25). While the cause and effect relationship is unclear, these observations are highly suggestive of an essential role of FX directly or indirectly in development.

Furthermore, FX(-/F) mice provide an opportunity to assess contribution of maternal FX to embryonic survival. Comparison between FX(-/F) intercross and FX(+/-) intercross suggests the following: 1) maternal transfer of FX or a direct relationship between maternal levels of FX activity and embryonic survival of FX knock-out mice with higher maternal levels of FX activity resulting in a greater representation of FX knock-out mice at birth; 2) rescue of FX knock-out mice from both embryonic and perinatal lethality is likely due to restoration of FX catalytic activity and not due to establishment of FX antigen.

Detection of the FX transcript in various tissues of adult mice also supports a hypothesis of multiple FX functions. Thus, coupled with other findings on FX, a detailed delineation of the embryonic pattern of FX expression may uncover additional clues to define the exact role of FX with relation to embryonic development.

At this point, several important questions about FX functions remain to be addressed. While complete FX deficiency is lethal and expression of a FX variant [i.e. FX(-/F)] with 1-3% FX activity and/or 50% antigen levels is compatible with life, the minimal characteristics of a FX molecule that are required to support embryonic or postnatal survival remain to be demonstrated. The utility of the plug-and-socket targeting strategy is that it will be possible to separate the roles of antigen and activity in embryonic survival. For example, one can characterize the embryonic effects resulting from expression of an active site mutation such as homozygous FX Stockton with no detectable activity but normal antigen levels.⁵⁷ Furthermore, one can evaluate the embryonic effects of a human FX variant with less than 1% activity and circulating antigen level (i.e. FX Stuart).^{68,69} Studies of these additional FX variants should define those characteristics of a FX molecule that are minimally required for embryonic development. As a matter of fact, these studies are already in progress.

Although the data presented in this study suggest maternal transfer of FX during development and that relative embryonic success of FX knock-out embryos depends on the maternal levels of FX activity, they are not absolutely

final. However, these results can be confirmed in mice backcrossed onto an inbred genetic strain such as C57/BL6 strain.

Finally, the challenge to elucidate the role of FX in development remains. Though a system [i.e. FX(-/F)] is in place to study the developmental role of FX, much remains to be learned. This work would entail the examination at different developmental time points of a large number of FX(-/-) embryos born to low FX(-/F) mothers and their comparison to FX(-/-) embryos born to FX(+/-) mothers with a much higher FX activity. This work would also involve a detailed examination of vasculature development in the yolk sacs as well as in the embryos themselves. One interesting experiment to pursue is to attempt rescue of FX knock-out mice through yolk sac-specific expression of FX. In other words, can the embryonic phenotype of FX knock-out mice as exemplified by the absence of yolk sac vasculature and re-absorption of embryos be rescued by restoration of FX expression in the yolk sac. This rescue would provide evidence for FX function in vasculature development and/or maintenance and the phenotypic characteristics of the FX(-/-) embryos from the rescued yolk sacs can then be evaluated. Although the exact cause of embryonic lethality in FX knock-out mice remains to be defined, this study and future studies outlined above will provide a better understanding of an elusive yet essential role of FX in development.

List of References

1. Rosen ED, Chan JC, Idusogie E, et al. Mice lacking factor VII develop normally but suffer fatal perinatal bleeding. *Nature*. 1997;390:290-294.
2. Bi L, Lawler AM, Antonarakis SE, High KA, Gearhart JD, Kazazian HH. Targeted disruption of the mouse factor VIII gene produces a model of haemophilia A. *Nature Genet*. 1995;10:119-121.
3. Kundu RK, Sangiorgi F, Wu L-Y, et al. Targeted inactivation of the coagulation factor IX gene causes hemophilia B in mice. *Blood*. 1998;92:168-174.
4. Lin H-F, Maeda N, Smithies O, Straight DL, Stafford DW. A coagulation factor IX-deficient mouse model for human hemophilia B. *Blood*. 1997;90:3962-3966.
5. Gailani D, Lasky NM, Broze GJ. A murine model of factor XI deficiency. *Blood Coag Fibrinol*. 1997;8:134-144.
6. Suh TT, Holmback K, Jensen NJ, et al. Resolution of spontaneous bleeding events but failure of pregnancy in fibronogen-deficient mice. *Genes Dev*. 1995;9:2020-2033.
7. Shivdasani RA, Orkin SH. Erythropoiesis and globin gene expression in mice lacking the transcription factor NF-E2. *Proc Natl Acad Sci U S A*. 1995;92:8690-8694.
8. Jalbert LR, Rosen ED, Moons L, et al. Inactivation of the gene for anticoagulant protein C causes lethal perinatal consumptive coagulopathy in mice. *J Clin Invest*. 1998;102:1481-1488.
9. Yin Z-F, Huang Z-F, Cui J, et al. Prothrombotic phenotype of protein Z deficiency. *Proc Natl Acad Sci USA*. 2000;97:6734-6738.
10. Cui J, O'Shea KS, Purkayastha A, Saunders TL, Ginsburg D. Fatal haemorrhage and incomplete block to embryogenesis in mice lacking coagulation factor V. *Nature*. 1996;384:66-68.
11. Sun WY, Witte DP, Degen JL, et al. Prothrombin deficiency results in embryonic and neonatal lethality in mice. *Proc Natl Acad Sci USA*. 1998;95:7597-7602.

12. Xue J, Wu Q, Westfield LA, et al. Incomplete embryonic lethality and fatal neonatal hemorrhage caused by prothrombin deficiency in mice. *Proc Natl Acad Sci USA*. 1998;95:7603-7607.
13. Toomey JR, Kratzer KE, Lasky NM, Stanton JJ, Broze GLJ. Targeted disruption of the murine tissue factor gene results in embryonic lethality. *Blood*. 1996;88:1583-1587.
14. Bugge TH, Xiao Q, Kombrinck KW, et al. Fatal embryonic bleeding events in mice lacking tissue factor, the cell-associated initiator of blood coagulation. *Proc Natl Acad Sci USA*. 1996;93:6258-6263.
15. Carmeliet P, Mackman N, Moons L, et al. Role of tissue factor in embryonic blood vessels development. *Nature*. 1996;383:73-75.
16. Huang Z-F, Higuchi D, Lasky N, Broze GJ. Tissue factor pathway inhibitor gene disruption produces intrauterine lethality in mice. *Blood*. 1997;90:944-951.
17. Healy AM, Rayburn HB, Rosenberg RD, Weiler H. Absence of the blood-clotting regulator thrombomodulin causes embryonic lethality in mice before development of a functional cardiovascular system. *Proc Natl Acad Sci USA*. 1995;92:850-854.
18. Liang Z, Cooper A, Rosen ED, Castellino FJ. Chromosomal arrangement of the murine coagulation factor VII and factor X genes. *Thromb Haemost*. 1998;80:524-525.
19. Gilgenkrantz S, Briquel ME, Andre E, et al. Structural genes of coagulation factors VII and X located on 13q34. *Ann Genet*. 1986;29:32-35.
20. Jagadeeswaran P, Reddy SV, Rao KJ, Hamsabhushanam K, Lyman G. Cloning and characterization of the 5' end (exon 1) of the gene encoding human factor X. *Gene*. 1989;84:517-519.
21. Leytus SP, Foster DC, Kurachi K, Davie EW. Gene for human factor X: a blood coagulation factor whose gene organization is essentially identical with that of factor IX and protein C. *Biochemistry*. 1986;25:5098-5102.
22. Cooper A, Liang Z, Castellino FJ, Rosen ED. Cloning and characterization of the murine coagulation factor X gene. *Thromb Haemost*. 2000;83:732-735.
23. Idusogie E, Rosen ED, Carmeliet P, Collen D, Castellino FJ. Nucleotide structure and characterization of the murine blood coagulation factor VII gene. *Thromb Haemost*. 1996;76:957-964.

24. Foster DC, Yoshitake S, Davie EW. The nucleotide sequence of the gene for human protein C. *Proc Natl Acad Sci U S A*. 1985;82:4673-4677.
25. Yoshitake S, Schach BG, Foster DC, Davie EW, Kurachi K. Nucleotide sequence of the gene for human factor IX (antihemophilic factor B). *Biochemistry*. 1985;24:3736-3750.
26. Heidtmann HH, Kontermann RE. Cloning and recombinant expression of mouse coagulation factor X. *Thromb Res*. 1998;92:33-41.
27. Liang Z, Cooper A, DeFord ME, et al. Cloning and characterization of a cDNA encoding murine coagulation factor X. *Thromb Haemost*. 1998;80:87-91.
28. Stanton C, Ross RP, Hutson S, Wallin R. Processing and expression of rat and human clotting factor-X-encoding cDNAs. *Gene*. 1996;169:269-273.
29. Rudolph AE, Mullane MP, Porche-Sorbet R, Miletich JP. Expression, purification, and characterization of recombinant human factor X. *Protein Expr Purif*. 1997;10:373-378.
30. James HL, Larson PJ, Chao YB, Yan SB, Kim DJ. Isolation and characterization of mouse coagulation factor X -- biophysical and enzymological properties. *Thromb Haemost*. 1997;78:1049-1054.
31. Leytus SP, Chung DW, Kisiel W, Kurachi K, Davie EW. Characterization of a cDNA coding for human factor X. *Proc Natl Acad Sci U S A*. 1984;81:3699-3702.
32. McMullen BA, Fujikawa K, Kisiel W, et al. Complete amino acid sequence of the light chain of human blood coagulation factor X: evidence for identification of residue 63 as beta-hydroxyaspartic acid. *Biochemistry*. 1983;22:2875-2884.
33. Hojrup P, Magnusson S. Disulphide bridges of bovine factor X. *Biochem J*. 1987;245:887-891.
34. Di Scipio RG, Hermodson MA, Davie EW. Activation of human factor X (Stuart factor) by a protease from Russell's viper venom. *Biochemistry*. 1977;16:5253-5260.
35. Fujikawa K, Legaz ME, Davie EW. Bovine factor X 1 (Stuart factor). Mechanism of activation by protein from Russell's viper venom. *Biochemistry*. 1972;11:4892-4899.
36. Titani K, Hermodson MA, Fujikawa K, et al. Bovine factor X 1a (activated Stuart factor). Evidence of homology with mammalian serine proteases. *Biochemistry*. 1972;11:4899-4903.

37. Esmon CT, Owen WG, Jackson CM. The conversion of prothrombin to thrombin. II. Differentiation between thrombin- and factor Xa-catalyzed proteolyses. *J Biol Chem.* 1974;249:606-611.
38. Mann KG. Prothrombin. *Methods Enzymol.* 1976;45:123-156.
39. Haley PE, Doyle MF, Mann KG. The activation of bovine protein C by factor Xa. *J Biol Chem.* 1989;264:16303-16310.
40. Foster WB, Nesheim ME, Mann KG. The factor Xa-catalyzed activation of factor V. *J Biol Chem.* 1983;258:13970-13977.
41. Donath MJ, Lenting PJ, Van Mourik JA, Mertens K. Kinetics of factor VIII light-chain cleavage by thrombin and factor Xa. A regulatory role of the factor VIII heavy-chain region Lys713-Arg740. *Eur J Biochem.* 1996;240:365-372.
42. Radcliffe R, Nemerson Y. Activation and control of factor VII by activated factor X and thrombin. Isolation and characterization of a single chain form of factor VII. *J Biol Chem.* 1975;250:388-395.
43. Owen WG. Evidence for the formation of an ester between thrombin and heparin cofactor. *Biochim Biophys Acta.* 1975;405:380-387.
44. Gitel SN, Medina VM, Wessler S. Inhibition of human activated Factor X by antithrombin III and alpha 1-proteinase inhibitor in human plasma. *J Biol Chem.* 1984;259:6890-6895.
45. Fuchs HE, Pizzo SV. Regulation of factor Xa in vitro in human and mouse plasma and in vivo in mouse. Role of the endothelium and plasma proteinase inhibitors. *J Clin Invest.* 1983;72:2041-2049.
46. Broze GJ, Jr. Tissue factor pathway inhibitor and the revised theory of coagulation. *Annu Rev Med.* 1995;46:103-112.
47. Hung HL, High KA. Liver-enriched transcription factor NHF-4 and ubiquitous factor NF-Y are critical for expression of blood coagulation factor X. *J Biol Chem.* 1996;271:2323-2330.
48. Senden NH, Jeunhomme TM, Heemskerk JW, et al. Factor Xa induces cytokine production and expression of adhesion molecules by human umbilical vein endothelial cells. *J Immunol.* 1998;161:4318-4324.
49. Camerer E, Rottengen J-A, Gjernes E, et al. Coagulation factors VIIa and Xa induce cell signaling leading to up-regulation of the *egr-1* gene. *J Biol Chem.* 1999;271:32225-32233.

50. Camerer E, Rottingen JA, Iversen JG, Prydz H. Coagulation factors VII and X induce Ca^{2+} oscillations in Madin-Darby canine kidney cells only when proteolytically active. *J Biol Chem.* 1996;271:29034-29042.
51. Nicholson AC, Nachman RL, Altieri DC, et al. Effector cell protease receptor-1 is a vascular receptor for coagulation factor Xa. *J Biol Chem.* 1996;271:28407-28413.
52. Herbert J, Bono F, Herault J, et al. Effector protease receptor 1 mediates the mitogenic activity of factor Xa for vascular smooth muscle cells in vitro and in vivo. *J Clin Invest.* 1998;101:993-1000.
53. Gasic GP, Arenas CP, Gasic TB, Gasic GJ. Coagulation factors X, Xa, and protein S as potent mitogens of cultured aortic smooth muscle cells. *Proc Natl Acad Sci U S A.* 1992;89:2317-2320.
54. Bono F, Herault JP, Avril C, Schaeffer P, Lormeau JC, Herbert JM. Human umbilical vein endothelial cells express high affinity receptors for factor Xa. *J Cell Physiol.* 1997;172:36-43.
55. Ong K, Horsfall W, Conway EM, Schuh AC. Early embryonic expression of murine coagulation system components. *Thromb Haemost.* 2000;84:1023-1030.
56. Detloff PJ, Lewis J, John SW, et al. Deletion and replacement of the mouse adult beta-globin genes by a "plug and socket" repeated targeting strategy. *Mol Cell Biol.* 1994;14:6936-6943.
57. Messier TL, Wong CY, Bovill EG, Long GL, Church WR. Factor X Stockton: a mild bleeding diathesis associated with an active site mutation in factor X. *Blood Coagul Fibrinolysis.* 1996;7:5-14.
58. Hooper M, Hardy K, Handyside A, Hunter S, Monk M. HPRT-deficient (Lesch-Nyhan) mouse embryos derived from germline colonization by cultured cells. *Nature.* 1987;326:292-295.
59. DeLisser HM, Christofidou-Solomidou M, Strieter RM, et al. Involvement of endothelial PECAM-1/CD31 in angiogenesis. *Am J Pathol.* 1997;151:671-677.
60. DeLisser HM, Newman PJ, Albelda SM. Molecular and functional aspects of PECAM-1/CD31. *Immunol Today.* 1994;15:490-495.
61. Xu H, Bickford JK, Luther E, Carpenito C, Takei F, Springer TA. Characterization of murine intercellular adhesion molecule-2. *J Immunol.* 1996;156:4909-4914.

62. Xu H, Tong IL, De Fougerolles AR, Springer TA. Isolation, characterization, and expression of mouse ICAM-2 complementary and genomic DNA. *J Immunol.* 1992;149:2650-2655.
63. Dewerchin M, Liang Z, Moons L, et al. Blood coagulation factor X deficiency causes partial embryonic lethality and fatal neonatal bleeding in mice. *Thromb Haemost.* 2000;83:185-190.
64. Romero EE, Velazquez-Estades LJ, Deo R, Schapiro B, Roth DA. Cloning of rat vitamin K-dependent gamma-glutamyl carboxylase and developmentally regulated gene expression in postimplantation embryos. *Exp Cell Res.* 1998;243:334-346.
65. James HL, Girolami A, Fair DS. Molecular defect in coagulation factor XFriuli results from a substitution of serine for proline at position 343. *Blood.* 1991;77:317-323.
66. Reid LH, Gregg RG, Smithies O, Koller BH. Regulatory elements in the introns of the human HPRT gene are necessary for its expression in embryonic stem cells. *Proc Natl Acad Sci U S A.* 1990;87:4299-4303.
67. Pawlinski R, Fernandes A, Kehrl B, et al. Tissue factor deficiency causes cardiac fibrosis and left ventricular dysfunction. *Proc Natl Acad Sci U S A.* 2002;99:15333-15338.
68. Hougie C, Barrow EM, Graham JB. Stuart clotting defect. I. Segregation of an hereditary hemorrhagic state from the heterogeneous group heretofore called stable factor (SPCA, proconvertin, factor VII) deficiency. *J Clin Invest.* 1957;36:485-496.
69. Cooper DN, Millar DS, Wacey A, Pemberton S, Tuddenham EG. Inherited factor X deficiency: molecular genetics and pathophysiology. *Thromb Haemost.* 1997;78:161-172.
70. Salier JP, Hirosawa S, Kurachi K. Functional characterization of the 5'-regulatory region of human factor IX gene. *J Biol Chem.* 1990;265:7062-7068.
71. Crossley M, Brownlee GG. Disruption of a C/EBP binding site in the factor IX promoter is associated with haemophilia B. *Nature.* 1990;345:444-446.
72. Santoro C, Mermoud N, Andrews PC, Tjian R. A family of human CCAAT-box-binding proteins active in transcription and DNA replication: cloning and expression of multiple cDNAs. *Nature.* 1988;334:218-224.
73. Shikamoto Y, Morita T. Expression of factor X in both the rat brain and cells of the central nervous system. *FEBS Lett.* 1999;463:387-389.

74. Wilberding JA, Castellino FJ. Characterization of the murine coagulation factor X promoter. *Thromb Haemost.* 2000;84:1031-1038.
75. Ogasawara T, Gotoh B, Suzuki H, et al. Expression of factor X and its significance for the determination of paramyxovirus tropism in the chick embryo. *Embo J.* 1992;11:467-472.
76. Ko FN, Yang YC, Huang SC, Ou JT. Coagulation factor Xa stimulates platelet-derived growth factor release and mitogenesis in cultured vascular smooth muscle cells of rat. *J Clin Invest.* 1996;98:1493-1501.
77. Gajdusek C, Carbon S, Ross R, Nawroth P, Stern D. Activation of coagulation releases endothelial cell mitogens. *J Cell Biol.* 1986;103:419-428.

Vita

Shing Jen Tai, author of the scientific work presented here, received her Bachelor of Art degree in biology from the University of Pennsylvania in 1996. She began her graduate study in 2000. In September 2005, she will receive the degree of Doctor of Philosophy in biomedical science from the School of Biomedical Engineering, Science, and Health Systems in Drexel University, Philadelphia, PA. During the course of her graduate study, author presented her work in the Meeting of American Society of Hematology, Meeting of American Heart Association, and in the Conference on Atherosclerosis, Thrombosis, and Vascular Biology. A manuscript of her work has also been submitted for publication.